UNDERSTANDING BIOFILM FORMATION IN CO-CULTURES OF *CANDIDA ALBICANS* AND *CANDIDA GLABRATA*

A Dissertation

by

MICHELLE LYNN OLSON

Submitted to the Office of Graduate and Professional Studies of
Texas A&M University
in partial fulfillment of the requirements for the degree of

DOCTOR OF PHILOSOPHY

Chair of Committee,	Arul Jayaraman
Co-Chair of Committee,	Katy C. Kao
Committee Members,	Pushkar Lele
	Xiaorong Lin
Head of Department,	M. Nazmul Karim

December 2018

Major Subject: Chemical Engineering

ABSTRACT

Candida spp. are commensal opportunistic fungal pathogens that often colonize and infect mucosal surfaces of the human body. *Candida*, along with other microbes in the microbiota, generally grow as biofilms in a polymicrobial environment. Due to the nature of cellular growth in a biofilm (such as production of a protective extracellular matrix) and the recalcitrance of biofilms, infections involving biofilms are very difficult to treat with antibiotics and perpetuate the cycle of infection. The two most commonly isolated *Candida* spp. from *Candida* infections are *Candida albicans* and *Candida glabrata*, and the presence of both of these species results in increased patient inflammation and overall biofilm formation. In this work, we investigate the interspecies interactions between *C. albicans* (Ca) and *C. glabrata* (Cg) in co-culture through understanding biofilm formation, transcriptomic analysis, and the involvement of the quorum-sensing molecule farnesol in biofilm formation. We report that biofilm formation in co-culture populations of Ca and Cg is dependent on the relative starting concentrations of each species, with the highest biofilm formation in a ratio of Ca:Cg 1:3. Confocal microscopy analysis revealed increased biofilm heterogeneity and Ca hyphae length in co-culture biofilm compared to mono-culture biofilms. Several genes involved in Ca adhesion (*HWP1* and *ALS3*) were up-regulated in Ca:Cg 1:3 co-culture biofilms and there was also an increase in resistance to the antifungal drug caspofungin in co-culture biofilms. Next, we utilized transcriptomic analysis to further understand Ca:Cg interspecies interactions within co-culture biofilms. We found that, in co-culture biofilms, lipid and cell wall

biosynthesis genes were significantly down-regulated and perturbed in both Ca and Cg, and it was demonstrated that cell wall lipid content is increased in co-culture biofilms in *C. albicans* via confocal microscopy. Finally, we investigated the relationship and mechanisms of farnesol with *C. glabrata* cultures and also the impact of farnesol on co-culture biofilm formation. Results show possible Cg sequestration of farnesol and that there are other factors likely at play during co-culture biofilm formation that leads to increased biofilm formation, especially in the highest biofilm former Ca:Cg 1:3.

DEDICATION

To my Mom, who taught me that knowledge is power and to never stop dreaming.

ACKNOWLEDGEMENTS

First, I sincerely thank both of my advisors Dr. Katy Kao and Dr. Arul Jayaraman for their guidance and support over the course of my graduate studies. I feel very fortunate to have been co-advised, for it has given me two perspectives on how to approach research, effectively collaborate, and think critically. Thank you for the constant support, challenging me, and encouraging me to grow.

I would also like to thank and acknowledge my family and friends that got me to where I am today. Thanks to my Mom who has been my biggest supporter and showed me that anything is possible, my Dad for always believing in me and teaching me the importance of perseverance, Tom for the continued support, and my sister Erika for the laughs and fun times along the way. For my friends who have been a rock throughout my life, especially Megan. Also to my fifth floor family – you have been that constant light through many challenges and between learning from each one of you and all the good times, you have been everything in this journey. A special recognition should go to Quint Peabody, Ravi Chawla, Daniel Peñarete, Nandita Kohli, Melanie DeSessa, Jon Raftrey, Duanduan Han, and Katie Ford. Recognition is also due to the one and only Princess Cottage: Cory Klemashevich, Pranav Kannan, and Susmitha Kotu. My sanity endlessly thanks you and I will miss our office; I could not have asked for better officemates and comrades over the course of my Ph.D. In addition, an overwhelming thanks to Connie for the clarity, support, and mind power.

Lastly, I would like to thank the pioneers in the microbiome research area and those that have developed the many useful tools to study *Candida* (*i.e.* Candida Genome Database). These efforts have helped immensely in the development of my thesis.

CONTRIBUTORS AND FUNDING SOURCES

This work was supported by a dissertation committee consisting of Professor Katy C. Kao (co-advisor), Professor Arul Jayaraman (co-advisor), and Professor Pushkar Lele of the Department of Chemical Engineering and Professor Xiaorong Lin of the Department of Microbiology at the University of Georgia.

The RNA-sequencing data analysis was provided in part by Professor Ulisses Braga-Neto and his graduate student Mahdi Imani in the Department of Electrical and Computer Engineering at Texas A&M University (Section 3). Smriti Shankar and Cory Klemashevich of the Integrated Metabolomics Analysis Core at Texas A&M University aided in experimental design and farnesol quantification optimization (Section 4). Michelle Olson completed all other work for the dissertation independently.

Graduate study was supported by a Graduate Teaching Fellowship from the Dwight Look College of Engineering.

Funding for all projects and additional support were provided by the Nesbitt Chair Endowment to Professor Arul Jayaraman and NSF grant MCB-1054276 to Professor Katy C. Kao.

NOMENCLATURE

Ca	*Candida albicans* (*C. albicans*)
Cg	*Candida glabrata* (*C. glabrata*)
qRT-PCR	Reverse transcription-quantitative PCR
PCR	Polymerase Chain Reaction
OD_{600}	Optical Density at 600 nanometers
RNA	Ribo Nucleic Acid
RNA-seq	RNA-sequencing
GFP	Green Fluorescent Protein
RFP	Red Fluorescent Protein
GO	Gene Ontology
CGD	Candida Genome Database

TABLE OF CONTENTS

Page

LIST OF FIGURES

Page

LIST OF TABLES

Page

1. INTRODUCTION

1.1 General Background

The human microbiota is composed of a wide and diverse array of bacterial and fungal species. The interactions that take place between the host cells and the microbiota have the potential to be beneficial or detrimental to overall host health. The opportunistic fungal pathogens *Candida albicans* and *Candida glabrata* are common commensal microorganisms found in the human body. *Candida* is isolated in about 70% of healthy individuals and often colonizes mucosal surfaces such as the oral cavity, gastrointestinal (GI) tract, urogenital tract, and also the skin [1]. Often times the colonizing *Candida* species changes overtime and is not fixed at a particular site [2]. Despite being commensal microorganisms, *Candida* spp. are the fourth leading cause of nosocomial infections and are the leading or second-leading cause of patient death [3, 4]. Candidiasis, a *Candida* infection, may range from mucosal to a deep tissue infection. Disseminated candidiasis (candidemia) often affects patients taking broad-spectrum antibiotics or antifungal drugs, patients with chronic inflammation, nosocomial patients, and patients that are immunocompromised, such as those with HIV or AIDS [5, 6]. Consequently, candidemia mortality rates may be as high as 50% [7, 8]. From clinical data of nosocomial candidemia, reports show that multiple *Candida* species are present during an infection. *C. albicans* is often the leading cause of candidiasis and candidemia, with *C. glabrata* frequently reported as the second most common *Candida* isolate in infections within North America [7, 9-11].

1.2 *Candida* lifestyle and biofilm formation

A unique feature of *C. albicans* is that it is polymorphic and has the ability to grow as yeast, pseudohyphae, and hyphae. The hyphal morphology of *C. albicans* is associated with increased virulence as it allows for active penetration of mucosal surfaces into host tissue, which can lead to disseminated candidiasis. In contrast, *C. glabrata* mainly grows as budding yeast. *C. glabrata* has been shown to piggyback onto the hyphae of *C. albicans* in order to invade tissue and cause an infection [12]. As part of the microbiome, fungal species such as *Candida* are incorporated into biofilms throughout the human body. Biofilms are the principal form of growth for microorganisms and are often composed of polymicrobial communities. Biofilms act as a protective niche for cells from stress and starvation, which makes them more resistant to antifungal agents and also allows them to go unnoticed by the host immune system [13, 14]. Additionally, it is estimated that 65% – 80% of human infections originate from biofilms [15]. *C. albicans* is capable of forming very robust biofilms because of their polymorphic capabilities, which contributes to its pathogenicity and results in higher mortality rates over other fungal species that lack biofilm-forming capabilities [13, 16].

Candida biofilm development is divided into four stages: (1) adherence to a surface, (2) proliferation on a surface, (3) maturation into a complex biofilm, (4) dispersion of cells from the biofilm and into the surrounding for further spread of cells [17-21]. A biofilm initiates as a monolayer of cells, which then expands and proliferates into a multilayer complex. As the biofilm matures, an extracellular matrix (ECM) develops and allows the cells to grow into a three-dimensional structure. The extracellular matrix is

a hydrated exopolymeric substance (EPS) that encases the cells and acts as a protective mechanism against nutritional deprivation and environmental factors such as desiccation, host immune defenses, and antifungal treatments. Synthesized mostly from the cells themselves, the *C. albicans* EPS has been shown to include polysaccharides (~25% [wt/wt]), lipids (~15% [wt/wt]), proteins (~55% [wt/wt]), and nucleic acids (~5% [wt/wt]) [22]. The most studied component of *Candida* biofilms is β-1,3-glucan, which is the major cell wall polysaccharide. It has been shown to act as a "drug sponge" and sequester antifungal molecules that only increases the cells resistance to the drug [22]. Polysaccharides represent about 25% of the *C. albicans* biofilm EPS by weight, and monosaccharide analysis indicates that arabinose, mannose, glucose, and xylose are the four most abundant sugars. Interestingly, the *C. albicans* major cell wall polysaccharide component β-1,3-glucan only represents a low amount of sugars in the EPS. Other polysaccharides such as α-1,2 branched and α-1,6-mannans comprise ~87% of EPS polysaccharides. These two polysaccharides are known to be associated with unbranched β-1,3-glucans and form a type of complex through physical interactions [22].

The material and growth substrate of *Candida* cells greatly impacts its ability to form biofilms. The media composition, temperature, and the type of growth surface *Candida* is exposed to all affect biofilm formation [2]. Growth conditions closer to a physiological pH and temperature induce *C. albicans* hypha formation, however it was demonstrated that medium composition modulates adherence and biofilm formation in *C. albicans* and *C. glabrata* more than pH [23]. The cellular growth surface also influences the morphological state and biofilm formation of *C. albicans*. For example, biofilms on

silicone elastomer catheter material were much thicker than biofilms formed on denture material Poly(methyl methacrylate) (PMMA). Interestingly, both hypha and yeast forms of *C. albicans* are able to produce biofilms and one type of cell is not absolutely essential for biofilm formation. Additionally, the presence of flow in the system has been shown to significantly increase *C. albicans* ECM production and biofilm strength [21]. Overall, *Candida* biofilm formation can vary greatly depending on the system conditions.

For mixed fungal biofilms, especially between *Candida* species, there is limited knowledge on how species interact and influence overall microbial pathogenicity. Considering that *C. albicans* and *C. glabrata* are the two most common species in candidiasis and pose a threat for human health, there is clinical relevance to study the interspecies interactions during biofilm development. In contrast to *C. albicans*, *C. glabrata* is able to adhere to some surfaces but forms weak biofilms by themselves. *C. glabrata* has the ability to cause candidiasis and worsen infections when other *Candida* species, such as *C. albicans*, are present. For example, *C. albicans* is required for *C. glabrata* to contribute to oropharyngeal candidiasis [12]. Several studies have looked at the interactions taking place in co-culture *C. albicans* and *C. glabrata* biofilms. Mixed species biofilms of *C. albicans* and *C. glabrata* have previously been shown to have a higher biomass than monoculture biofilms [23, 24]. In addition, it has been demonstrated that *C. glabrata* physically adheres to *C. albicans* hyphae and that adherence requires the adhesin proteins of both fungal species to be present [12].

1.3 Genetic control of *C. albicans* and *C. glabrata* biofilm formation

For genetic regulation of biofilms, *C. glabrata* has several known adhesion genes, many of which are in the *EPA* gene family. The *EPA* genes are located at subtelomeres and expression of several *EPA* genes is regulated by chromatin silencing. *EPA6* and *EPA7* are known adhesion genes in *C. glabrata* that are involved in biofilm formation. Epa1-5 do not appear to have a substantial role in biofilm formation despite similar structure to Epa6-7. *EPA1* has been demonstrated to contribute to the interactions between *C. glabrata* and epithelial cells; however *EPA1* is highly expressed during exponential growth phase [25]. Studies also show that *C. glabrata* undergoes cell wall remodeling and changes in cell surface physical properties during biofilm formation. Genes involved in cell surface hydrophobicity and phospholipid synthesis, such as *PDR16* and *PGS1*, have been shown to alter and decrease *C. glabrata* biofilm formation, respectively [26, 27].

In *C. albicans*, there are several known pathways and genes responsible for biofilm formation. The Als proteins are adhesins that are regulated by Tor1. In the presence of nutrients, adhesion gene expression is repressed by Tup1 and Nrg1. Once nutrients are depleted, there is no longer repression of Bcr1 and Efg1 and the proteins can aid in activating transcription of adhesion genes [28]. Gene regulation in *C. albicans* biofilms changes over the course of biofilm growth and development [29]. In the early stages of *C. albicans* biofilm growth, farnesol concentration is low and adherence is determined by Efg1 and Eap1. After attachment of cells to a surface, *HWP1*, one of the genes responsible for hyphae formation, is activated in *C. albicans* and cells begin to form filaments and a structured biofilm. The biofilm continues to mature and produce more farnesol, which

promotes the yeast form of *C. albicans*. When the biofilm is in the dispersal stage, Nrg1 modulates *C. albicans* adhesion genes so cells may detach from the biofilm substrate [29].

In previous co-culture *C. albicans* and *C. glabrata* biofilm studies, *C. glabrata* adhesion-associated genes were upregulated in the presence of *C. albicans*. The *C. glabrata* upregulated genes were cell wall protein coding genes *EPA8*, *EPA19*, *AWP2*, *AWP7*, and *CAGL0F00181* and they were suggested to mediate the adhesion of *C. glabrata* to *C. albicans* hyphae [12]. In another study that looked at co-culture biofilms of *C. albicans* and *C. glabrata*, they found that at 12 and 24 hour biofilm formation the *C. albicans* biofilm-associated genes *ALS3*, *HWP1*, *PLB2*, *LIP9*, and *SAP5* were all slightly upregulated in the co-culture biofilm compared to the monoculture *C. albicans* biofilm. This suggests a seemingly neutral or synergistic relationship between the two *Candida* species [30]. Neutral relationships between *C. albicans* and *C. glabrata* have also been reported, where the number of cells of each species in a culture is not affected by the presence of the other [31, 32].

1.4 Antifungal resistance of *C. albicans* and *C. glabrata* biofilms

Since biofilms are a tightly organized community of cells, they have inherent resistance to antimicrobial drugs in comparison to planktonic cells. A biofilm promotes infection and persistence of microorganisms in the host, which is why being able to properly treat a biofilm is crucial to host survival. Due to the structure of a biofilm, during treatment, the outer cells of the biofilm have exposure to the therapeutic and the cells that do not die will persist and potentially gain resistance against the drug. In addition,

antifungal resistance increases with biofilm development. In one study, early *C. albicans* biofilms had high susceptibility for various antifungal drugs. By mature biofilm formation at 72 hours, *C. albicans* cells were highly resistant [33]. *C. glabrata* also exhibits an innate resistance to antifungal drugs, especially azoles, which makes the treatment of co-culture *Candida* biofilms even more difficult to treat [34]. Additionally, a report looked at the effect of glucose concentration on *C. glabrata* biofilm formation and found that glucose concentration modulates *C. glabrata* biofilm formation and lower glucose promotes biofilm formation and increased resistance to amphotericin B [35].

C. albicans and *C. glabrata* strains that are resistant or susceptible to antifungal drugs also form different types of biofilms. *C. albicans* that is resistant to fluconazole forms more biofilm than the susceptible strains, mostly because of the increased hydrophobicity of the cell surface and cell wall polysaccharides that aid in adhesion [36]. *C. albicans* biofilms, regardless of susceptibility, are a dense accumulation of cells composed of blastospores, pseudohyphae, and hyphae partially embedded in an ECM. *C. glabrata* resistant cells form a compact layered biofilm composed of only blastospores, whereas the susceptible strains form a discontinuous structured biofilm [37]. Since *C. glabrata* forms weaker and thinner biofilms in comparison to *C. albicans*, the biofilm formation seen in *C. glabrata* resistant cells may contribute to the increased pathogenesis of the species.

1.5 Quorum sensing in *C. albicans* and *C. glabrata*

Candida albicans and *Candida glabrata* regulate virulence traits through a minimum of two quorum sensing (QS) signaling molecules, *E,E*-farnesol and tyrosol. Through these QS molecules, cells are able to monitor their population density. In *C. albicans*, both molecules affect the morphological transition from yeast to hyphae and also biofilm formation. There is tight positive and negative control over the production of these molecules in *C. albicans* based on environmental conditions. The production of *E,E*-farnesol and farnesoic acid is stimulated by high biomass and reduces *C. albicans* hyphae formation [38-40]. Indeed, the expression of a hypha-specific cell wall protein *HWP1* is decreased in *C. albicans* after exposure to farnesol [41]. Tyrosol, on the other hand, is produced and secreted when cell density is low, thus promoting hyphae formation and growth. Tyrosol secretion is at least 50% higher in *C. albicans* biofilms compared to planktonic cells and takes effect most significantly during the early and intermediate stages of biofilm formation. Tyrosol stimulation of *C. albicans* hyphae formation seems to occur in the early stages of biofilm formation (1 to 6 hours); however, farnesol appears to have a dominant affect over tyrosol when both compounds are together at later biofilm times (48 to 72 hours) [42].

Farnesol and tyrosol are also produced by *C. glabrata*, but at much lower levels than *C. albicans*. *C. albicans* has been reported to produce ~ 10 – 60 µM farnesol (depending on the medium), whereas *C. glabrata* only produces on the order of ~ 1 µM farnesol. Treatment with *E,E*-farnesol does not affect biofilm formation of *C. glabrata* but slightly decreases the growth rate of the fungus [43]. For tyrosol, *C. glabrata* produces on

the order of ~ 1 µM and *C. albicans* produces closer to ~ 10 – 50 µM tyrosol [42, 44]. *C. glabrata* total biofilm biomass was shown to be not affected by tyrosol concentrations in the medium [45].

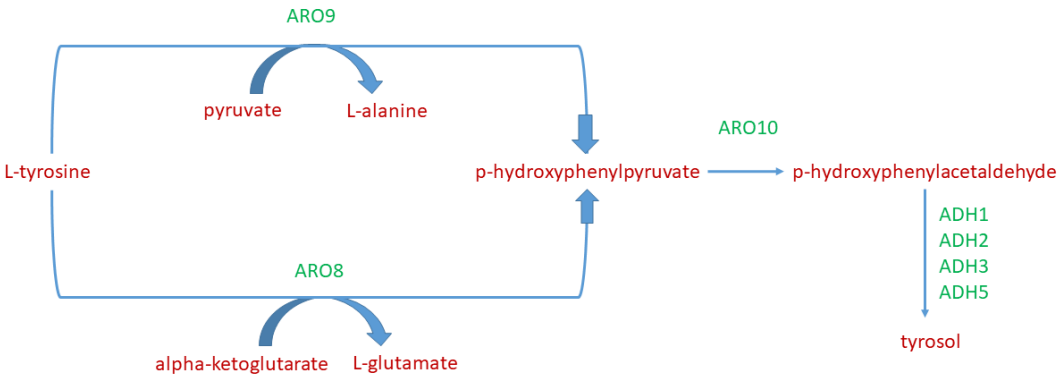

Figure 1. Tyrosol biosynthesis pathway in *Candida albicans*. Genes in green are fully characterized and confirmed to be involved in tyrosol biosynthesis.

Tyrosol biosynthesis pathway, as seen in Figure 1, begins with L-tyrosine and several alcohol dehydrogenases convert p-hydroxyphenylacetaldehyde to tyrosol [46-48]. Figure 2 shows the known genes involved in the farnesol biosynthesis pathway. *ERG9* is fully characterized in *Candida*, and *IDI1*, *ERG20*, and *DPP3* have putative roles in farnesol biosynthesis based on homology in *S. cerevisiae* [49-51]. *DPP3* is not fully characterized for its involvement in FPP to farnesol conversion (Figure 2), however it was demonstrated that the deletion of *DPP3* resulted in six times less farnesol production compared to wild type *C. albicans* [52]. *DPP3* is the only gene that has been characterized and linked to farnesol production in *C. albicans* [53-55]. Several other genes have been

suggested to be involved in FPP conversion to farnesol (e.g. *DPP2*) [56], but studies remain to confirm their role in farnesol biosynthesis. Farnesoic acid (Figure 2) has been reported to be produced in some *C. albicans* strains [40], where others report only farnesol production in *C. albicans* [57].

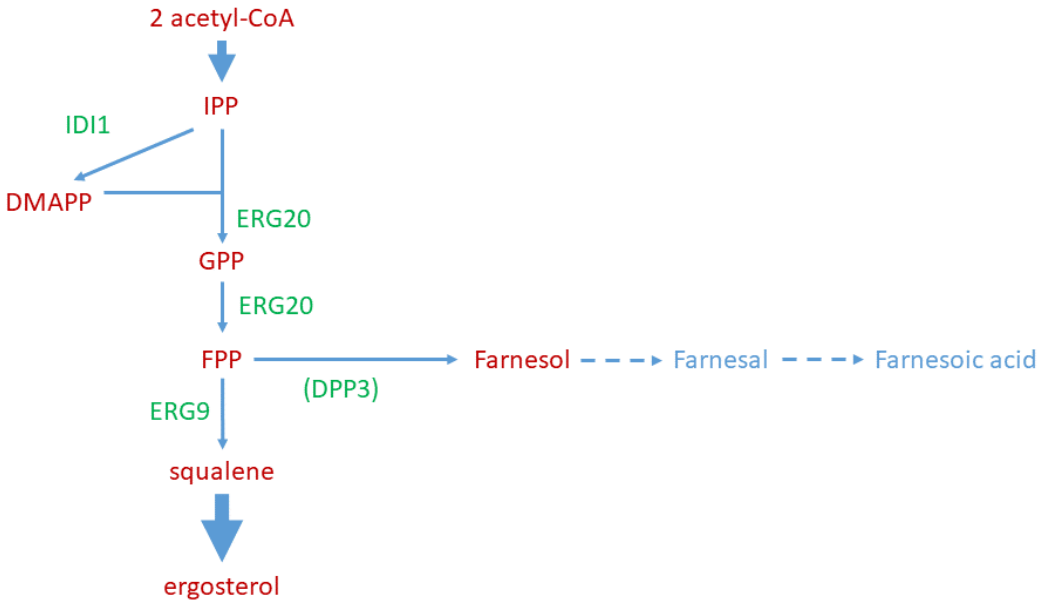

Figure 2. Farnesol biosynthesis pathway in *Candida albicans*. Genes in parentheses are considered to be involved in pathway biosynthesis. Light blue are reported derivatives and dotted blue arrows show biosynthesis known in some *Candida* spp.

The metabolic response of *C. albicans* to farnesol is just beginning to be understood. A report by Han et al. investigated the metabolic response of farnesol treated *C. albicans* cells [58]. Intracellular metabolites were identified after cells were exposed to farnesol. What was found was that saturated fatty acid (myristate) and amino acids such as phenylalanine and leucine were decreased whereas amino acids such as tryptophan and histidine were increased [58]. Looking at pathways differentially expressed under farnesol treatment, pathways involved in nitrogen and amino acid metabolism, fatty acid metabolism, and acetyl CoA biosynthesis were all upregulated. Downregulated pathways included those involved in tryptophan metabolism which is associated with tyrosol production [58].

What is still not known in yeast is if there is a receptor or sensor for farnesol, how farnesol synthesis is regulated, if there is active uptake and transport of farnesol, and the exact relationship between farnesol and the commitment to a yeast or hyphae morphology [53, 59]. What is also not fully understood is if active degradation of farnesol occurs in yeast [53]. It has been demonstrated that farnesol is secreted by white cells only (versus opaque) [60], and that secreted farnesol acts as a chemoattractant for macrophages which enables the yeast to multiply and spread during infection [61]. What is known about farnesol regulation is that biosynthesis is diminished under anaerobic growth [62] and that farnesol resistance is a factor of the growth phase where cells have increased resistance to farnesol in the stationary phase over the exponential phase [63]. There are several transcriptional morphogenic repressor genes: *TUP1*, *NRG1*, and *EED1*. *TUP1*, *NRG1*, and *EED1* mutants all over produce farnesol and are proposed to be regulators in the cellular

farnesol response [64]. Interestingly, even with over production of farnesol in the three mutants there were no reported changes in *DPP3* expression levels suggesting that *DPP3* is not the only gene involved in farnesol production [64-66]. Additionally, *EED1* (epithelial escape and dissemination 1) has been shown to regulate hyphal maintenance in *C. albicans* and the *EED1* mutant can form hyphae but it cannot switch back to the yeast form of growth and is hypersensitive to farnesol [66]. These findings suggest that *EED1* might play a role in farnesol membrane transport. Overall, it is not clear how yeast cells sense farnesol, but binding is very specific as subtle changes in the molecular structure of farnesol was sufficient to reduce biological activity [67]. It is possible that farnesol binds to a nuclear receptor in *C. albicans*, similar to what is observed in mammalian cells [68].

In mammalian cells, free farnesol has been shown to be utilized for isoprenoid biosynthesis which is incorporated into cholesterol [69]. Farnesol activates a nuclear hormone receptor complex, retinoid X – farnesoid X nuclear receptor (FXR), which mediates the transcription of steroids and retinoids [68]. Farnesol also increases the degradation of HMG-CoA reductase, which is upstream of the mevalonate pathway and converts HMG-CoA to mevalonic acid [70]. In plant cells, farnesol is incorporated into sterols by FPP when exogenous farnesol is supplied which demonstrates the conversion of farnesol to farnesyl monophosphate (FP) to eventually FPP [71]. Tyrosol similarly is not well characterized in yeast but has been studied in mammalian cells to some extent. What was demonstrated is that tyrosol is poorly metabolized in hepatocytes [72] and that in epithelial cells, tyrosol is metabolized into glucuronides [73].

2. RELATIVE ABUNDANCE OF CANDIDA ALBICANS AND CANDIDA GLABRATA IN IN VITRO CO-CULTURE BIOFILMS IMPACTS BIOFILM STRUCTURE AND FORMATION[1]

2.1 Summary

Candida is a member of the normal human microbiota and often resides on mucosal surfaces such as the oral cavity or the gastrointestinal tract. In addition to their commensality, *Candida* species can opportunistically become pathogenic if the host microbiota is disrupted or if the host immune system becomes compromised. An important factor for *Candida* pathogenesis is its ability to form biofilm communities. The two most medically important species - *Candida albicans* and *Candida glabrata* - are often co-isolated from infection sites, suggesting the importance of *Candida* co-culture biofilms. In this work, we report that biofilm formation of the co-culture population depends on the relative ratio of starting cell concentrations of *C. albicans* (Ca) and *C. glabrata* (Cg). When using a starting ratio of Ca:Cg of 1:3, a ~6.5- and ~2.5-fold increase in biofilm biomass was observed relative to Ca monoculture and a Ca:Cg ratio of 1:1, respectively. Confocal microscopy analysis revealed heterogeneity and complex structures composed of long Ca hyphae and Cg cell clusters in the co-culture biofilms, and qRT-PCR studies showed an increase in the relative expression of the *HWP1* and *ALS3* adhesion genes in

---

[1] Reprinted with permission from Olson, M. L., Jayaraman, A., & Kao, K. C. (2018). Relative Abundance of Candida albicans and Candida glabrata in In Vitro Co-Culture Biofilms Impacts Biofilm Structure and Formation. *Applied and Environmental Microbiology*, 84(8), e02769-17,

the Ca:Cg 1:3 biofilm compared to Ca monoculture biofilm. Additionally, only the 1:3 Ca:Cg biofilm demonstrated increased resistance to the antifungal drug caspofungin. Overall, the results suggest that interspecific interactions between these two fungal pathogens increase biofilm formation and virulence-related gene expression in a co-culture composition-dependent manner.

2.2 Introduction

The human microbiota is composed of a diverse array of bacterial and fungal species that colonize different sites in the body [74, 75]. Although the composition and function of the bacteria in the microbiota have been extensively studied [76-80], the mycobiota, or fungal members of the microbiome, remains largely understudied [74]. In the gastrointestinal tract, shotgun sequencing revealed that fungi compose approximately 0.1% of the microorganisms [81, 82], yet this is likely an underrepresentation [74]. One of the most common fungi in the human body is *Candida* spp., which colonize mucosal surfaces such as the oral cavity, gastrointestinal (GI) tract, urogenital tract, and also the skin in approximately 70% of healthy individuals [1]. An expansion in the *Candida* population may lead to mucosal and deep tissue infections (candidiasis), while disseminated candidiasis (candidemia) often affects patients on broad-spectrum antibiotics or antifungal drugs, patients with chronic inflammation, nosocomial patients, and patients that are immunocompromised, such as those with HIV or AIDS [5, 6]. Not surprisingly, *Candida* is the fourth leading cause of nosocomial infections, and candidemia mortality rates may be as high as 50% [3, 7, 8].

Of the various *Candida* spp., the opportunistic pathogens *Candida albicans* (Ca) and *Candida glabrata* (Cg) account for roughly 60% of *Candida* spp. in the human body. Ca is often the leading cause of candidiasis and candidemia, with Cg frequently reported as the second most common *Candida* isolate in infections within North America [7, 9-11]. Ca and Cg are often co-isolated together during an infection, and isolation of single species Cg from infection sites is rare [83]. Additionally, the co-isolation of Ca and Cg has been linked with increased pathogenesis as the occurrence of co-isolation was reported in almost 80% of patients with high inflammation [84]. The inherent resistance of Cg against commonly used antifungals such as fluconazole and amphotericin B is generally higher than Ca [85, 86]. The abundance of Cg and non-*Candida albicans* (non-Ca) species has been shown to increase in a clinical study during a course of antifungal treatment against *Candida* spp. [7]. Nguyen et al. [9] observed 427 nosocomial patients with candidemia and found that after treatment with amphotericin B, Cg was the most common non-Ca species to cause candidemia mainly due to the persistence of Cg and resistance to antifungal treatment [9].

Biofilm communities provide a protective niche for microorganisms from stress and external perturbations, and it is estimated that 65% – 80% of human infections originate from biofilms [87]. Fungal species such as *Candida* are also found in polymicrobial biofilms in the human body and are generally more resistant to antifungal agents than when present in suspension [88]. It has also been shown that the biofilm microenvironment facilitates *Candida* to evade the host immune system and persist in the body [13, 14]. *Candida albicans* not only resides in the biofilm but also contributes to its

development as it is also capable of forming robust biofilms [16, 89]. This is primarily due to its polymorphic nature where it is able to grow as yeast, pseudohyphae, and hyphae. The hyphal morphology of Ca is associated with increased virulence as it allows for active penetration of mucosal surfaces into host tissue, which can lead to disseminated candidiasis. On the other hand, Cg mainly grows as budding yeast and has been shown to attach to the hyphae of Ca in order to invade tissue [12]. The presence of *Candida* spp. in a polymicrobial biofilm not only promotes its virulence but also increases the biofilm formation and antimicrobial resistance of other pathogenic bacteria, as has been demonstrated for *Staphylococcus aureus* [90].

Despite the synergism between Ca and Cg, there is limited information on the underlying mechanisms involved in the interaction between the two fungal species and their effect on virulence and invasion. Recent work by Pathak et al. with Ca and Cg co-cultures demonstrated that co-cultures with a 1:1 initial ratio of Ca:Cg yielded the highest biofilm biomass over any other *Candida* species combination as well as over single species biofilms [24]. In addition, a recent host microbiome study showed that the abundance of fungal species, including *C. albicans*, changed with diet, and potentially contributed to disease [91]; thus, it is conceivable that the relative abundance of fungal species within a polymicrobial biofilm can impact pathogenesis. However, there is little knowledge regarding the relative abundance of each species in a biofilm and how that contributes to biofilm formation and pathogenesis. In this work, we investigated the effect of how varying the initial Ca and Cg ratio impacts biofilm formation, structure and antifungal drug susceptibility.

2.3 Materials and Methods

2.3.1 Microorganisms and growth conditions

C. albicans (SC5314, J. Berman, ENO1-RFP::Nat1) [92] and *C. glabrata* (ATCC 2001, GFP-labeled) were used in this study. Prior to the experiments, strains were cultured on Yeast Peptone Dextrose (YPD) agar plates for 48 hours at 30°C. For all experiments, single colonies were isolated from YPD agar plates and inoculated into 25 mL YNB medium (50 mM glucose and pH 7, Amresco). Cultures were grown overnight at 30°C and 170 rpm for 12 hours prior to experiments.

2.3.2 Biofilm quantification assay

Biofilms were grown in either 96-well polystyrene plates (Corning®), or on glass or acrylic coverslips (VWR®) in 6-well tissue cultures plates. 96-well plates or coverslips were incubated in heat-inactivated fetal bovine serum (HI FBS) overnight at 37°C. Prior to experiment, coverslips or wells were washed once in 1X phosphate buffered saline (PBS, pH 7.4) and the coverslips were placed into 6-well tissue culture plates. Overnight cultures were washed twice with PBS and resuspended in fresh YNB medium. A hemocytometer was used to calculate cell density and cell cultures were diluted to a final concentration of 10^7 cells/mL. A final volume of 4 mL cell culture was added to each well with a coverslip and 100 µL was added to the 96-well plates. Wells with media only were used as controls. Biofilms were allowed to grow at 37°C for 48 hours without agitation. After 48 hours, the coverslips were removed from the 6-well plates using tweezers and washed twice with PBS. For the 96-well plates, wells were washed twice with 200 µL PBS. Coverslips were placed in a new 6-well plate, where 2 mL (200 µL for microtiter

plates) of 99% methanol was added to each biofilm. After 15 minutes, excess methanol was removed from the well and biofilms were allowed to dry completely. Once dry, 2 mL (200 µL for microtiter plates) of 0.1% crystal violet was added to each biofilm and incubated at room temperature for 20 minutes [93]. Plates were rinsed gently under DI water to remove excess crystal violet stain from the wells and biofilms. Excess water was removed from the well and 1 mL (150 µL for microtiter plates) of 33% acetic acid was added to each biofilm. Acetic acid samples were diluted 50-fold in a black walled clear bottom 96-well Corning® plate and absorbance was measured at 590 nm in a plate reader (Molecular Devices SpectraMax® 340PC).

2.3.3 Confocal Laser Scanning Microscopy

For CLSM biofilm analysis, biofilms were grown in 2-well chambered coverglass slides (Nunc® Lab-Tek™) that were pre-incubated overnight with HI FBS at 37°C. Cultures of *C. albicans* and *C. glabrata* were grown overnight in YNB medium. Cultures were washed twice in PBS and adjusted to a cell density of 10^7 cells/mL. A final volume of 2 mL per well was used. Biofilms were allowed to grow for 48 hours at 37°C and no agitation. After 48 hours growth, biofilms were washed gently with PBS and fixed with 4% paraformaldehyde (room temperature, dark, 30 min). Images were acquired using Zeiss LSM 780 NLO Multiphoton microscope (Zeiss, USA) using the Plan-Apo 40X/1.4 oil DIC M27 objective with 488 nm and 543 nm laser lines to image GFP and RFP simultaneously. To analyze the structure of the biofilms, a series of optical sections were taken at 1 µm intervals throughout the depth of the biofilm. 3 biological replicates were imaged and up to 3 images were taken per biofilm sample and used in both Comstat2 and

ImageJ analysis. Image J [94] was used to adjust brightness of images, render 3D image stacks, and quantify hyphae length and cell clustering. Comstat2 [95, 96] was used for calculating biofilm thickness.

2.3.4 RNA extraction and qRT-PCR analysis

As described above, biofilms were grown for 6, 12, and 24 hours on glass coverslips in 6-well tissue culture plates. Biofilms were washed off of the coverslip with pre-chilled sterile Millipore water and cells were collected by centrifugation (2000 x g, 5 minutes, 4°C). Supernatant was removed and cell pellets were flash-frozen in liquid nitrogen prior to placing in a lyophilizer for drying. Cell pellets were allowed to dry for 24 hours. Acid-washed glass beads (Sigma-Aldrich) were added to the dried cell pellets and disrupted in the Disruptor Genie for 2 minute cycles for up to 10 minutes. Lysis buffer from the GE Illustra RNAspin Mini kit was added to the disrupted cell powder and RNA was extracted using the kit protocol with on-column DNase I treatment. RNA quality and concentration were determined using a Nanodrop® and Qubit™, respectively.

For qRT-PCR, qScript™ One-Step SYBR® Green qRT-PCR kit (Quanta Biosciences™) was used in a Roche LightCycler® 96 system. 50 ng of RNA was used per reaction. *ADH1* was the reference gene used for ΔC_T analysis. For $\Delta\Delta C_T$ analysis, mono-culture biofilm ΔC_T was subtracted from the co-culture biofilm ratios. $2^{-\Delta\Delta CT}$ analysis was used to determine fold-change gene expression. Standard deviation was taken from $2^{-\Delta\Delta CT}$ values of three biological replicates. Primers used are listed in Table 1.

Table 1. qRT-PCR primer list.

Gene	Primer
HWP1 (Ca)	F: 5'-TTGGCTAGTGAAACCTCACCAA-3' R: 5'-GGCAGATGGTTGCATGAGTG-3'
ALS3 (Ca)	F: 5'-ACTTTGTGGTCTACAACTTGGG-3' R: 5'-CCAGATGGGGATTGTAAAGTGG-3'
PLB5 (Ca)	F: 5'-CATTTGACTCGTCCGGCTCT-3' R: 5'-ATGATGCCTGGGCAGAGGA-3'
SAP9 (Ca)	F: 5'-TGTAACTTGGCCGACTCCAG-3' R: 5'-ACGAGCTTGACGATTGTTGCAT-3'
EPA1 (Cg)	F: 5'-ACCTAGCCCATACGGACCAA-3' R: 5'-TCTGAGAAAGCATACTCGCTTGA-3'
EPA6 (Cg)	F: 5'-TCCGAATTATCCTCGAACAGGC-3' R: 5'-ATCAAACAGCGAAGTACACCC-3'
ADH1 (Ca)	F: 5'-TGGGTGCTGAAGCTTACGTT-3' R: 5'-TGACTTTAGCGTGAGCTGGT-3'
ADH1 (Cg)	F: 5'-GAGCCGTCTTCCCTTCCA-3' R: 5'-CGTGTTCGATTCGGTAACGC-3'

2.3.5 Antifungal susceptibility test

Caspofungin (GoldBio, St. Louis, MO) was dissolved in sterile MilliQ water to a concentration of 1 mg/mL. Caspofungin stock solution was stored at -80°C in individual aliquots for one time use. CLSI M27-A2 [97] testing standard was slightly modified and used to test *Candida* planktonic caspofungin susceptibility. Cells were diluted to a concentration of 5.0×10^2 to 2.5×10^3 cells/mL in YNB medium (50 mM glucose, pH 7). Cultures were allowed to grow for 48 hours in test tubes at 37°C without agitation. OD_{600} of planktonic cultures was measured after 48 hours. To test biofilm susceptibility, 96-well microtiter plates were coated with HI FBS and placed at 37°C overnight. Wells were washed once with PBS before inoculating with prepared cell cultures as mentioned above. Final volume in the wells was 100 µL. Biofilms were allowed to grow for 24 hours at

37°C. After 24 hours, biofilms were washed twice with 200 µL PBS and fresh YNB medium or YNB medium with caspofungin was added to the wells. Plates were placed back at 37°C for 24 hours. After 48 hours of total growth, biofilms were washed twice with 200 µL PBS and processed with either the XTT assay or CLSM for biofilm cell counts.

Quantitation of *Candida* biofilms was performed as described previously [98, 99] using both a biochemical assay, the 2,3-bis(2-methoxy-4-nitro-5-sulfophenyl)-5-[(phenylamino) carbonyl]-2H-tetrazolium hydroxide (XTT) reduction assay, and CFU measurements via confocal microscopy. XTT (Sigma Chemical Co., St. Louis, Mo.) is reduced by mitochondrial dehydrogenase into a water-soluble formazan product that is measured spectrophotometrically. Briefly, XTT (Amresco) was dissolved in PBS to a final concentration of 0.5 mg/mL and filter sterilized. Menadione (Spectrum, NJ) was dissolved in acetone to a final concentration of 10 mM. XTT and menadione aliquots were stored at -80°C for future use. Menadione solution was added to the XTT solution for a final concentration of 1 µM. 100 µL of XTT-menadione solution was added to the wells and the plates were wrapped in foil and incubated at 37°C for 3 hours. 80 µL of supernatant was added to a new 96 well plate and measured at 490 nm (TECAN Infinite® M200). The % viability was calculated using the following equation: % viability = 100*(A_{490} treated - A_{490} background)/(A_{490} untreated – A_{490} background).

To count biofilm cells from the antifungal susceptibility test, cells were removed from the 96 well plates by addition of 100 µL PBS and scraped with a pipette tip. A total of 3 technical replicates were collected and combined for one sample in a microcentrifuge

tube. Samples were vortexed vigorously and 10 μL of cell suspension was added to a coverslip and imaged. Images were taken using a Leica TCS SP5 (Leica, Germany) using a HCX Plan-Apo 40X/0.85 dry objective with 488 nm and 543 nm laser lines with 1.7X zoom. 10 images were taken per sample and cell counts from a total of 3 biological replicates were counted using Image J software [94].

2.4 Results

2.4.1 Increasing C. glabrata in a Candida co-culture on biofilm increases biofilm formation

We investigated the effect of varying the initial ratio of Ca and Cg on biofilm formation on glass surfaces. Figure 3 shows that the extent of biofilm formation after 48 h of culture was significantly impacted by the starting ratio of Ca to Cg at the three ratios tested (3:1, 1:1, and 1:3). Ca and Cg monocultures demonstrated comparable biofilm biomass formation on glass surfaces, as determined by crystal violet staining (Figure 3A). However, on polystyrene and acrylic surfaces, biofilm formation by Cg monocultures was lower than Ca monocultures (Figure 3B & Figure 4). Interestingly, while Cg monocultures showed lower biofilm formation compared with Ca on polystyrene surface, increasing the initial cell density of Cg in the mixed species biofilm led to an increase in total biofilm formation (see Figure 3B). A ratio of 1:3 (Ca:Cg) yielded the maximum biofilm growth and was significantly higher than that observed with both Ca monocultures and 3:1 and 1:1 initial ratio of Ca-Cg co-cultures. No additional increase in biofilm formation was observed when the ratio of Ca:Cg was increased to 1:5 and 1:10 (Figure 5).

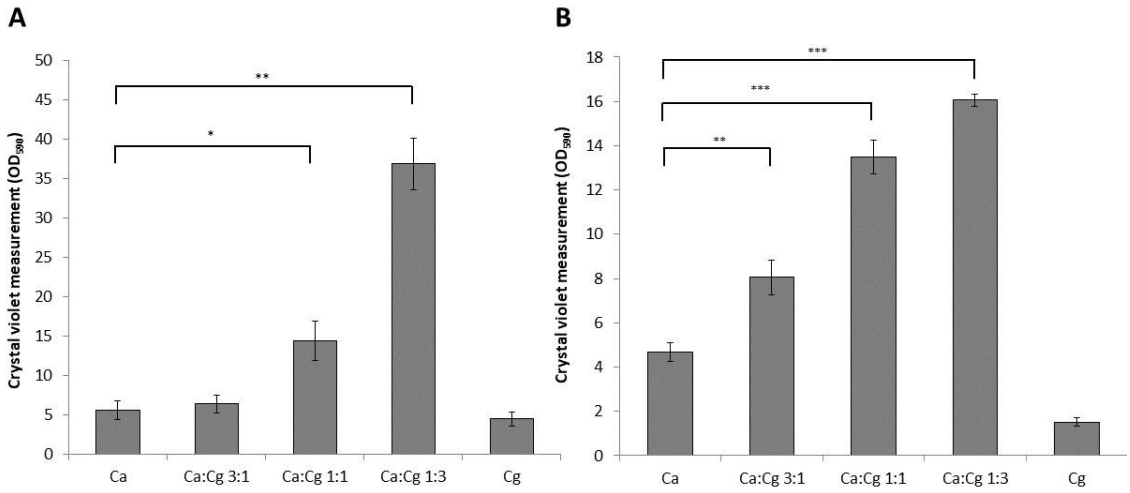

Figure 3. Effect of starting culture composition on *Candida* co-culture biofilm formation. Biofilms formed on glass coverslips (A) or polystyrene microtiter plates (B) for 48 hours. 4 biological replicates. Student's t-test, *:p-value < 0.05, **:p-value < 0.01, ***:p-value < 0.001 compared with *C. albicans* monoculture. Error bars are standard error of samples.

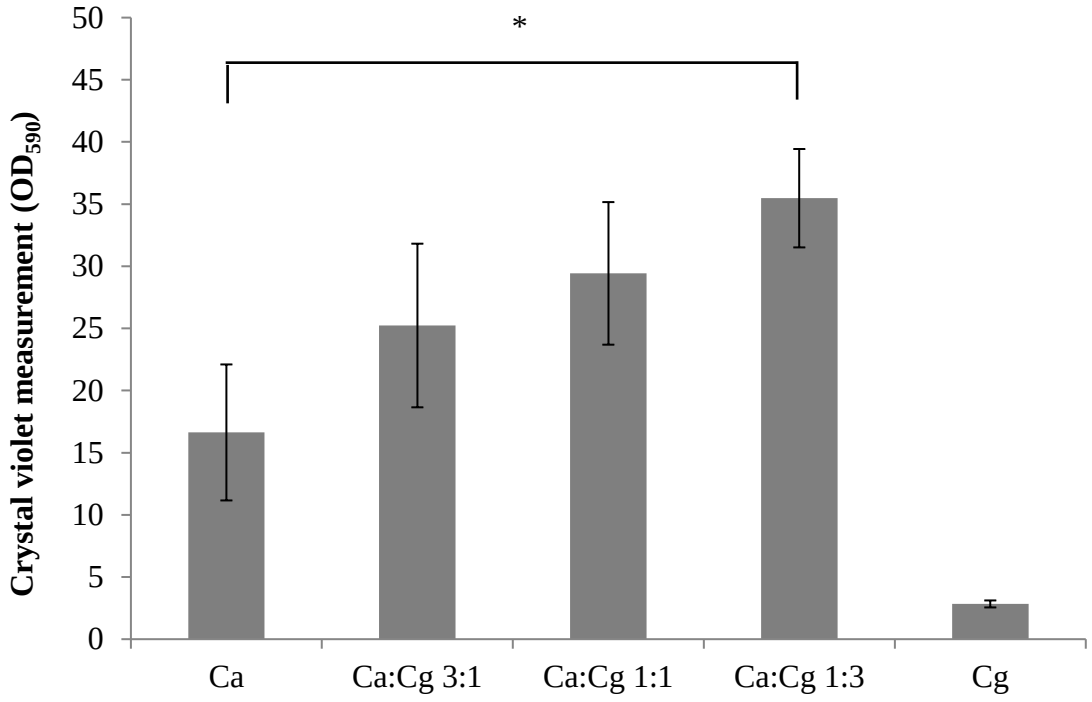

Figure 4. Biofilm formation on PMMA coverslips. 48 hours growth. Student's t-test, *: $p \leq 0.05$, compared to *C. albicans* monoculture. Error bars are standard error of 4 biological replicates.

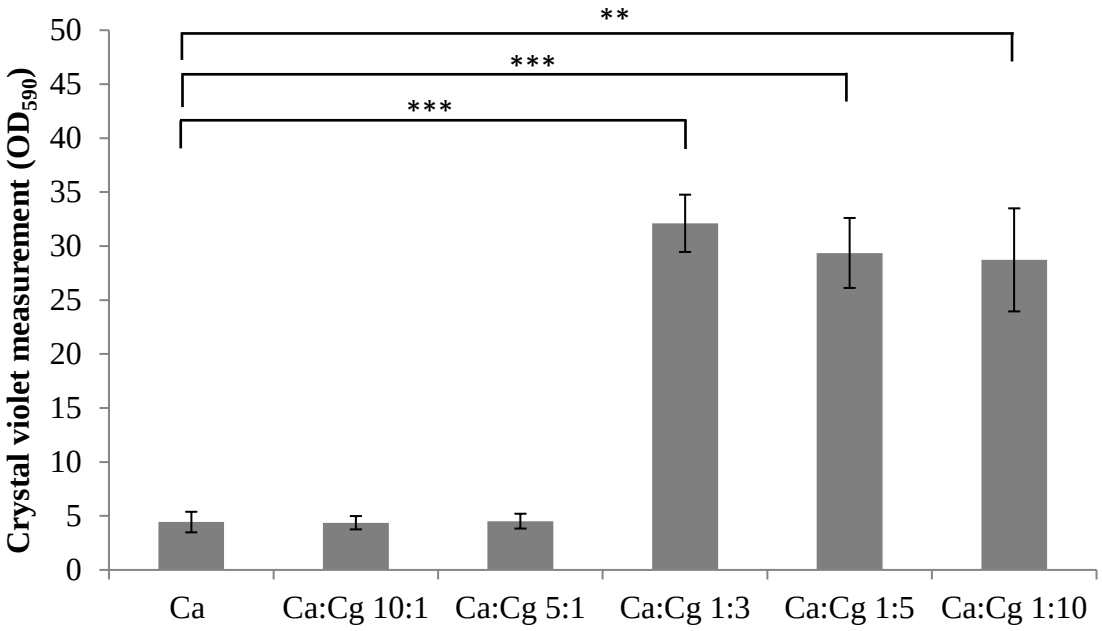

Figure 5. Biofilm formation on glass coverslips. 48 hours growth. Student's t-test, **: $p \leq 0.01$, ***: $p \leq 0.001$, compared to *C. albicans* monoculture. Error bars are standard error of 6 biological replicates.

We quantified the number of Ca and Cg cells in the co-culture biofilms to determine whether one species was more abundant in the biofilm. Our results showed that the ratio of Ca:Cg in mature biofilms after 48 hours remains approximately similar to the initial inoculum ratio (Figure 6), suggesting that one species does not have a significant fitness advantage over the other under the culture conditions that were used.

Since hyphae and biofilm formation in Ca increases in nutrient-limited conditions [100, 101], it may be possible that the increase in biofilm biomass observed in co-cultures is the result of nutrient competition in Ca:Cg co-cultures. As a control experiment, co-cultures of Ca and *Saccharomyces cerevisiae* (Sc) were used to mimic the nutrient

competition environment of co-cultures to ensure that the enhanced biofilm formation observed in Ca:Cg co-cultures are the result of potential interactions between Ca and Cg and not due to nutrient-limited conditions experienced by Ca in co-cultures. The data show that unlike the Ca:Cg co-cultures, biofilm formation with Ca:Sc 1:3 co-cultures was not greater than monocultures of Ca or Sc (Figure 7), suggesting that the enhanced biofilm formation observed in Ca:Cg co-cultures was not due to nutrient competition.

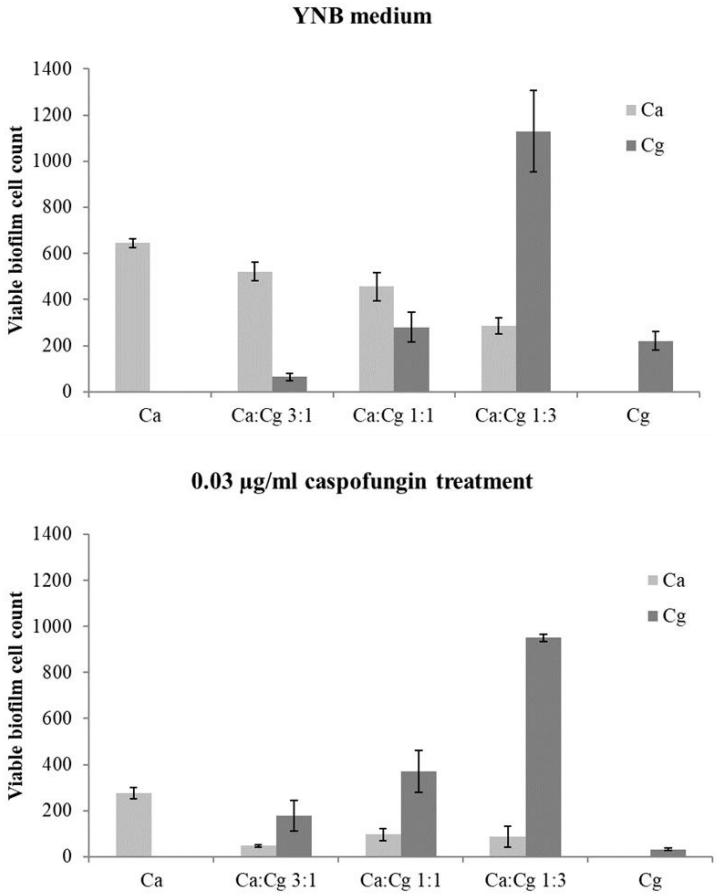

Figure 6. *Candida* co-culture biofilm cell counts before and after caspofungin treatment.

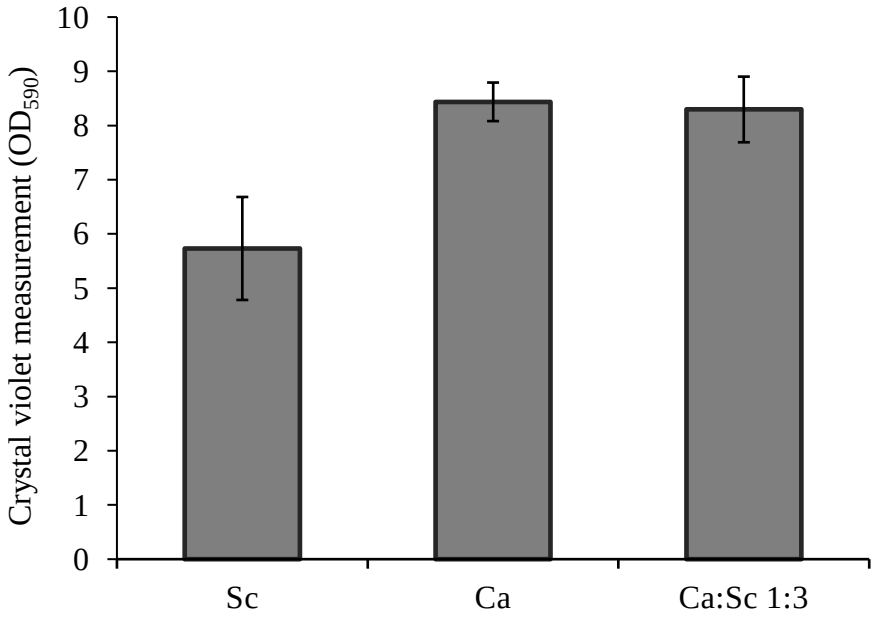

Figure 7. Biofilm formation in 96 well polystyrene plates after 48 hours growth. Error bars are standard error of 3 biological replicates.

2.4.2 Increased C. albicans hyphae and biofilm structural heterogeneity in Candida co-culture biofilms

The composition and structure of *Candida* co-culture biofilms were characterized using Confocal Laser Scanning Microscopy (CLSM). Biofilms were imaged after 6, 12, and 24 h upon initiation of co-culture to assess differences in biofilm composition and structure between varying initial Ca:Cg ratios. The biofilm images were used to reconstruct the 3D structures of mono- and co-culture biofilms. Image analysis revealed long Ca hyphae throughout the entire thickness of the Ca:Cg 1:3 co-culture biofilms and increased biofilm thickness compared to the other culture conditions during the early biofilm maturation phase after just 6 h of growth (Figure 8). Moreover, the thicknesses of

co-culture biofilms at Ca:Cg ratios of 1:1 and 1:3 were significantly higher than Ca monoculture biofilms at 6 h (p-value of 0.05 and 0.001 respectively) (Figure 8B). After 12 h, the co-culture biofilm thickness was comparable in all three Ca:Cg ratios, but still greater than Ca monoculture biofilms (Figure 8B). The reconstructed 3D biofilms also revealed extensive heterogeneity in the Ca:Cg 1:3 co-cultures, which differed from the other two ratios tested. In the Ca:Cg 1:3 biofilm, there was increased clustering of Ca hyphae and Cg yeast cells as well as variation in biofilm structure and thickness over the entire surface of the biofilm. Interestingly, the thickness of Ca:Cg 1:3 biofilms varied across the entire surface of the biofilm, revealing a more heterogeneous biofilm topology; whereas the thickness of Ca:Cg 3:1 and 1:1 biofilms were more uniform across the entire biofilm (Figure 9A, Figure 10, Figure 11). The length of *C. albicans* hyphae was estimated from the reconstructed 3D biofilms. At each time point, hyphae length increased significantly with increasing Cg concentration in the co-culture biofilm, with the Ca:Cg 1:3 biofilm exhibiting the longest hyphae at all three time points (Figure 9B).

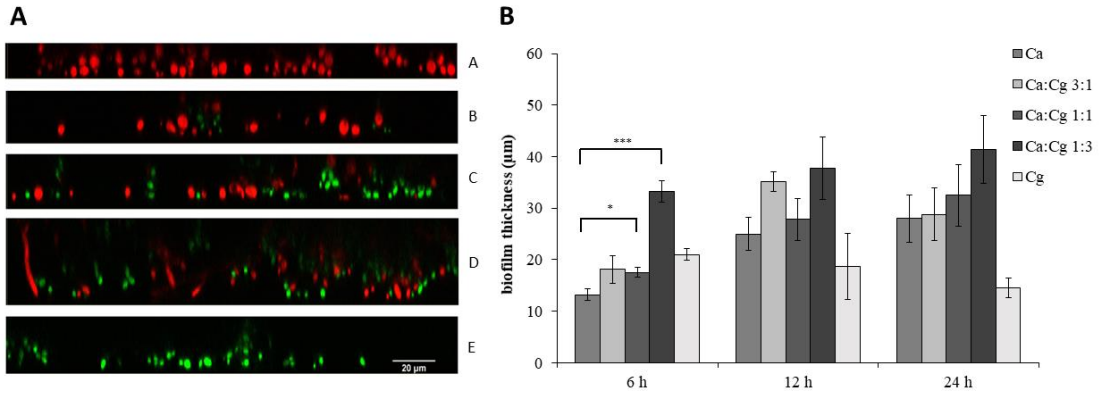

Figure 8. Confocal microscopy analysis of *Candida* co-culture biofilm thickness. (A) Representative 6-hour 3D *Candida* biofilm cross-sectional views. *C. albicans* = red, *C. glabrata* = green. A - Ca, B - Ca:Cg 3:1, C - Ca:Cg 1:1, D - Ca:Cg 1:3, E - Cg. (B) Biofilm thickness at 6, 12, 24 hours. Student's t-test, *:p-value < 0.05, ***:p-value < 0.001 compared with *C. albicans* monoculture. Error bars are standard error of 3 biological replicates.

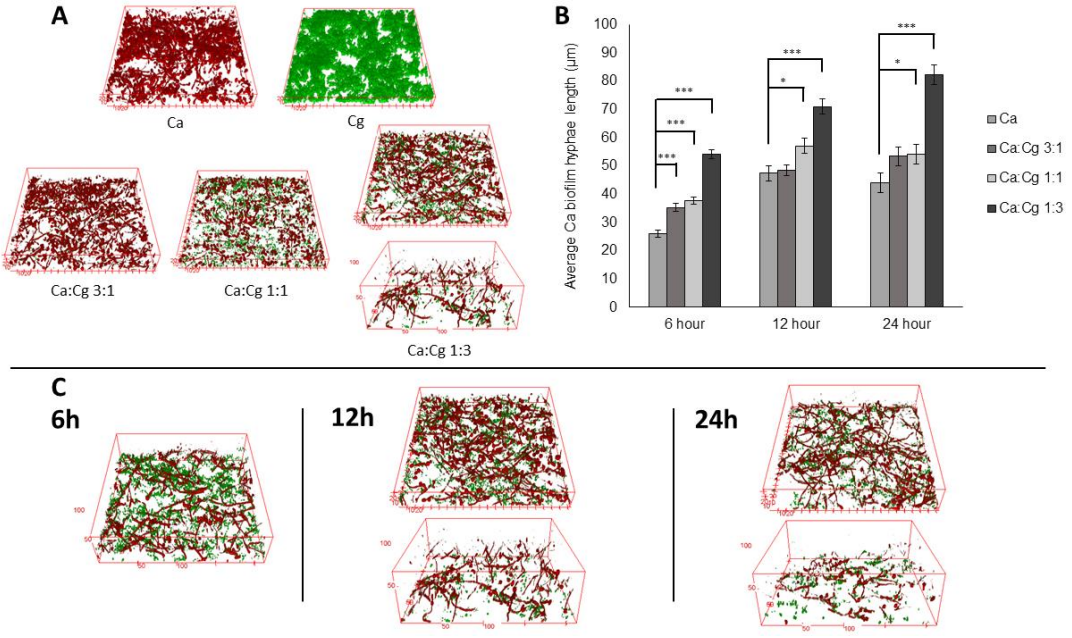

Figure 9. Effects of culture composition on biofilm structure. (A) Representative 12 hour 3D biofilm. Scale bar in microns. (B) Average *C. albicans* hyphae length in biofilms. (C) Representative 3D biofilm images of Ca:Cg 1:3 at 6, 12, and 24 hours. Scale bar in microns. Student's t-test, *:p-value < 0.05, **:p-value < 0.01, ***:p-value < 0.001 compared with *C. albicans* monoculture. Error bars are standard error of 3 biological replicates.

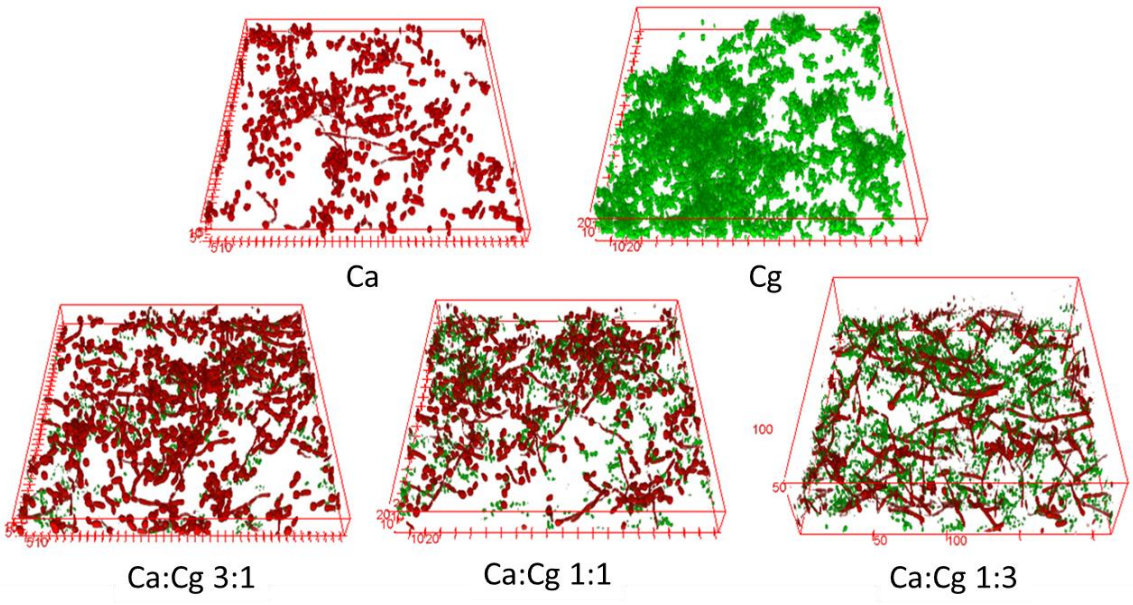

Figure 10. Representative 6 hour 3D *Candida* biofilms. Scale bar in microns.

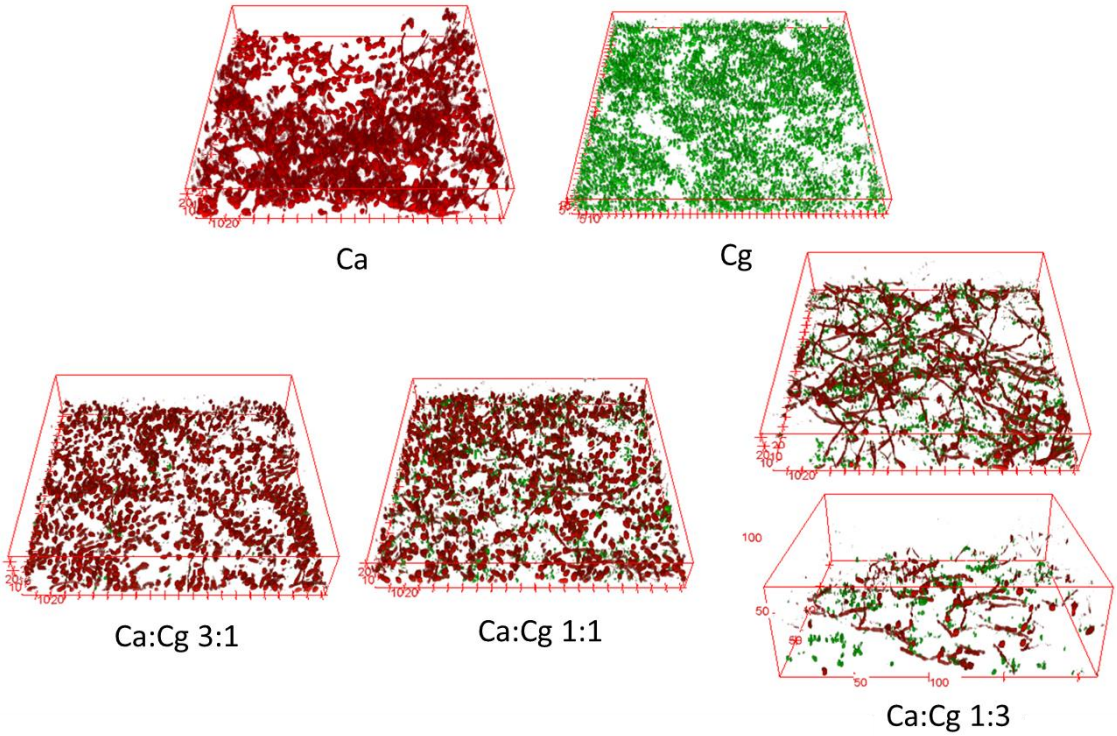

Figure 11. Representative 24 hour 3D *Candida* biofilms. Scale bar in microns.

Ca monoculture biofilms were thinner compared to co-culture biofilms and composed of both yeast and hyphae cells in a dense mat that were tightly interwoven as evident by the close clustering of red in the representative images (Figure 9A, Figure 10, Figure 11, Figure 12). Cg monoculture biofilms were composed of yeast cells but formed small clusters of cells that contributed to a thin biofilm layer (Figure 8A, Figure 10, Figure 11, Figure 12). However, co-culture biofilms with an initial Ca:Cg ratio of 1:3 demonstrated different characteristics. Two distinct features were observed – a dense, but not thick, region that was comprised of a mat of Ca hyphae and Cg cells, and a less dense, but thicker, region with long and elongated Ca hyphae that contributed to the increased

thickness and volume, with few Cg cells (Figure 9A,C). The denser regions of the Ca:Cg 1:3 biofilm were similar to those observed with Ca monoculture biofilms, or co-culture biofilms started with Ca:Cg at 1:1 and 3:1 (Figure 9A, Figure 10, Figure 11).

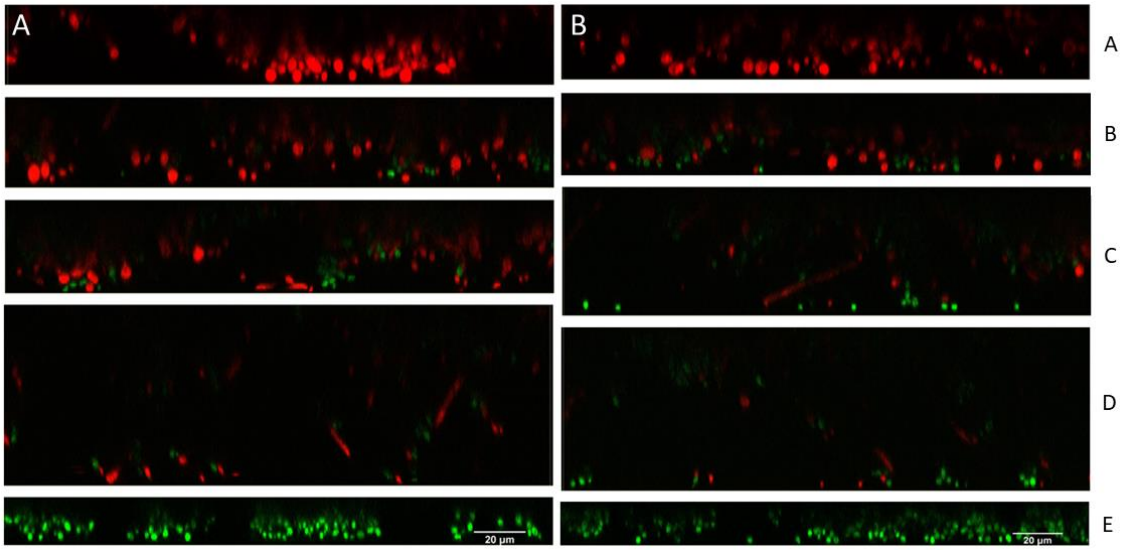

Figure 12. Representative cross-sectional views of *Candida* biofilms. (A) 12 hour (B) 24 hour. A - Ca, B - Ca:Cg 3:1, C - Ca:Cg 1:1, D - Ca:Cg 1:3, E - Cg. Scale bar = 20 µm.

In addition to increased thickness and Ca hyphae length in the *Candida* co-culture biofilms, the observed physical associations between Ca and Cg in the mixed species biofilm were quantified. Cg appears to preferentially attach to the hyphae of Ca (Figure 13A-C), which has previously been observed [12]. The clustering between the two *Candida* species was most abundant in the Ca:Cg 1:3 biofilm, where the percent of Cg

attached to Ca hyphae was significantly higher than Ca:Cg 3:1 at 12 and 24 h and Ca:Cg 1:1 ratio at 6 and 12 h (Figure 13D).

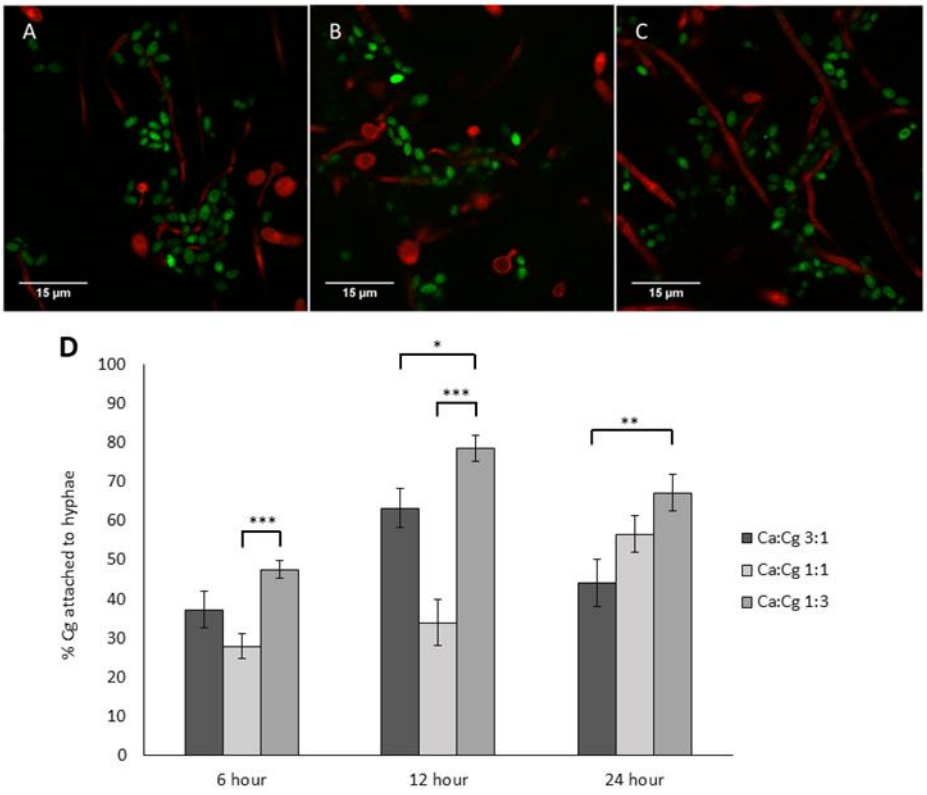

Figure 13. Physical association of *C. glabrata* with *C. albicans* hyphae in biofilms. (A): Ca:Cg 3:1, (B): Ca:Cg 1:1, (C): Ca:Cg 1:3, (D) percent *C. glabrata* attached to *C. albicans* hyphae in *Candida* co-culture biofilm. Student's t-test, *:p-value < 0.05, ***:p-value < 0.001 compared with *C. albicans* monoculture. Error bars are standard error of 3 biological replicates.

2.4.3 Gene expression analysis of adhesion genes in C. albicans biofilms

Quantitative real-time PCR was utilized to analyze gene expression at 6, 12, and 24 h in all Ca:Cg co-culture biofilms. For Ca, four adhesion and invasion associated genes

(*HWP1*, *ALS3*, *PLB5*, and *SAP9)* were chosen whereas two Cg adhesion genes (*EPA1* and *EPA6*) were chosen as representative Cg genes (see Materials and Methods). *HWP1*, *ALS3*, *PLB5*, and *SAP9* are all genes that contribute to Ca cell wall integrity and adhesion during biofilm formation. In Cg, *EPA1* and *EPA6* are known adhesion genes that have been demonstrated to be upregulated in biofilms [102]. All of these genes have been previously reported to be involved in biofilm formation and *Candida* virulence [30, 103-106]. The expression of *HWP1* increased with increasing Cg in the co-culture biofilm. The maximum increase in *HWP1* expression was observed at 12 h and was significantly different between Ca monoculture biofilms, or co-culture biofilms at 3:1 and 1:3 ratios (t-test, $p < 0.01$). At 24 h, *HWP1* gene expression in Ca:Cg 1:1 and Ca:Cg 1:3 was significantly higher compared to Ca monoculture biofilm (Table 2).

ALS3 gene expression increased as the ratio of Ca:Cg decreased and the maximum increase was again observed at 12 h. *ALS3* gene expression was significantly higher in Ca:Cg 3:1 biofilm at 24 h and in Ca:Cg 1:3 biofilm at 6 and 24 h compared to the Ca monoculture biofilm (t-test, $p < 0.05$) (Table 2). The expression of *PLB5* did not change significantly between Ca and the co-culture biofilms at all ratios at the three time points, whereas *SAP9* gene expression decreased at all time points in the co-culture biofilms compared to Ca monoculture (Table 3). The expression of Cg adhesion genes *EPA1* and *EPA6* was unchanged at all ratios and time points compared to Cg monoculture (Table 4).

Table 2. Relative *C. albicans* biofilm gene expression of *HWP1* and *ALS3*. Average gene expression level +/- standard error of 3 biological replicates with 3 technical replicates each. Statistical significance is with respect to Ca monoculture biofilm. Student's t-test, *:p-value < 0.05, **:p-value < 0.01.

		Gene expression level (relative to *ADH1*)		
Gene	Biofilm	6 hour	12 hour	24 hour
HWP1	Ca	0.352 ± 0.262	1.274 ± 0.280	0.151 ± 0.102
	Ca:Cg 3:1	0.357 ± 0.148	1.070 ± 0.330	0.465 ± 0.098
	Ca:Cg 1:1	0.680 ± 0.237	2.141 ± 0.822	0.621 ± 0.114 (*)
	Ca:Cg 1:3	0.774 ± 0.157	3.827 ± 0.369 (**)	0.829 ± 0.095 (**)
ALS3	Ca	0.095 ± 0.053	0.359 ± 0.103	0.052 ± 0.021
	Ca:Cg 3:1	0.146 ± 0.075	0.238 ± 0.065	0.157 ± 0.019 (*)
	Ca:Cg 1:1	0.257 ± 0.089	0.345 ± 0.088	0.177 ± 0.055
	Ca:Cg 1:3	0.337 ± 0.052 (*)	0.714 ± 0.084	0.163 ± 0.007 (*)

Table 3. Relative *C. albicans* biofilm gene expression of *PLB5* and *SAP9*. Average gene expression level +/- standard error of 3 biological replicates with 3 technical replicates each. Statistical significance is with respect to Ca monoculture biofilm. Student's t-test, *:p-value < 0.05, **:p-value < 0.01.

		Gene expression level (relative to *ADH1*)		
Gene	Biofilm	6 hour	12 hour	24 hour
PLB5	Ca	0.004 ± 0.000	0.007 ± 0.002	0.008 ± 0.004
	Ca:Cg 3:1	0.003 ± 0.000	0.005 ± 0.001	0.005 ± 0.002
	Ca:Cg 1:1	0.003 ± 0.000	0.006 ± 0.001	0.003 ± 0.001
	Ca:Cg 1:3	0.004 ± 0.000	0.012 ± 0.002	0.003 ± 0.000
SAP9	Ca	0.018 ± 0.000	0.585 ± 0.148	0.552 ± 0.199
	Ca:Cg 3:1	0.014 ± 0.001	0.214 ± 0.082	0.214 ± 0.093
	Ca:Cg 1:1	0.014 ± 0.001	0.113 ± 0.022	0.064 ± 0.020
	Ca:Cg 1:3	0.014 ± 0.002	0.083 ± 0.020	0.055 ± 0.006

Table 4. Relative *C. glabrata* biofilm gene expression. Average gene expression level +/- standard error of 3 biological replicates with 3 technical replicates each.

		Gene expression level (relative to *ADH1*)		
Gene	Biofilm	6 hour	12 hour	24 hour
EPA1	Cg	0.026 ± 0.005	0.032 ± 0.011	0.078 ± 0.023
	Ca:Cg 3:1	0.014 ± 0.004	0.040 ± 0.014	0.197 ± 0.063
	Ca:Cg 1:1	0.013 ± 0.003	0.049 ± 0.008	0.256 ± 0.098
	Ca:Cg 1:3	0.011 ± 0.002	0.048 ± 0.015	0.192 ± 0.074
EPA6	Cg	0.442 ± 0.201	0.407 ± 0.211	0.256 ± 0.149
	Ca:Cg 3:1	0.635 ± 0.268	0.676 ± 0.447	0.380 ± 0.234
	Ca:Cg 1:1	0.510 ± 0.175	0.980 ± 0.656	0.402 ± 0.266
	Ca:Cg 1:3	0.430 ± 0.243	0.360 ± 0.193	0.346 ± 0.162

2.4.4 Candida co-culture biofilms demonstrate increased anti-fungal resistance

As biofilms are known to increase antimicrobial drug resistance [16, 88, 107], the increased biofilm thickness and structural complexity of Ca:Cg co-cultures can potentially result in enhanced antifungal drug resistance. Therefore, the impact of Ca:Cg ratio on the susceptibility of Ca and Cg biofilm cultures to caspofungin was tested. The MIC_{50} for planktonic culture of Cg and mixed Ca:Cg 1:1 was measured to be 0.0156 µg/mL which was double that of Ca monoculture (0.0078 µg/mL) and MIC_{90} was 0.0312 µg/mL for all conditions. The MIC_{50} and MIC_{90} of planktonic *Candida* cultures were lower than that observed in biofilms (Table 5).

Table 5. *Candida* biofilm cell viability after caspofungin treatment.

Condition	MIC_{50} (µg/ml)		MIC_{90} (µg/ml)	
Biofilm (24 h biofilm, 24 h caspofungin treatment) *(n=6)*	Ca	0.0234	Ca	0.0468
	Cg	0.0312	Cg	0.125
	Ca:Cg 3:1	0.0234	Ca:Cg 3:1	0.125
	Ca:Cg 1:1	0.0312	Ca:Cg 1:1	0.125
	Ca:Cg 1:3	0.0312	Ca:Cg 1:3	0.250

Due to differences in metabolism of XTT between *Candida* species, CLSM was utilized for cell enumeration and to quantify cell viability of caspofungin-treated biofilms. A caspofungin concentration of 0.03 µg/mL was chosen to analyze cell viability based on unpublished data from our laboratory showing that the MIC_{50} using the XTT assay was 0.03 µg/mL for Ca, Cg, and co-culture biofilms (Table 5). After caspofungin treatment, Cg monoculture biofilm had a viability of 14% ± 2.5% and Ca monoculture biofilm was 43% ± 4.4% viable compared to untreated control biofilms (Figure 14). In co-culture biofilm, total cell viability increased with increasing Cg in the biofilm. The Ca:Cg 1:3 biofilm had a cell viability of 75% ± 8.4%, which was significantly higher than the Ca:Cg 3:1 and Ca:Cg 1:1 biofilms which exhibited a viability of 37% ± 8.2% and 62% ± 5.7%, respectively (Figure 14). When considering the individual species viability in co-culture biofilms, Ca was more susceptible to caspofungin than Cg. In the mixed species biofilm, Cg continues to grow even after the addition of caspofungin.

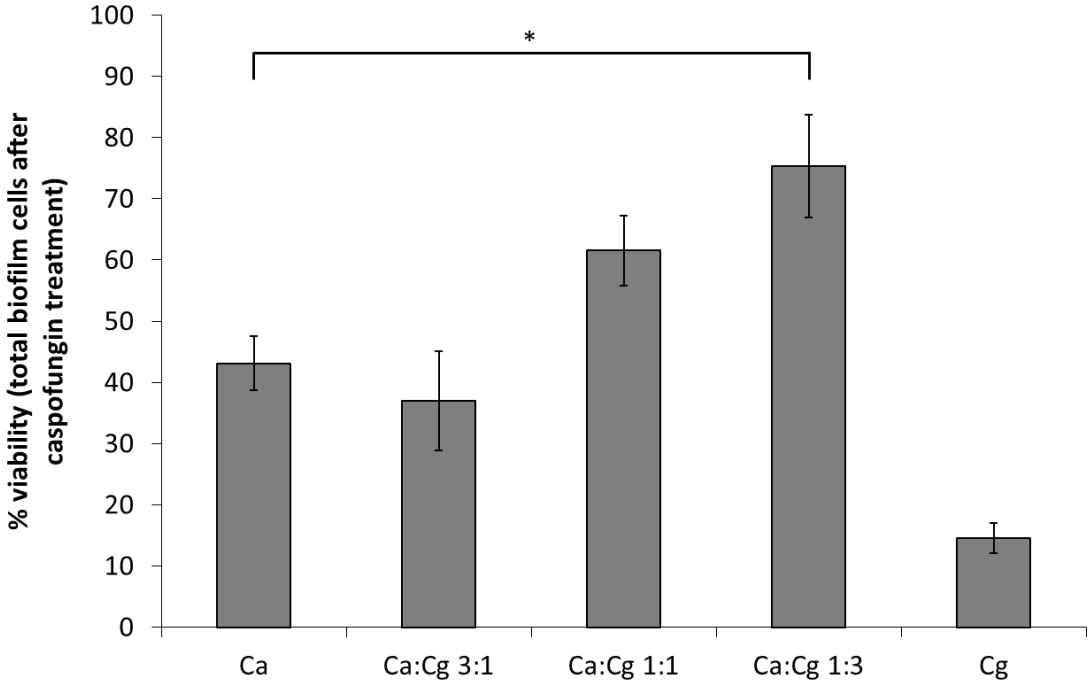

Figure 14. *Candida* biofilm viability after caspofungin treatment. Student's t-test, *: $p \leq 0.05$, compared to *C. albicans* monoculture. Error bars are standard error of 3 biological replicates.

2.5 Discussion

Recent microbiome studies have started to shed light on how composition of bacterial and fungal species can potentially correlate with health and disease [91, 108-110]. *Candida*, being a commensal fungal microorganism and opportunistic pathogen [1], is involved in this paradigm of health and disease. As *Candida* species exhibit variable susceptibility to antifungal treatments, changing prevalence of *Candida* spp. in candidiasis and candidemia on an epidemiological level [111-113] and changing colonization of fungal species over time at the single patient level have been observed [111, 114, 115],

suggesting changes in the mycobiome during the course of disease and treatment. *Candida* biofilms pose a high risk to human health, as high rates of infection and mortality are correlated with biofilm formation due to enhanced resistance to antimicrobials [116]. Clinical studies show that Ca and Cg are often co-isolated in infections [34, 111, 117], and the degree of infection is worsened by the presence of both species [84, 118]. While the clinical importance of *Candida* spp. in biofilms is evident, the interactions between Ca and Cg, in terms of their relative abundance and on the development of *Candida* biofilms, is poorly understood. In this work, we investigated the impact of varying the relative starting ratios of Ca and Cg in co-culture biofilms on biofilm formation and resistance to antifungal treatment. Our results clearly demonstrate that the relative abundance of each species has a significant impact on biofilm formation as biofilm increased with increased levels of Cg. This observation is especially interesting as we and others [23, 45, 119, 120] have shown that Cg in monocultures forms a weaker biofilm compared with Ca. The fact that this density-dependent effect was observed with biofilms grown on different surfaces (glass, polystyrene, and acrylic) suggests that this behavior is independent of the surface characteristics.

Analysis of biofilms using CLSM revealed that the ratio of Ca:Cg remained relatively constant at the levels in which they were seeded over the duration of the experiment. This suggests that one species did not have a nutritional or metabolic advantage to outgrow the other in the biofilm (Figure 6). Cataldi et al. [37] demonstrated that a complex biofilm structure (biofilm composed of blastospores, pseudohyphae, and hyphae cells) increased biofilm cell surface area, which can increase adhesion to host cell

surfaces and pathogenesis. Recently, Alonso et al. demonstrated that macrophage migration towards Ca, a mechanism for clearing infection and pathogens in the human body, is reduced two-fold when cells are in a biofilm, which was attributed to increased biofilm thickness and structure (extracellular matrix encasement of yeast and hyphal cells [121]), rather than the composition of the biofilm matrix [122]. In this work, we also observed increased structural complexity and heterogeneity in co-culture *Candida* biofilms compared to monoculture biofilms where the highest biofilm heterogeneity was seen in the Ca:Cg 1:3 biofilm. The increase in structural complexity was evident from the increase in Ca hyphae formation and uneven thickness across the biofilm, which resulted in a larger network of cells and more complex 3D structure (Figure 8, Figure 9, Figure 10, Figure 11, Figure 12).

Because of the increase in hyphae and uneven topology, overall biofilm thickness was not an appropriate metric for quantifying co-culture *Candida* biofilms. Instead, 3D biofilm reconstructed images were used for biofilm data interpretation. For example, the increase in hyphae length observed with the 1:3 Ca:Cg biofilms suggests that the Ca:Cg 1:3 biofilm is potentially more virulent than 1:1 or 3:1 ratio biofilms, as an increase in hyphae length is often associated with increased Ca virulence [123]. We observed that a majority of Ca yeast cells were on the bottom of the biofilm with hyphal cells growing upward (Figure 8 & Figure 12), which is similar to the observations reported by Kuhn et al. with monoculture Ca biofilms [124]. In our observations of Ca:Cg co-culture biofilms, Cg was evenly dispersed throughout the biofilm and aggregates formed around Ca hyphae (Figure 9C & Figure 13). While clustering of Cg around Ca hyphae was seen in all three

Ca:Cg ratios (Figure 13A-C), maximum clustering was observed in the Ca:Cg 1:3 biofilm. This observation is consistent with the longer hyphae that were observed in this co-culture condition (Figure 9B).

Previous studies have shown that several Ca genes (*e.g. HWP1, ALS3*) and Cg genes (*e.g. EPA1, EPA6*) are involved in increased adhesion and biofilm formation *in vitro* and *in vivo* [103, 105, 106]. In this study, both *HWP1* and *ALS3* gene expression increased in the co-culture biofilms compared to a Ca monoculture biofilm, and the highest fold-induction was observed with starting ratio of Ca:Cg 1:3 (Table 2). The increase in *HWP1* gene expression for the Ca:Cg 1:3 biofilm is consistent with the increased hyphae length seen in the biofilms (Figure 9B), as *HWP1* (Hyphal Wall Protein 1) is a Ca hyphal-associated gene involved in adhesion and invasion [125, 126]. *ALS3* gene expression was highest in Ca:Cg 1:3 co-culture biofilms compared to Ca monoculture biofilms at 6 and 24 h indicating that Als3 may be needed for the initial forming of *Candida* co-culture biofilms (at 6 h) and also maintenance of mature biofilm structure (at 24 h). Early activation of *ALS3* gene expression in *C. albicans* biofilms has previously been demonstrated by Nailis et al., where *ALS3* gene expression increases within 6 hours compared to planktonic cells and then is downregulated after 48 hours [127]. Increased expression of Ca cell wall adhesins *HWP1* and *ALS3* also suggest an increase in attachment of cells within the biofilm, which allows for more robust biofilm formation compared to biofilms with lower adhesin expression. Moreover, increased hyphae in Ca and increased *HWP1* expression is associated with increased yeast-hyphae cell interactions in the biofilm which contributes to increased structural complexity of cells

within the biofilm matrix (Figure 13D), and *ALS3* has been demonstrated to facilitate the binding of Cg to Ca in a biofilm further leading to biofilm robustness and thickness in co-culture [12]. Expression of *HWP1* and *ALS3* are also activated earlier on in the Ca:Cg 1:3 biofilm compared to Ca monoculture, indicating an earlier initiation of biofilm formation which possibly contributes to the higher biomass seen over time in the 1:3 ratio.

We observed an increase in the expression of the Cg adhesion gene *EPA1* at 24 hours in co-culture biofilms. Recently, Tati et al. demonstrated that several *EPA* adhesions genes (*EPA8* and *EPA19)* are upregulated in mixed species cultures of Ca and Cg [12]. While no significant change in the expression of *EPA1* or *EPA6* was observed between co-culture and monoculture biofilms (Table 4), it should be noted that *EPA1* has been primarily reported to be involved in adhesion to host tissue [106], and the lack of observed gene expression change in *EPA1* and *EPA6* could also be the result of sub-telomeric silencing [128-130].

In concordance with the biofilm data, Ca:Cg 1:3 co-culture biofilms exhibited the highest resistance to caspofungin treatment (Figure 14). Cataldi et al. [37] has reported that a non-uniform biofilm increases susceptibility to antifungal drugs due to a lower biofilm cell-matrix density and discontinuous cell embedding in the extracellular matrix, which could explain the increased resistance to caspofungin with the Ca:Cg 1:3 biofilm. Interestingly, while Ca monoculture biofilms were more susceptible to caspofungin, Cg biofilms cells in co-culture grew in the presence of 0.03 μg/mL caspofungin (Figure 6). It is unclear why Cg cell viability increases in co-culture biofilms in the presence of caspofungin and if this phenomenon is observed for other antifungal drugs as well.

Our study presents multiple lines of evidence to demonstrate that the initial relative cell densities of a Ca and Cg in a co-culture biofilm strongly influences the extent of biofilm formation as well as its structural complexity. The increased hyphae length in the Ca:Cg 1:3 biofilm contributes to a more complex biofilm structure, which increases the thickness and antifungal resistance of the biofilm. Additionally, increased hyphae also provides more hyphal surface area for Cg yeast cells to attach and cluster in the biofilm. These observations suggest that the changing *Candida* polymicrobial culture dynamics during biofilm formation may alter the course of the infection. Ongoing work in our laboratory focuses on investigating the transcriptomic changes in co-culture biofilms and identifying the molecular basis underlying *Candida* interspecies interactions.

3. TRANSCRIPTOMIC ANALYSIS OF CANDIDA CO-CULTURE BIOFILMS

3.1 Summary

Candida spp. are commensal opportunistic fungal pathogens that often colonize and infect mucosal surfaces of the human body. *Candida*, along with other microbes in the microbiota, generally grow as biofilms in a polymicrobial environment. Due to the nature of cellular growth in a biofilm (such as production of a protective extracellular matrix) and the recalcitrance of biofilms, infections involving biofilms are very difficult to treat with antibiotics and perpetuate the cycle of infection. The two most commonly isolated *Candida* spp. from *Candida* infections are *Candida albicans* and *Candida glabrata*, and the presence of both of these species results in increased patient inflammation and overall biofilm formation. This work aims to investigate the interspecies interactions between *C. albicans* (Ca) and *C. glabrata* (Cg) in co-culture through transcriptome analysis over the course of biofilm growth. We report that during co-culture, lipid biosynthesis and transporter genes were significantly modulated in both Ca and Cg. Differentially expressed genes in Ca during co-culture growth included putative transporter genes (C2_02180W_A and C1_09210C_B; up-regulated), amino acid biosynthesis (Ca*ARO7*; up-regulated most in Ca:Cg 1:3), and lipid-related genes (Ca*LIP3* and Ca*IPT1*; down-regulated). Differentially expressed genes in Cg in co-culture included putative transmembrane transporters (CAGL0H03399g and CAGL0K04609g; up-regulated), an oxidative stress response gene (CAGL0E04114g; down-regulated most in Ca:Cg 1:3), genes involved in the TCA cycle (Cg*LYS12* and CAGL0J06402g; down-

regulated), and several genes involved in cell wall/membrane biosynthesis (Cg*SEC53*, Cg*GAS2*, Cg*VIG9*; down-regulated). Additionally, confocal microscopy was utilized for cell membrane lipid analysis between mono-culture and co-culture biofilms. Through filipin-stained lipid analysis, we found that there was a significant increase in cell membrane lipid content in Ca:Cg 1:3 biofilms compared to Ca mono-culture biofilms. These results suggest significant modifications of both cell wall, cell membrane, and transporters in both Ca and Cg during the time course of co-culture growth, which allows for increased biofilm formation and virulence in Candida co-culture biofilms.

3.2 Introduction

Candida spp. are commensal opportunistic fungal pathogens in the human body and often reside on skin or mucosal surfaces [74, 131]. It was recently described by Auchtung et al. [132] that *C. albicans* is a more transient member in the GI tract than once believed and that the fungi will thrive only in the gut of certain individuals. However, if a patient has inflammation, is immunocompromised, or has a compromised gut microbiota, *Candida* spp. may become virulent and invade host tissue leading to an infection [5, 6]. These infections mainly occur on mucosal surfaces, which are colonized and inhabited by many types of bacterial and fungal species [75, 133, 134]. Within these polymicrobial niches, certain communities exhibit antagonistic (oral – *C. albicans* and *Pichia* [135], vaginal – *C. albicans* and *Lactobacillus* [136]) or synergistic interactions (oral – *C. albicans* and *Streptococcus mutans* [109], GI tract – *C. albicans* and *C. parapsilosis* [137, 138]). During the course of a *Candida* infection (*i.e.* candidiasis), *C. albicans* (Ca) and *C.*

glabrata (Cg) are often co-isolated [83]. Coco et al. reported that patients with the combination of these two *Candida* species exhibit a higher level of inflammation at the site of infection [84]. Additionally, *in vitro* experiments show that co-culture of *C. albicans* and *C. glabrata* produces higher biofilm formation over mono-culture biofilms alone [23, 24, 139]. Additionally, our lab has recently demonstrated that the relative abundance of Ca and Cg in co-cultures impacts overall biofilm formation; and increased co-culture *Candida* biofilm formation is associated with increased antifungal resistance and virulence gene expression [139]. In the highest biofilm former with initial culture Ca:Cg ratio of 1:3, there was increased Ca hyphae, increased Cg attachment to Ca hyphae, and increased expression of Ca virulence genes over time [139]. Thus, it is important to elucidate the interspecies interactions between Ca and Cg in a biofilm to improve therapeutic strategies for treating fungal infections throughout different areas of the human body.

The survival of *C. albicans* and *C. glabrata* in different host niches and its potential to cause disease relies largely on its ability to alter its transcriptome in response to different environmental stimuli and stresses [140, 141]. In *C. albicans*, a complex transcriptional circuitry exists for the regulation of yeast to hyphae morphogenesis (an important virulence factor) in response to certain stimuli [142]. Changes in the transcriptional network also allows *C. albicans* to grow in a variety of environments with a range of pH and stresses from the immune system [143-145]. Furthermore, it was demonstrated by Rajendran et al. [146] that amino acid metabolism in *C. albicans* is up-regulated in high biofilm forming conditions and shown by Lattif et al. [147] that *C. albicans* biofilm cells

have a higher content of phospholipids and sphingolipids than planktonic cultures. On the other hand, little is currently known about the transcriptional dynamics during growth and biofilm formation in *C. glabrata*. Since *C. glabrata* is inherently difficult to treat with certain antifungal drugs (*i.e.* azole drugs [148]), studies have focused on investigating the genes involved in Cg drug resistance. It was recently reported by Rodrigues et al. that several genes involved in beta-1,3-glucans and mannans biosynthesis (identified via RT-qPCR) were an essential component of Cg biofilm growth and play an important role in antifungal drug resistance in biofilms [149]. Additionally, Linde et al. looked at transcriptional regulatory differences between Ca and Cg under nutrient-rich medium, nitrosative stress, and pH shifts using RNA-seq analysis [141], and found that iron homeostasis was altered in Cg in response to pH changes, whereas Ca exhibited less of a response. For adaptation to nitrosative stress, 'RNA polymerase III activity' (which has global impacts on gene expression) and 'oxidation-reduction process' (which signifies the cells are encountering and responding to stress) were significantly enriched in Cg, but not in Ca, suggesting different patterns of adaptation to pH shift and stress between *C. glabrata* and *C. albicans* [141].

While several studies have explored transcriptome dynamics in mono-cultures of Ca or Cg, few studies have focused on Ca and Cg co-culture biofilms. One report demonstrated that several genes involved in *C. albicans* adhesion (i.e. Ca*ALS3*, Ca*HWP1*) were down-regulated in co-cultures with *C. glabrata* [30]; however, our lab recently reported an increase in gene expression of Ca adhesion genes Ca*ALS3* and Ca*HWP1* during Ca:Cg co-culture biofilm formation over 24 hours [139]. The differences in gene

expression results may be due to varied approaches in culturing *Candida* biofilms. Furthermore, work by Tati et al. showed that CaAls1 and CaAls3 adhesins are needed for Cg virulence in co-culture [12]. Overall, studies have demonstrated that there is transcriptome modulation in both Ca and Cg during co-culture biofilm growth. Here we investigate the transcriptome profiles of *C. albicans* and *C. glabrata* co-culture biofilms as a function of Ca:Cg ratios and explore any temporal shifts in gene expression in mono- and co-culture biofilms. The result shows significant changes in transcriptional regulation in both Ca and Cg over time during biofilm development and specifically in co-cultures that leads to increased overall biofilm formation and potentially virulence. Interestingly, the results showed substantially more genes to be differentially expressed in *C. glabrata* compared to *C. albicans* in co-cultures. During co-culture growth, several transporters and genes responsible for lipid biosynthesis were perturbed in *C. albicans*. In *C. glabrata*, genes involved in amino acid and lipid membrane biosynthesis were significantly modulated in co-culture biofilms. Additionally, we found that through filipin-stained cell membrane lipids, there was a significant increase in membrane lipids in Ca:Cg 1:3 compared to both Ca mono-culture and Ca:Cg 3:1 co-culture biofilm. Increased lipid content in Ca:Cg 1:3 suggests that lipid biosynthesis is indeed modulated in co-culture, as found from transcriptomic analysis, and biosynthesis is most significantly altered in the highest biofilm former Ca:Cg 1:3. This work elucidates physiological and metabolic shifts as a result of interspecies interactions between *C. albicans* and *C. glabrata* during co-culture biofilm growth via transcriptome analysis, and reveals potential adaptations of

Candida spp. during *in vitro* co-culture biofilm formation that may lead to an overall increase in virulence.

3.3 Materials and Methods

3.3.1 Microorganisms and growth conditions

C. albicans (SC5314, J. Berman, ENO1-RFP::Nat1) (58) and *C. glabrata* (ATCC 2001, GFP-labeled) were used in this study. Prior to the experiments, strains were cultured on Yeast Peptone Dextrose (YPD) agar plates for 48 hours at 30°C. For all experiments, single colonies were isolated from YPD agar plates and inoculated into 25 mL YNB medium (50 mM glucose and pH 7, Amresco). Cultures were grown overnight at 30°C and 170 rpm for 12 hours prior to experiments.

3.3.2 Biofilm quantification assay

Biofilms were grown in 96-well polystyrene plates (Corning®). 96-well plates were incubated in heat-inactivated fetal bovine serum (HI FBS) overnight at 37°C. Overnight cultures were washed twice with PBS and resuspended in fresh YNB medium. A hemocytometer was used to estimate cell density, and cell cultures were diluted to a final concentration of 10^7 cells/mL. A final volume of 100 µL was added to the 96-well plates. Wells with media only were used as controls. Biofilms were allowed to grow at 37°C for 48 hours without agitation. After 48 hours, wells were washed twice with 200 µL PBS. Then 200 µL of 99% methanol was added to each well and after 15 minutes, excess methanol was removed from the wells and biofilms were allowed to dry completely. Once dry, 200 µL of 0.1% crystal violet was added to each biofilm and

incubated at room temperature for 20 minutes [93]. Plates were rinsed gently under DI water to remove excess crystal violet stain from the wells and biofilms. Excess water was removed from the well and 150 μL of 33% acetic acid was added to each well. Acetic acid samples were diluted 10-fold in a clear walled clear bottom 96-well Corning® plate and absorbance was measured at 590 nm in a plate reader (Molecular Devices SpectraMax® 340PC).

3.3.3 Filipin Staining and Confocal Laser Scanning Microscopy

For CLSM biofilm-derived cell analysis, biofilms were grown in 96-well microtiter polystyrene plates (Corning®) that were pre-incubated overnight with HI FBS at 37°C. Cultures of *C. albicans* and *C. glabrata* were grown overnight in YNB medium. Cultures were washed twice in PBS and adjusted to a cell density of ~10^7 cells/mL. A final volume of 100 μl was used per well. Biofilms were allowed to grow for 24 hours at 37°C and no agitation. After 24 hours growth, biofilms were washed gently with PBS, and 100 μL of PBS was added per well to scrape and remove attached biofilm cells. Biofilm cells were centrifuged in a microcentrifuge tube and resuspended in 50 μg/ml filipin complex (Sigma-Aldrich) solution in PBS. Samples were incubated at room temperature for 20 minutes. To make the filipin complex solution, filipin was prepared in DMSO to a concentration of 5 mg/mL and aliquots were stored in rubber-sealed vials at -20C with only one freeze thaw. Prior to imaging for filipin staining, cells were washed once with PBS, and mounted on a glass coverslip and imaged using a Leica SP8 (Leica, USA) using the Leica HC PL APO CS2 63x/1.2 water objective (zoom = 3) with 405, 488 nm and 561 nm laser lines. 3 biological replicates were imaged and 10 images were taken per biofilm

sample. Comstat2 was used to quantify the surface area of filipin staining per image [95, 96]. Automatic thresholding was used in Comstat2 and filipin surface area quantification (μm^2) for *C. albicans*-RFP only cells in co-culture biofilms was calculated by subtracting the GFP-associated filipin surface area from raw images prior to Comstat2 analysis. For biofilm images without filipin dye, images were taken in the chambered coverglass slides (2 mL biofilm volume, previously fixed with 4% paraformaldehyde, 1 hour in the dark at room temperature) and acquired with a Zeiss LSM 780 NLO Multiphoton microscope (Zeiss, USA) using the Plan-Apo 40X/1.4 oil DIC M27 objective with 488 nm and 543 nm laser lines to image GFP and RFP simultaneously. To analyze the structure of the biofilms, a series of optical sections were taken throughout the chamber slides at 1 μm intervals throughout the depth of the biofilm. 3 biological replicates were imaged and 3 images were taken per biofilm sample and used in ImageJ analysis [94].

3.3.4 RNA extraction

Biofilms were grown for 6, 12, and 24 hours as described in "Biofilm quantification assay," except on glass coverslips (pre-incubated in HI FBS) in 6-well tissue culture plates. Biofilms were washed off of the coverslip with pre-chilled sterile MilliQ water and cells were collected by centrifugation (2000 x g, 5 minutes, 4 °C). Supernatant was removed and cell pellets were flash-frozen in liquid nitrogen prior to lyophilization for 24 hours. Acid-washed glass beads (Sigma-Aldrich) were added to the dried cell pellets and disrupted in the Disruptor Genie for 2 minute cycles for up to 10 minutes. Lysis buffer from the GE Illustra RNAspin Mini kit was added to the disrupted cell powder and RNA was extracted using the kit protocol with on-column DNase I

treatment. RNA quality and concentration were determined using a Nanodrop® and Qubit™, respectively.

3.3.5 RNA-sequencing and analysis

RNA-sequencing was done through the Texas A&M AgriLife Research center. RNA libraries were constructed using TruSeqRNA kit and processed (125SE) on an Illumina® HiSeq 2500v4 High Output instrument. RNA-sequencing analysis was done using the Galaxy interface [150] through the Texas A&M High Performance Research Computing Center. In Galaxy, raw reads were trimmed of adapter sequences using Trimmomatic and mapped to the reference genome using Tophat2 [151, 152]. In Trimmomatic, TruSeq3 adapter sequences were used and selected operations were MINLEN (20), LEADING (3), TRAILING (3). MINLEN drops reads below a specified length (in this case 20 bp), and LEADING/TRAILING cuts off bases from the start/end of the read if the quality is below a certain threshold (set to default of 3). In Tophat2, intron length was set to 10 – 1500 bp as previously described and all other parameters were set to default [140]. Average sequencing depth for *C. albicans* genome was 95 and 126 for the *C. glabrata* genome, which indicates how many times each base in the genome was sequenced on average. Coverage rate equation used: Coverage = (read length)*(number of reads)/(size of haploid genome). “Number of reads” used in the equation were taken from the average mapped reads over all time points of monoculture biofilm to reference genome. The percent of mapped reads for *C. albicans* was 83% and 84% for *C. glabrata*. Percent mapped reads was calculated from the average of monoculture mapped reads over 6, 12, and 24 hour time points. After mapping, HTseq-counts was used to count how many reads mapped to

each feature of the genome using the aligned sequencing reads and a list of genomic features as the input [153]. The Bioconductor DEseq2 package [154] was used to analyze HTseq-count data for differentially expressed genes, and Candida Genome Database GO Term Finder was used for statistically significant Gene Ontology analysis and GO Slim Mapper was used for broad categorization of terms [155]. Data analysis schematic represented in Figure 15. A p-adjusted value was calculated by taking all conditions (biofilm condition and time points) into account for use of comparisons within and between conditions.

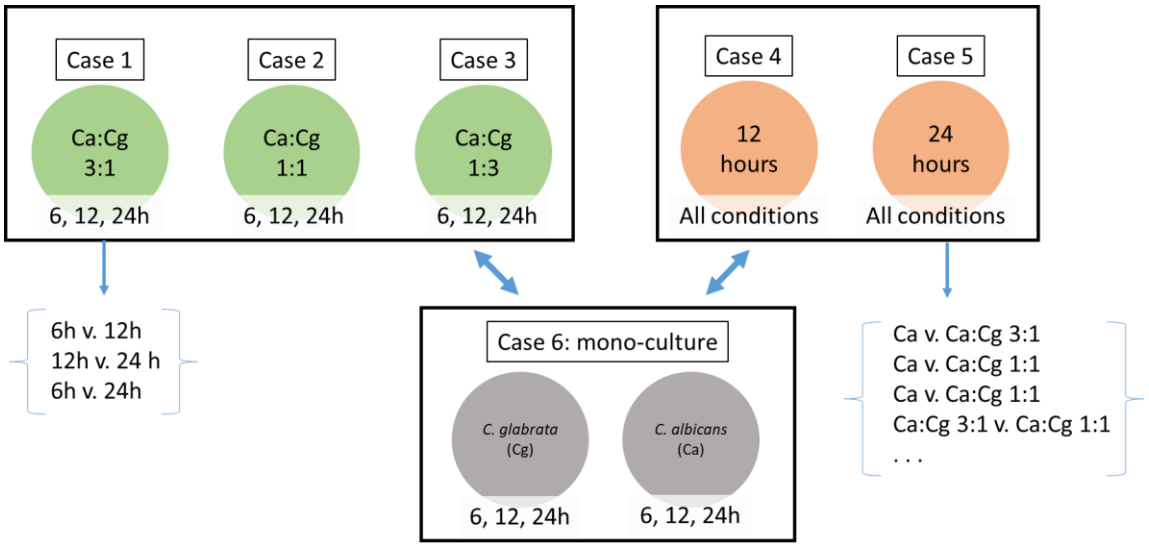

Figure 15. RNA-seq analysis schematic.

3.4 Results and Discussion

3.4.1 Confocal images demonstrate differences between mono-culture and co-culture Candida biofilms

It was previously demonstrated that relative abundance of *Candida* spp impacts co-culture biofilm formation [139]; we observed an increase in Ca hyphae length and overall biofilm formation in *C. glabrata* and *C. albicans* co-cultures (Figure 16). Furthermore, an increase in antifungal drug resistance was also observed in the co-culture with the highest biofilm formation (Ca:Cg ratio of 1:3) [139]. These results suggest interspecies interactions between Ca and Cg, which allow for increased biofilm formation and Ca hyphal growth. To investigate this further, RNA-seq analysis was utilized to determine the influence of co-culture on *Candida* gene expression over time at 6, 12, and 24 hours of growth.

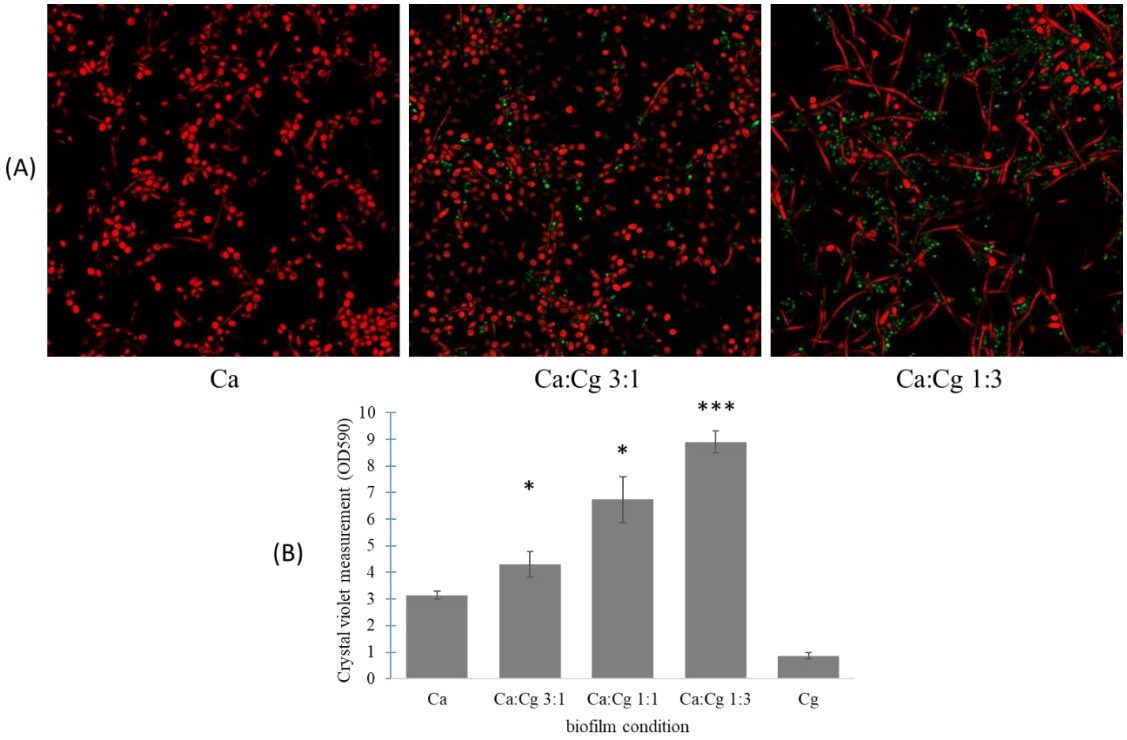

Figure 16. Increased hyphae and biofilm formation in *Candida* co-culture biofilms. (A): Representative 24-hour *Candida* biofilm z-slice cross-sectional views. *C. albicans* (Ca) = red, *C. glabrata* (Cg) = green. (B): *Candida* biofilm formation in 96-well polystyrene plates, data from 3 biological replicates. Student's t-test, *:p-value < 0.05, ***:p-value < 0.001 compared with *C. albicans* monoculture. Error bars are standard error of samples.

3.4.2 Significant C. albicans genes in mono-culture and co-culture biofilms

Biofilm samples for initial co-culture ratios of Ca:Cg 3:1, 1:1, and 1:3 and monocultures were taken after 6, 12, and 24 hours of biofilm growth and subjected to RNA-seq analysis. Multifactor analysis was carried out with the RNA-seq data, which included a linear model fitted to sample p-value and $\log_2$ fold change for all transcripts and takes into account all time points and biofilm conditions. For *C. albicans* genes, there were 128 significantly perturbed genes in *C. albicans* during biofilm growth from the

multifactor analysis (p-adjusted value less than 0.1 and $\log_2$ fold change greater than 1.2). Of the 128 significant Ca genes, 14 genes had unknown protein function (Table 6). Eleven out of the 14 genes of unknown function were noted to be induced in Spider-medium biofilms. Additionally, among the set genes with unknown functions, C3_07980C_A was also upregulated in *Candida* co-culture biofilms and is reported to be regulated by Plc1 which is involved in hyphal growth and biofilm formation (Table 6).

Table 6. *C. albicans* significant genes from multifactor analysis with unknown function.

Systematic Name	Description (CGD)
C2_00860C_A	Protein of unknown function; Spider biofilm induced [156]
C5_03430W_B	Protein of unknown function; Spider biofilm induced [156]
CR_06570C_B	Protein of unknown function; Spider biofilm induced [156]
C4_06960W_B	Protein of unknown function; Spider biofilm induced [156]
C3_03020W_A	Protein of unknown function; flow model biofilm induced [157]
C6_04420W_A	Protein of unknown function; GlcNAc-induced protein; Spider biofilm induced; rat catheter biofilm repressed [156, 158, 159]
C1_05900W_A	Protein of unknown function; mRNA binds to She3; Hap43 repressed gene; Spider biofilm induced [156, 160, 161]
C3_01020W_A	Protein of unknown function; opaque-specific transcript; induced during chlamydospore formation in both *C. albicans* and *C. dubliniensis*; Hog1-repressed; Spider biofilm induced [145, 156, 162, 163]
CR_06500C_B	Protein of unknown function; Hap43-induced; regulated by Nrg1, Tup1; repressed by alpha pheromone in SpiderM medium; Spider biofilm induced; Bcr1-repressed in RPMI a/a biofilms [156, 161, 164-166]
C1_05920W_A	Protein of unknown function; induced during chlamydospore formation in both *C. albicans* and *C. dubliniensis*; Spider biofilm induced [156, 163]
C3_07980C_A	Protein of unknown function; Plc1-regulated; transcript detected in high-resolution tiling arrays [167, 168]
C7_03150W_A	Protein of unknown function; rat catheter and Spider biofilm induced [156, 158]
C1_12470W_A	Protein of unknown function; induced by Mnl1 under weak acid stress [169]
C3_02330C_A	Protein of unknown function; Spider biofilm induced [156]

Using the GO Term Finder on CGD [155], there were significant genes in both gene ontology terms ‘molecular function’ and ‘cellular component’ for *C. albicans* multifactor analysis (Table 7) [155]. Under ‘molecular function’, significant gene ontology categories included kininogen binding, cell adhesion molecular binding, and several transmembrane transporter activities (Table 7). ‘Kininogen binding’ GO term included the adhesin gene Ca*ALS3*. Significant ‘cell adhesion’ genes included Ca*HWP1*, Ca*INT1*, and Ca*ALS3*. Transmembrane transporters were those involved in inorganic molecular entity, L-proline, and ion transport. For the L-proline transporters, Ca*GNP1* is fluconazole and caspofungin induced and is reported to be similar to asparagine and glutamine permease [157, 170]. Genes involved in ion transmembrane transporter activity included zinc (Ca*ZRT1*, Ca*ZRT2*), as well as a putative serine transporter (Ca*AGP3*), glycerophosphocholine transporter (Ca*GIT4*), and glycerophosphoinositol permease which is involved in the utilization of glycerophosphoinositol as a phosphate source (Ca*GIT1*) (Table 7) [171].

Genes categorized under ‘cellular component’ included cell surface, cell wall, hyphal cell wall, and cell periphery (Table 7). Genes associated with cell surface and cell wall/hyphal cell wall included adhesion genes (Ca*ALS3*, Ca*PGA59*), as well as several chitinase genes (Ca*CHS1*, Ca*CHT2*) and many GPI-anchored proteins (i.e. Ca*EXG2*, Ca*ECM331*, Ca*IHD1*, Ca*HYR1*, Ca*PGA10*). For those genes associated with cell periphery, there were many overlaps with cell wall and cell surface. Genes associated with cell periphery included those involved in septin (Ca*SEP7*), alternative oxidase (Ca*AOX2*),

and an oligopeptide transporter (Ca*PTR22*). Septin is involved in Ca hyphal cell growth, which is a major component of Ca biofilm formation.

Table 7. GO analysis of *C. albicans* multifactor analysis significant genes.

Biological process: no significant ontology term		
Molecular function		
GO term	Gene(s) annotated to the term	Corrected p-value
kininogen binding	ENO1, HYR1, ALS3	0.01012
high molecular weight kininogen binding	ENO1, HYR1, ALS3	0.01012
cell adhesion molecule binding	HWP1, INT1, ALS3	0.01996
inorganic molecular entity transmembrane transporter activity	HSP31, ATP1, ZRT2, GIT1, FUR4, GAP2, VMA6, AGP3, ZRT1, GIT4, HIP1, GNP1, CM_00250W	0.03458
L-proline transmembrane transporter activity	GAP2, GNP1	0.05354
ion transmembrane transporter activity	HSP31, ATP1, ZRT2, GIT1, FUR4, GAP2, VMA6, AGP3, ZRT1, GIT4, HIP1, GNP1, CM_00250W	0.07962
Cellular component		
GO term	Gene(s) annotated to the term	Corrected p-value
cell surface	EXG2, BMH1, ATP1, PGA26, PGA45, ENO1, FGR41, HYR1, ACT1, SOD5, TOS1, PGA10, RPL20B, PGA59, CRH11, HWP1, ECM331, INT1, CHT2, FET99, IHD1, PGA61, CHS1, PGA34, IFF9, ALS3	1.45E-12

Table 7. Continued.

Cellular component		
GO term	Gene(s) annotated to the term	Corrected p-value
cell wall	EXG2, CDC12, BMH1, ATP1, PGA45, ENO1, HYR1, SOD5, TOS1, PGA10, CSP2, PGA59, CRH11, HWP1, ECM331, INT1, C5_02500C_A, CHT2, IFF9, ALS3	6.14E-09
fungal-type cell wall	EXG2, CDC12, BMH1, ATP1, PGA45, ENO1, HYR1, SOD5, TOS1, PGA10, CSP2, PGA59, CRH11, HWP1, ECM331, INT1, C5_02500C_A, CHT2, IFF9, ALS3	6.14E-09
external encapsulating structure	EXG2, CDC12, BMH1, ATP1, PGA45, ENO1, HYR1, SOD5, TOS1, PGA10, CSP2, PGA59, CRH11, HWP1, ECM331, INT1, C5_02500C_A, CHT2, IFF9, ALS3	6.88E-09
cell periphery	SEP7, EXG2, CDC12, BMH1, ATP1, PGA45, ENO1, AOX2, C1_10540C_A, HYR1, ACT1, SOD5, ZRT2, GIT1, TOS1, FUR4, PTR22, GAP2, PGA10, CSP2, PGA59, QCR9, CRH11, HWP1, VPS1, ECM331, INT1, C5_02500C_A, CHT2, CAG1, FET99, CR_02210W_A, OPT4, IFF9, ALS3	0.0000353
hyphal cell wall	ATP1, ENO1, HYR1, SOD5, TOS1, CRH11, HWP1, ALS3	0.00924

For analysis of *C. albicans* significant genes that were only differentially expressed in *Candida* co-culture biofilms, a threshold of p-adjusted value (see Materials and Methods) less than 0.1 and $\log_2$ fold change greater than 2 was used. For this analysis, significant genes were first categorized based on 6 different conditions (see Materials and Methods): genes unique to mono-culture (Ca or Cg), Ca:Cg 3:1, Ca:Cg 1:1, Ca:Cg 1:3, 12 hour growth, and 24 hour growth. To analyze significantly perturbed genes in co-cultures, two different analyses were considered: 1) comparing genes differentially expressed at 12

and 24 hours in all biofilm conditions compared to mono-culture at either 6, 12, or 24 hours (time-course analysis) and 2) comparing the three co-culture biofilm conditions (Ca:Cg 3:1, Ca:Cg 1:1, Ca:Cg 1:3) to mono-culture at the same time points (either 6, 12 or 24 hours). Combining all cases, there were a total of 29 significant genes unique to *Candida* co-culture and biofilm growth time (at 12 and 24 hours compared to 6 hours): 16 genes were up-regulated and 13 genes were down-regulated in comparison to Ca mono-culture. None of these genes had significant gene ontology terms for process, function, or component analysis. The GO Slim Mapper was used to give high-level parent GO terms. For the up-regulated genes, these included those involved in transport and response to chemical, stress and drug (Table 8). For the down-regulated genes, GO terms included lipid metabolic process, as well as response to stress, chemical, and drug (Table 9).

Table 8. GO analysis for *C. albicans* up-regulated genes in co-culture.

C. albicans **up-regulated**	**GO term**	**Gene(s)**
	transport	C2_04850C_A, C1_09210C_A, LTE1, C2_02180W_A
	biological_process	C3_01090W_A, C1_08390C_A, C1_07010W_A, C3_01020W_A
	regulation of biological process	LTE1, HOT1, PST1
	carbohydrate metabolic process	C1_02320C_A, MNN47
	response to chemical	C1_09210C_A, PST1
	organelle organization	C2_04850C_A, MEF2
	response to stress	HOT1, PST1
	vesicle-mediated transport	C2_04850C_A, LTE1
	cytoskeleton organization	C2_04850C_A
	RNA metabolic process	HOT1
	response to drug	C1_09210C_A
	signal transduction	LTE1
	interspecies interaction between organisms	PST1
	cellular homeostasis	C2_02180W_A
	pathogenesis	PST1

Table 9. GO analysis for *C. albicans* down-regulated genes in co-culture.

C. albicans **down-regulated**	**GO term**	**Gene(s)**
	biological_process	C1_05390C_A, C2_10090C_A, C2_08740W_A, C1_01610C_A
	response to stress	C3_02770C_A, YIM1, IPT1
	lipid metabolic process	LIP3, IPT1
	RNA metabolic process	YPT1, C1_01160C_A
	response to chemical	YPT1, IPT1
	response to drug	YPT1, IPT1
	organelle organization	CSE4, YPT1
	regulation of biological process	YPT1, IPT1
	ribosome biogenesis	C1_01160C_A
	cellular respiration	MRPS9
	translation	MRPS9
	generation of precursor metabolites and energy	MRPS9
	transport	YPT1
	filamentous growth	IPT1
	signal transduction	YPT1
	cell cycle	CSE4
	interspecies interaction between organisms	IPT1
	DNA metabolic process	C3_02770C_A
	biofilm formation	IPT1
	vesicle-mediated transport	YPT1

In the time-course analysis for Ca significant genes, there were 10 genes that were up-regulated in the 12- and 24-hour time point samples in co-culture biofilms (Figure 17, Table 10). In *C. albicans*, there were two genes specific to 12 hours that were up-regulated – Ca*CTF1* and Ca*MEF2*. Ca*CTF1* is a putative transcription factor that activates genes for fatty acid degradation. Ca*CTF1* has been shown to regulate beta-oxidation of fatty acids in *C. albicans*, which is required for the full virulence of *C. albicans* [172]. In co-culture biofilms, Ca*CTF1* was most up-regulated in Ca:Cg 1:3 biofilm. At 24 hours, two genes were up-regulated and specific to co-culture: Ca*PST1* and Ca*MNN47*. Ca*PST1* is a flavodoxin-like protein (FLP) induced by Ca hyphae formation and is involved in oxidative stress protection and virulence of Ca; FLPs are a membrane protein and are critical for fungal survival in the host [173]. Ca*MNN47* was also only upregulated at the later stages of biofilm growth and is a protein of unknown function but is thought to be a part of a MNN4-like gene family of phosphomannosyltransferases, which are responsible for phosphomannosylation that modifies mannan cell wall proteins (Table 10) [174]. At both 12 and 24 hours, Ca*ARO7* and C1_02320C_B were upregulated suggesting an increase in both amino acid metabolism and glycolysis, respectively (Figure 18). Ca*ARO7* is a putative chorismate mutase and has been shown to be involved in Ca response to pH [144] and Ca*ARO1*, another gene involved in the shikimate pathway, has been shown to alter Ca cell wall properties and also increase expression of adhesin genes Ca*ALS1* and Ca*ALS3* [175]. This signifies that amino acid metabolism may also modulate increased biofilm formation in co-culture through increased adhesin/cell wall architecture. Ca*HOT1* was upregulated in Ca in co-culture biofilms at 12 and 24 hours, which is a putative

transcription factor required for the response of Ca to farnesoic acid by increasing expression on Ca*PHO81* that reduces hyphal growth [176]. Several putative transporters were also upregulated: C2_02180W_A (ortholog is zinc transporter) and C1_09210C_B which is similar to the Sit1p siderophore iron transporter associated with epithelial invasion and penetration [177]. Also to note, two genes with unknown functions (C3_01090W_A and C3_01020W_A) were among the highest expressed genes in Ca:Cg 1:3 biofilms, which suggests that these two ORFs may be involved in interspecies interactions in co-culture biofilm and warrant further investigation in future work.

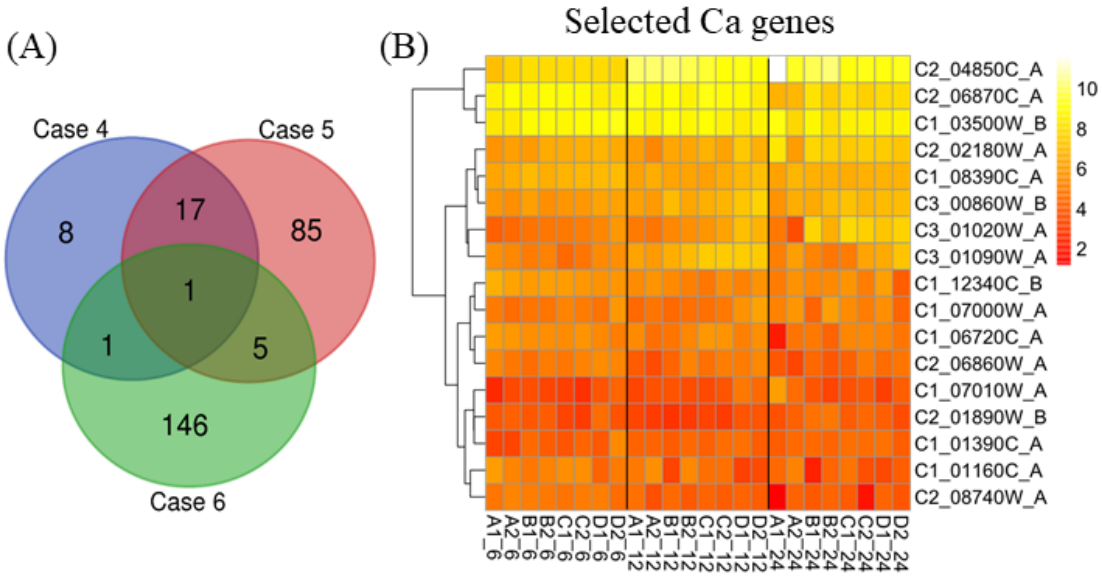

Figure 17. (A): Venn diagram of Ca significant genes in co-culture at 12 and 24 hours. Case 4: 12 hour, Case 5: 24 hour, Case 6: Ca mono-culture. (B): Heat map of Ca significant genes in co-culture at 12 and 24 hours. A: Ca, B: Ca:Cg 3:1, C: Ca:Cg 1:1, D: Ca:Cg 1:3. 2 biological replicates (i.e. A1 and A2). Normalized count data Log_2(counts).

Table 10. Significant genes in *C. albicans* co-culture over 12 and 24 hours.

Systematic Name	Standard Name	Description
C1_08390C_B		Ortholog of *S. cerevisiae* : YPL247C, *C. glabrata* CBS138 : CAGL0H00781g, *C. dubliniensis* CD36 : Cd36_07900, *C. parapsilosis* CDC317 : CPAR2_207070 and *Candida tenuis* NRRL Y-1498 : CANTEDRAFT_121354
C3_01090W_A		Ortholog of *C. parapsilosis* CDC317 : CPAR2_103040, Candida tenuis NRRL Y-1498 : CANTEDRAFT_116324, *Debaryomyces hansenii* CBS767 : DEHA2G01980g and *Pichia stipitis* Pignal : PICST_45936
C1_01160C_B		Exosome non-catalytic core component; involved in 3'-5' RNA processing and degradation in the nucleus and cytoplasm; Spider biofilm induced [156]
C2_08740W_A		Has domain(s) with predicted ATP binding, nucleoside-triphosphatase activity, nucleotide binding activity
C1_01390C_B	HOT1	Putative transcription factor; required for inhibition of filamentous growth by farnesoic acid and for expression of PHO81; filament induced [65, 176]
C2_04850C_B		Ortholog(s) have actin filament binding activity, role in actin cortical patch localization, actin filament bundle assembly, endocytosis and actin cortical patch localization
C1_07010W_A		Ortholog of *C. dubliniensis* CD36 : Cd36_06550, *C. parapsilosis* CDC317 : CPAR2_209030, *Candida tenuis* NRRL Y-1498 : CANTEDRAFT_111035 and *Debaryomyces hansenii* CBS767 : DEHA2F25300g
C1_03500W_A	YPT1	Functional homolog of *S. cerevisiae* Ypt1p, which is an essential small Ras-type GTPase involved in protein secretion at ER-to-Golgi; dominant-negative mutation causes SAP secretion defect and accumulation of intracellular secretory vesicles [178, 179]
C2_01890W_A	CTF1	Putative zinc-finger transcription factor, similar to *A. nidulans* FarA and FarB; activates genes required for fatty acid degradation; induced by oleate; null mutant displays carbon source utilization defects and slightly reduced virulence [172, 180]

Table 10. Continued.

Systematic Name	Standard Name	Description
C3_01020W_A		Protein of unknown function; opaque-specific transcript; induced during chlamydospore formation in both *C. albicans* and *C. dubliniensis*; Hog1-repressed; Spider biofilm induced [145, 156, 162, 163]
C2_06860W_B	LTE1	Protein similar to GDP/GTP exchange factors; repressed by alpha pheromone in Spider medium; flow model biofilm repressed [157, 165]
C1_07000W_B	MEF2	Putative mitochondrial translation elongation factor; caspofungin induced [181]
C1_12340C_A	MRPS9	Mitochondrial ribosomal protein S9; has N-terminal mitochondrial targeting signal and an S9 consensus motif; overexpression in *S. cerevisiae* causes respiratory defect that is reversible upon cessation of *C. albicans* gene expression [182]
C2_02180W_B		Ortholog of *S. cerevisiae* Zrt3, vacuolar membrane zinc transporter; predicted Kex2 substrate; induced in oralpharyngeal candidiasis; flow model biofilm induced; Spider biofilm induced [156, 157, 183, 184]
C1_06720C_A		Ortholog(s) have mitochondrion localization
C3_00860W_B	CSE4	Centromeric histone H3 variant; role in structural changes of centromeric nucleosomes during cell cycle; 4 nucleosomes bind 1 centromere, each has 1 Cse4 molecule during most of cell cycle, 2 molecules in anaphase; Spider biofilm repressed [156, 185-189]
C2_06870C_A	PST1	Flavodoxin-like protein involved in oxidative stress protection and virulence; putative 1,4-benzoquinone reductase; hyphal-induced; regulated by Cyr1, Ras1, Efg1, Nrg1, Rfg1, Tup1; Hap43-induced; Spider biofilm induced [65, 156, 161, 173, 190, 191]

At both time points of 12 and 24 hours, several genes were downregulated involved in cell membrane (Figure 17, Figure 18). Ca*YPT1* is a functional homolog of *S. cerevisiae* Ypt1p, which is involved in protein secretion between ER and Golgi and overexpression in Ca and has been shown to inhibit growth and aspartyl protease secretion [178]. Ca*IPT1* was also downregulated in co-culture biofilms (and most downregulated in Ca:Cg 1:3), which is involved in sphingolipid biosynthesis and is responsible for proper membrane transporter localization and drug resistance [192, 193] signifying that the cell membrane of Ca is significantly modulated in co-culture biofilm formation through modulation of cell membrane sphingolipids. Ca*LIP3* and Ca*YIM1* were downregulated (Table 11) and Ca*LIP3* – a secreted lipase - has been shown to be downregulated at later time points of *C. albicans* infection in a mouse model [194]. Ca*YIM1* (most down-regulated in Ca:Cg 1:3 biofilms) was reported to be down-regulated when *C. albicans* is in the presence of macrophages [195].

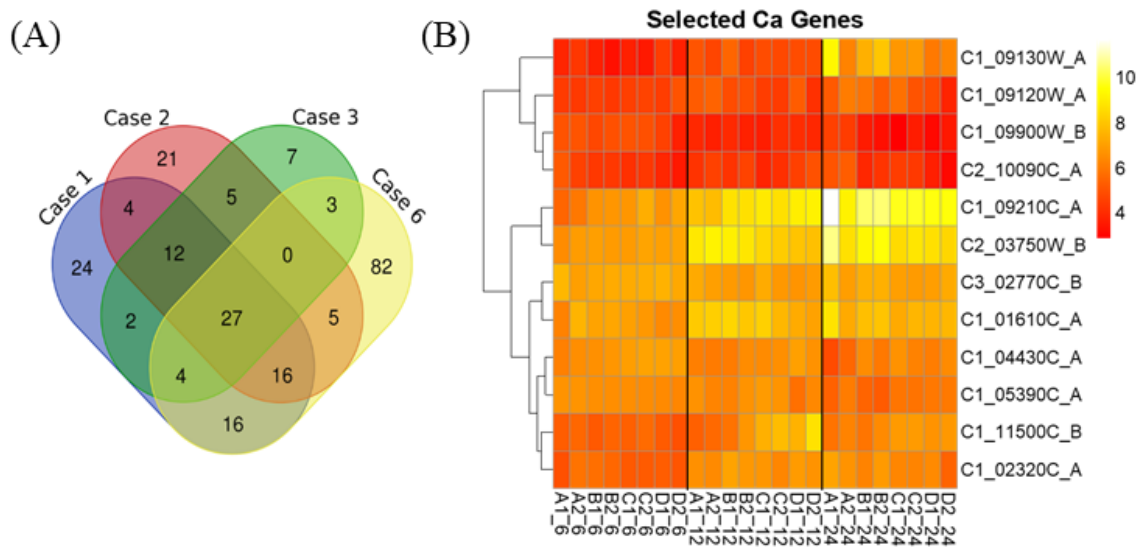

Figure 18. (A):Venn diagram of Ca significant genes in co-culture compared to monoculture. Case 1: Ca:Cg 3:1 biofilm, Case 2: Ca:Cg 1:1 biofilm, Case 3: Ca:Cg 1:3 biofilm, Case 6: Ca mono-culture. (B): Heat map of Ca significant genes in co-culture at 6, 12, and 24 hours. A: Ca, B: Ca:Cg 3:1, C: Ca:Cg 1:1, D: Ca:Cg 1:3. 2 biological replicates (i.e. A1 and A2). Normalized count data Log_2(counts).

Table 11. Significant genes to co-culture in *C. albicans* over all time points (Case 123 v. 6).

Systematic name	Standard name	Description
C1_09130W_A	MNN47	Protein of unknown function; Spider biofilm induced [156]
C1_09210C_B		Putative transporter; slightly similar to the Sit1p siderophore transporter; Gcn4p-regulated; fungal-specific; induced by Mnl1p under weak acid stress [169, 177, 196, 197]
C1_11500C_A	ARO7	Putative chorismate mutase; fungal-specific (no human or murine homolog); alkaline upregulated [144]
C2_10090C_B		Ortholog of *S. cerevisiae* : MRX1, *C. glabrata* CBS138 : CAGL0J03278g, *C. dubliniensis* CD36 : Cd36_24130, *C. parapsilosis* CDC317 : CPAR2_407430 and *Candida tenuis* NRRL Y-1498 : cten_CGOB_00234
C2_03750W_A	YIM1	Protein similar to protease of mitochondrial inner membrane; increased transcription is observed upon benomyl treatment; macrophage-downregulated gene [195, 198]
C1_09900W_A	LIP3	Secreted lipase; gene family member whose members are expressed differentially in response to carbon source and infection; possible role in nutrition and/or in creating an acidic microenvironment; flow model biofilm induced [157, 194, 199]
C1_02320C_B		Putative protein similar to 6-phosphofructo-2-kinase/fructose-2,6-bisphosphatase; expression downregulated in an ssr1 null mutant [200]
C1_05390C_B		Ortholog of *C. dubliniensis* CD36 : Cd36_05120, *C. parapsilosis* CDC317 : CPAR2_107740, *Candida tenuis* NRRL Y-1498 : CANTEDRAFT_136277 and *Debaryomyces hansenii* CBS767 : DEHA2A02266g
C3_02770C_B		Ortholog(s) have role in transcription-coupled nucleotide-excision repair and Ddb1-Ckn1 complex localization
C1_01610C_B		Protein of unknown function; Hap43-induced; Spider biofilm induced [156, 161]
C1_04430C_B		Putative protein of unknown function; clade-associated gene expression [201]
C1_09120W_B	IPT1	Inositol phosphoryl transferase; catalyzes the synthesis of the most abundant sphingolipid, mannose-(inositol-P)2-ceramide, M(IP)2C, from MIPC; required for wild-type membrane localization of Cdr1; Spider biofilm induced [156, 192, 193]

3.4.3 Significant C. glabrata genes in mono-culture and co-culture biofilms

For the multifactor analysis with *C. glabrata* genes, there were 763 significantly differentially expressed genes (p-adjusted value less than 0.1 and $\log_2$ fold change greater than 1.2). Compared to *C. albicans*, which had 128 significant genes, *C. glabrata* had many more differentially expressed genes (763 genes), which is interesting to note. To reduce the list of genes for further analysis, multiple factors were taken into account: multifactor analysis, biofilm condition (mono-culture and co-culture), and time course (12 and 24 hour significant transcripts) which resulted in a total of 63 significant genes in Cg over all time points and biofilm conditions. Looking at a heat map of the 63 significant transcripts in Cg (Figure 19), Cg significant genes were down-regulated over time in 12h and 24h and significant genes were also down-regulated in co-culture biofilms. This can be seen in Ca:Cg 3:1 (B), Ca:Cg 1:1 (C), and also in Ca:Cg 1:3 (D) where there are significant decreases in transcripts in co-cultures compared to mono-culture (E) and also specifically at 12h and 24h compared to 6h (Figure 19). Of these 63 significant genes, there was only significant GO 'function' term for ligase activity (Table 12) which included CgFOL3 (role in folic acid biosynthesis). Looking at GO slim mapper 'component' analysis, which finds global GO trends with less stringency than GO term finder, most genes were involved in cytoplasm and membrane component groups including genes involved in glycosylation (i.e. GDP-mannose for protein glycosylation (Cg*VIG9*), CAGL0L07172g, CAGL0K05005g, CAGL0A00209g, CAGL0L00693g), predicted GPI-anchor (Cg*GAS2*), and a membrane anchor for oligosaccharides (CAGL0A00209g). Additionally, Cg*CRN1* was a reported gene in GO analysis, which has been reported as

upregulated in Δ*ACE2* strains and noted to be involved in cell fate and cell type differentiation in *C. glabrata* [202, 203], indicating that there may be some cell wall and morphology adaptations of *C. glabrata* in co-culture *Candida* biofilms. It was demonstrated by de Groot et al. that the cell wall proteins of *C. glabrata* (specifically the adhesion-like proteins) depended on the growth stage of the cell, where there was increased adhesion and cell surface hydrophobicity of Cg during the stationary phase over the log phase of growth [204]. Additionally, it was recently reported by Charlet et al. that the *C. glabrata* cell wall underwent several changes during *in vivo* mouse colonization such as a significant increase in cell wall chitin after exposure to a mouse gastrointestinal tract [205]. For the Cg stress response, it was reported by Ramírez-Quijas et al. that oxidative stress (a common environmental stress) modified the cell wall morphology and of *C. glabrata* [206]. Transport genes from GO analysis included those involved in ion, DNA, and transmembrane transport, indicating a potential increase or decrease in cellular uptake. Several genes involved in DNA and RNA assembly, amino acid biosynthesis (histidine, lysine, folic acid derivative), and protein localization (nucleus, mitochondria, and endoplasmic reticulum) were represented in GO analysis. A change in DNA and RNA assembly may suggest a modification of gene expression and cell growth and amino acid biosynthesis indicates a potential change in growth requirements of *C. glabrata* during biofilm formation. It has been previously suggested that alterations of amino acid (i.e. methionine) biosynthesis results in modulation of azole susceptibility in *C. albicans* [207].

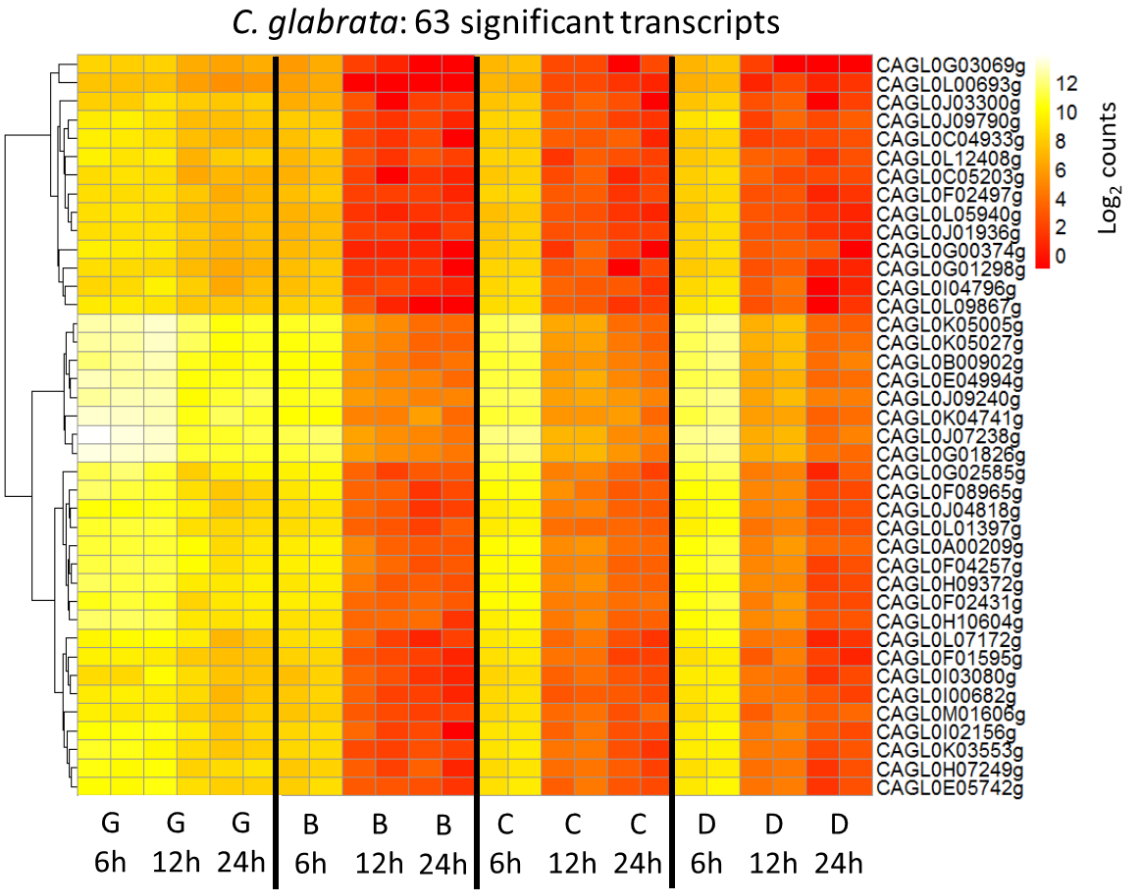

Figure 19. Normalized count data heat map for Cg significant transcripts. Grouped based on *Candida* biofilm condition. G: Cg, B: Ca:Cg 3:1, C: Ca:Cg 1:1, D: Ca:Cg 1:3. 2 biological replicates (i.e. B1 and B2). Normalized count data Log_2(counts).

Table 12. Gene ontology for significant *C. glabrata* genes from multifactor analysis (63 genes).

Biological process: no significant ontology term		
Molecular function		
GO term	Gene(s) annotated to the term	Corrected p-value
Ligase activity	FRS1, CAGL0H09372g, CAGL0K00913g, FOL3, CAGL0K05027g, CAGL0M01606g	0.07963
Cellular component: no significant ontology term		

To select significant genes in *C. glabrata* unique to *Candida* co-culture, a threshold of p-adjusted value less than 0.02 and $\log_2$ fold change greater than 2.7 was used. Combining both co-culture conditions and the effect of time (12 and 24 hours compared to 6 hours), there were a total of 49 significant *C. glabrata* genes unique to co-culture and time (Table 13, Table 14). 4 genes were up-regulated (Table 15) and 45 of these genes were down-regulated (Table 16) in comparison to mono-culture Cg as seen in Table 15 and Table 16 respectively for GO slim analysis. In GO slim analysis for up-regulated genes, GO terms included transport, cell cycle, and response to chemical and drug (Table 15). For GO slim analysis for down-regulated genes, general categories of GO included organelle organization, transport, lipid metabolic process, and response to stress, chemical, and drug (Table 16).

Table 13. Significant genes in *C. glabrata* in co-culture at 12 and 24 hours (Case 45 v. 6).

Systemic name	Standard name	Description
CAGL0B02409g		Ortholog of *S. cerevisiae* : YML119W and *Saccharomyces cerevisiae* S288C : YML119W
CAGL0C00517g		Ortholog(s) have protein-arginine omega-N monomethyltransferase activity, protein-arginine omega-N symmetric methyltransferase activity
CAGL0D04708g		Ortholog(s) have copper ion transmembrane transporter activity, role in copper ion import, iron ion transmembrane transport and plasma membrane localization
CAGL0D05434g	ROX1	Protein of unknown function
CAGL0E04114g		Ortholog(s) have role in cellular response to oxidative stress, protein import into peroxisome matrix, protein quality control for misfolded or incompletely synthesized proteins and mitochondrial inner membrane localization
CAGL0G02585g	LYS12	Homo-isocitrate dehydrogenase [203]
CAGL0F07601g	CWP1.1	GPI-linked cell wall protein [208, 209]
CAGL0I02156g		Ortholog(s) have role in endocytosis
CAGL0J09746g		Ortholog(s) have tRNA (guanine-N7-)-methyltransferase activity, role in tRNA methylation and tRNA methyltransferase complex localization
CAGL0J11264g		Has domain(s) with predicted oxidoreductase activity and role in metabolic process
CAGL0K05027g		Ortholog(s) have DNA replication origin binding, adenylosuccinate synthase activity, sulfinylpropanyl adenylate synthase activity and role in 'de novo' AMP biosynthetic process, cellular response to cadmium ion, fumarate metabolic process
CAGL0L13178g		Ortholog(s) have role in mitochondrial respiratory chain complex III assembly and integral component of mitochondrial inner membrane localization
CAGL0M09614g		Ortholog(s) have plasma membrane localization

Table 14. Significant genes to co-culture in *C. glabrata* over all time points (Case 123 v. 6).

Systematic name	Standard name	Description
CAGL0A03190g		Ortholog(s) have kinetochore localization
CAGL0C05313g		Protein of unknown function
CAGL0D01716g		Ortholog(s) have DNA polymerase processivity factor activity
CAGL0D01034g	VIG9	GDP-mannose pyrophosphorylase involved in the synthesis of GDP-mannose for protein glycosylation [210]
CAGL0D04444g		Ortholog(s) have role in mitotic sister chromatid cohesion, negative regulation of chromosome condensation, negative regulation of maintenance of mitotic sister chromatid cohesion and nuclear cohesin complex localization
CAGL0D05742g		Has domain(s) with predicted dolichyl-diphosphooligosaccharide-protein glycotransferase activity, role in protein glycosylation and endoplasmic reticulum, integral component of membrane localization
CAGL0D01012g		Ortholog(s) have RNA polymerase II proximal promoter sequence-specific DNA binding, transcriptional activator activity, RNA polymerase II proximal promoter sequence-specific DNA binding activity
CAGL0F02431g	ACO2	Ortholog(s) have role in mitochondrial translation and mitochondrion, nucleus localization
CAGL0F06941g	PYC1	Putative pyruvate carboxylase isoform; gene is upregulated in azole-resistant strain [211]
CAGL0G02585g	LYS12	Homo-isocitrate dehydrogenase [203]
CAGL0I05764g		Ortholog(s) have repressing transcription factor binding, transcription factor activity, transcription factor binding activity and role in negative regulation of transcription involved in G1/S transition of mitotic cell cycle
CAGL0G04851g	SUR4	Predicted fatty acid elongase involved in production of very long chain fatty acids for sphingolipid biosynthesis; mutants show reduced sensitivity to caspofungin and increased sensitivity to micafungin [212]
CAGL0H07183g		Ortholog(s) have role in regulation of DNA methylation
CAGL0I00484g		Ortholog(s) have cell adhesion molecule binding, glucan endo-1,6-beta-glucosidase activity, glucan exo-1,3-beta-glucosidase activity
CAGL0F08437g		Ortholog(s) have steryl deacetylase activity, role in response to toxic substance, sterol deacetylation and endoplasmic reticulum lumen, integral component of membrane, lipid droplet localization
CAGL0F07865g	UPC2B	Putative Zn(2)-Cys(6) binuclear cluster transcriptional regulator of ergosterol biosynthesis [213]

Table 14. Continued.

Systematic name	Standard name	Description
CAGL0H03399g		Ortholog(s) have (R)-carnitine transmembrane transporter activity, choline transmembrane transporter activity, ethanolamine transmembrane transporter activity
CAGL0I08371g		Ortholog(s) have DNA replication origin binding activity and role in DNA replication initiation, chromatin silencing at silent mating-type cassette, pre-replicative complex assembly involved in nuclear cell cycle DNA replication
CAGL0I01210g		Ortholog(s) have [cytochrome c]-lysine N-methyltransferase activity, role in peptidyl-lysine methylation and cytosol localization
CAGL0J04378g		Ortholog(s) have role in glycolipid translocation and endoplasmic reticulum membrane localization
CAGL0J05676g	INN1	Ortholog(s) have enzyme regulator activity, role in chromosome organization, division septum assembly and HICS complex, cellular bud neck contractile ring localization
CAGL0J06402g		Ortholog(s) have homocitrate synthase activity, role in DNA repair, histone displacement, lysine biosynthetic process via aminoadipic acid and nucleus localization
CAGL0K11506g		Ortholog(s) have 5'-3' exodeoxyribonuclease activity involved in UV-damage excision repair, 5'-flap endonuclease activity, double-stranded DNA 5'-3' exodeoxyribonuclease activity, single-stranded DNA 5'-3' exodeoxyribonuclease activity
CAGL0K12870g		Ortholog(s) have role in mitochondrial respiratory chain complex IV assembly and mitochondrion localization
CAGL0K01001g		Ortholog(s) have role in protein localization to plasma membrane, protein targeting to vacuole, receptor-mediated endocytosis, response to pheromone and actin cortical patch, cytosol, endosome, plasma membrane localization
CAGL0K00605g		Ortholog(s) have ATP binding, ATPase activity, DNA replication origin binding, GTP binding, GTPase activity, chromatin binding, protein serine/threonine kinase activity
CAGL0K00913g		Ortholog(s) have formate-tetrahydrofolate ligase activity, methenyltetrahydrofolate cyclohydrolase activity, methylenetetrahydrofolate dehydrogenase (NADP+) activity, single-stranded DNA binding activity
CAGL0K04609g		Has domain(s) with predicted role in transmembrane transport and integral component of membrane localization

Table 14. Continued.

Systematic name	Standard name	Description
CAGL0K12848g	SEC53	Putative phosphomannomutase; protein differentially expressed in azole resistant strain [203, 214]
CAGL0L01397g		Ortholog(s) have DNA replication origin binding, MCM complex binding, chromatin binding, single-stranded DNA-dependent ATP-dependent DNA helicase activity
CAGL0L11088g		Ortholog(s) have phosphatase activity and role in dephosphorylation
CAGL0L08184g	FEN1	Predicted fatty acid elongase with role in sphingolipid biosynthetic process; mutants show reduced sensitivity to caspofungin and increased sensitivity to micafungin [212]
CAGL0L09867g		Ortholog(s) have adenylate kinase activity, uridylate kinase activity, role in 'de novo' pyrimidine nucleobase biosynthetic process and mitochondrion, nucleus localization
CAGL0M14025g		Has domain(s) with predicted oxidoreductase activity and role in oxidation-reduction process
CAGL0M08448g		Ortholog(s) have mannose-ethanolamine phosphotransferase activity and role in ATP transport, GPI anchor biosynthetic process, conidium formation, regulation of growth rate
CAGL0M13849g	GAS2	Putative glycoside hydrolase of the Gas/Phr family; predicted GPI-anchor [209]

Table 15. GO slim analysis for *C. glabrata* in up-regulated significant genes in co-culture.

C. glabrata **up-regulated**	**GO term**	**Gene(s)**
	transport	CAGL0H03399g, CAGL0K04609g
	cell cycle	CAGL0K00605g
	response to chemical	CAGL0H03399g
	regulation of biological process	CAGL0K00605g
	response to drug	CAGL0H03399g
	biological_process	ROX1
	DNA metabolic process	CAGL0K00605g

Table 16. GO slim analysis for *C. glabrata* down-regulated genes in co-culture.

C. glabrata	**GO term**	**Gene(s)**
down-regulated	regulation of biological process	CAGL0D01716g, CAGL0C00517g, CAGL0L01397g, CAGL0M08448g, CAGL0I05764g, UPC2B, CAGL0D04444g, CAGL0H07183g, GAS2, CAGL0D01012g, CAGL0I08371g
	organelle organization	CAGL0L01397g, CAGL0K12870g, INN1, CAGL0J06402g, CAGL0K11506g, CAGL0L13178g, CAGL0D04444g, CAGL0E04114g, GAS2, CAGL0I08371g
	transport	FEN1, CAGL0D04708g, CAGL0M08448g, SEC53, CAGL0J04378g, CAGL0E04114g, CAGL0I02156g, CAGL0K01001g, SUR4
	cell cycle	CAGL0D01716g, CAGL0C00517g, CAGL0L01397g, CAGL0I05764g, INN1, CAGL0K11506g, CAGL0D04444g, CAGL0D01012g, CAGL0I08371g
	response to stress	CAGL0D01716g, CAGL0C00517g, CAGL0L01397g, CAGL0J06402g, UPC2B, CAGL0K11506g, CAGL0E04114g, GAS2
	response to chemical	CAGL0M08448g, UPC2B, CAGL0F08437g, CAGL0K05027g, CAGL0E04114g, CAGL0K01001g
	lipid metabolic process	FEN1, CAGL0M08448g, UPC2B, CAGL0F08437g, SUR4
	cellular protein modification process	CAGL0C00517g, CAGL0M08448g, CAGL0I01210g, VIG9, CAGL0D05742g
	DNA metabolic process	CAGL0D01716g, CAGL0L01397g, CAGL0J06402g, CAGL0K11506g, CAGL0I08371g
	carbohydrate metabolic process	CAGL0I00484g, PYC1, SEC53, GAS2
	biological_process	CAGL0M09614g, CAGL0B02409g, CAGL0C05313g, CAGL0A03190g
	vesicle-mediated transport	FEN1, CAGL0I02156g, CAGL0K01001g, SUR4
	RNA metabolic process	CAGL0D01716g, CAGL0K11506g, CAGL0J09746g
	cell wall organization	CAGL0I00484g, CWP1.1, GAS2

Table 16. Continued.

C. glabrata **down-regulated**	**GO term**	**Gene(s)**
	protein catabolic process	CAGL0C00517g, CAGL0E04114g
	response to drug	CAGL0M08448g, UPC2B
	interspecies interaction between organisms	CAGL0I00484g, GAS2
	cytokinesis	INN1
	cellular respiration	ACO2
	hyphal growth	GAS2
	cell development	CAGL0M08448g
	generation of precursor metabolites and energy	ACO2
	translation	ACO2
	cell adhesion	CAGL0I00484g
	vitamin metabolic process	CAGL0K00913g
	filamentous growth	GAS2
	conjugation	CAGL0I00484g
	biofilm formation	CAGL0I00484g
	pathogenesis	GAS2

The GO term mapper from CGD [155] was used to find statistically significant GO terms related to *C. glabrata* co-culture conditions. For genes involved in 'biological

process', significant genes included those involved in GDP-mannose processes (Cg*VIG9*, Cg*SEC53*) and 'small molecule biosynthetic process' such as Cg*PYC1* and Cg*LYS12* (Table 17). Cg*VIG9* is a GDP-mannose pyrophosphorylase involved in GDP-mannose synthesis [215]. Cg*SEC53* is a putative phosphomannomutase and was reported as differentially expressed in an azole resistant Cg strain [203, 214]. Both genes are also involved in the mannose metabolism pathway (Figure 20). Cg*PYC1* is a putative pyruvate carboxylase isoform and was up-regulated in azole-resistant strain [211] and Cg*LYS12* is a homo-isocitrate dehydrogenase [203] involved in lysine biosynthesis (Figure 21). These results suggest that the cell wall via mannose metabolism and amino acid biosynthesis were significantly altered during co-culture *C. glabrata* growth conditions. For GO 'molecular function', significant terms included fatty acid elongase and synthase activity (Cg*SUR4*, Cg*FEN1*), and DNA replication origin binding (Table 17). Cg*SUR4* is a predicted fatty acid elongase for the production of very long chain fatty acids for sphingolipid biosynthesis, which are major components of the Cg cell membrane [212]. Cg*FEN1* plays a role in sphingolipid biosynthesis as well and mutants in both genes (*SUR4* and *FEN1*) showed a reduced susceptibility to caspofungin [212]. In *C. albicans*, it was recently demonstrated by Alfatah et al. that Ca*FEN1* plays a critical role in Ca cell wall integrity and biofilm formation and that a double mutant of Ca*FEN1* and Ca*FEN12* resulted in defective hyphae formation, which is a major component of biofilm growth [216]. Our GO analysis results imply that there are substantial cell membrane changes in Cg under the exposure to Ca in co-culture biofilms and that these cell membrane changes increase biofilm formation in *C. glabrata*. In GO 'cellular component', significant genes

were associated with the DNA replication complex, and MBF transcription complex (Table 17). In *S. cerevisiae*, this complex is involved in the regulation of transcription during the G1/S transition of the cell cycle [217]. This information indicates that the cell growth (G1 phase) and DNA replication (S phase) is impacted when Cg is co-culture with Ca in biofilms.

Table 17. Significant Gene Ontology terms for *C. glabrata* co-culture specific significant genes.

Biological process		
GO term	Gene(s) annotated to the term	Corrected P-value
nuclear DNA replication	CAGL0D01716g, CAGL0I08371g, CAGL0K00605g, CAGL0K11506g, CAGL0L01397g	0.00256
cell cycle DNA replication	CAGL0D01716g, CAGL0I08371g, CAGL0K00605g, CAGL0K11506g, CAGL0L01397g	0.00285
GDP-mannose metabolic process	VIG9, SEC53	0.0332
GDP-mannose biosynthetic process	VIG9, SEC53	0.0332
pre-replicative complex assembly involved in cell cycle DNA replication	CAGL0I08371g, CAGL0K00605g, CAGL0L01397g	0.03559
pre-replicative complex assembly	CAGL0I08371g, CAGL0K00605g, CAGL0L01397g	0.03559
pre-replicative complex assembly involved in nuclear cell cycle DNA replication	CAGL0I08371g, CAGL0K00605g, CAGL0L01397g	0.03559
very long-chain fatty acid biosynthetic process	SUR4, FEN1	0.06613

Table 17. Continued.

Biological process		
GO term	Gene(s) annotated to the term	Corrected P-value
small molecule biosynthetic process	PYC1, UPC2B, LYS12, SUR4, CAGL0J06402g, CAGL0K00913g, SEC53, FEN1	0.07207
Molecular function		
GO term	Gene(s) annotated to the term	Corrected P-value
fatty acid elongase activity	SUR4, FEN1	0.0074
fatty acid synthase activity	SUR4, FEN1	0.051
DNA replication origin binding	CAGL0I08371g, CAGL0K00605g, CAGL0L01397g	0.05963
sequence-specific double-stranded DNA binding	CAGL0D01012g, UPC2B, CAGL0I08371g, CAGL0K00605g, CAGL0L01397g	0.07284
Cellular component		
GO term	Gene(s) annotated to the term	Corrected P-value
pre-replicative complex	CAGL0I08371g, CAGL0K00605g, CAGL0L01397g	0.00663
nuclear pre-replicative complex	CAGL0I08371g, CAGL0K00605g, CAGL0L01397g	0.00663
DNA replication preinitiation complex	CAGL0I08371g, CAGL0K00605g, CAGL0L01397g	0.01727
MBF transcription complex	CAGL0D01012g, CAGL0I05764g	0.01879

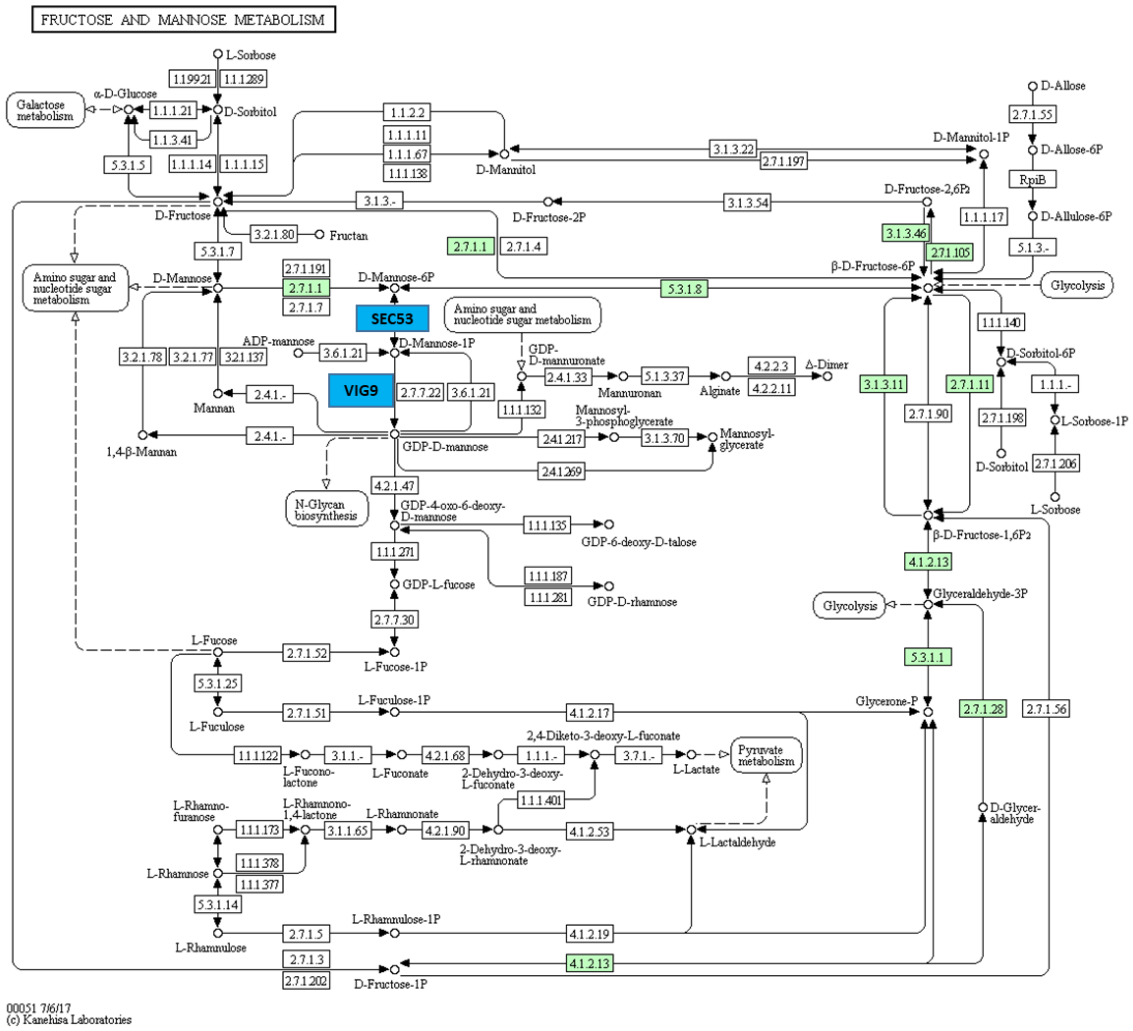

Figure 20. *C. glabrata* KEGG pathway for mannose metabolism [218-220]. Blue boxes indicate Cg co-culture down-regulated genes.

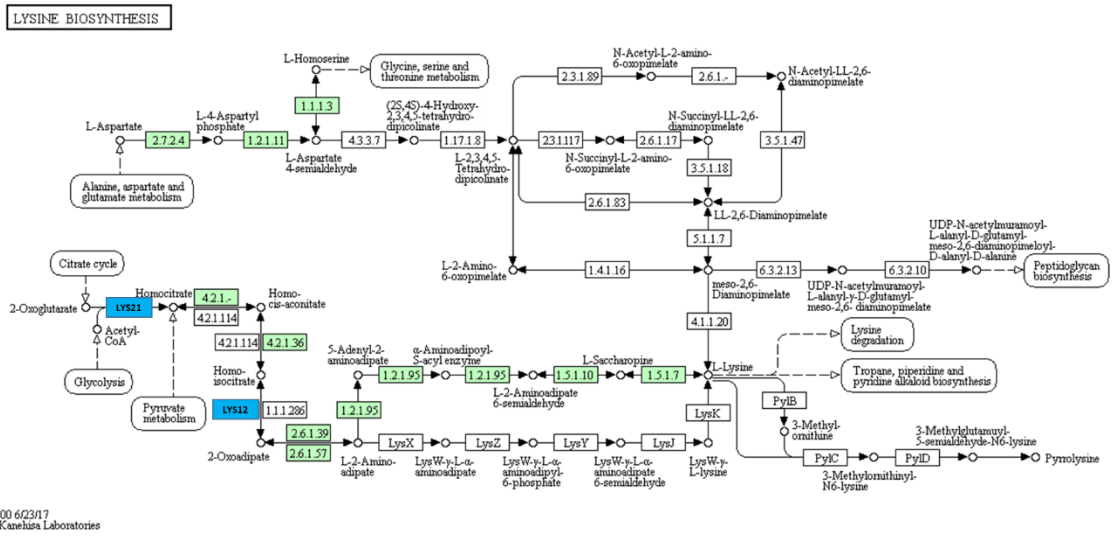

Figure 21. *C. glabrata* KEGG pathway for lysine biosynthesis [218-220]. Blue box indicate Cg co-culture down-regulated genes.

Looking at differential gene expression in *C. glabrata* in co-culture biofilms, there were several significant genes upregulated at 12 and 24 hours compared to 6 hour. Most of the *C. glabrata* significant genes were down-regulated in co-culture. Cg*ROX1*, which is a protein of unknown function in Cg, has an ortholog in *S. cerevisiae* that is a heme-dependent repressor of hypoxic genes. A previous study showed that biofilm formation was reduced in a Cg*ROX1* mutant under hypoxia [221], an important host factor, and Linde et al. linked the Cg stress response to iron homeostasis in Cg [141]. Biofilm formation is generally considered a stress and survival mechanism of Cg so our results also suggest the link of stress and biofilm formation to potentially up-regulation of iron homeostasis in Cg. CAGL0H03399g was also upregulated in co-culture, and orthologs of this gene have choline transmembrane transporter activity. It is reported that choline and inositol utilize the same transporter in the cell, and inositol is a precursor for sphingolipid

biosynthesis in yeast [222, 223]. Another gene up-regulated in Cg co-culture biofilms was CAGL0K04609g, which has predicted transmembrane transport association and an integral role in membrane localization.

Looking at down-regulated genes, 33 genes in Cg were down-regulated in co-culture biofilms (Table 18). 12 genes out of these 33 genes were involved in cell membrane and cell wall biosynthesis. Cell membrane sugars and lipid backbones positively impact the extracellular matrix of *Candida* biofilms and contribute to biofilm formation. The majority of the cell membrane-related down-regulated genes in Cg during co-culture biofilm growth were involved in the cell wall biosynthesis such as mannan and sphingolipid biosynthesis (Cg*CWP1.1* – GPI-linked cell wall protein most down-regulated in Ca:Cg 1:3, Cg*SEC53*, Cg*FEN1*, CgCAGL0M08448g – most down-regulated in Ca:Cg 1:3, Cg*GAS2*, Cg*VIG9*) (Figure 20, Figure 22, Figure 23). Additionally, Cg*SUR4* (a predicted fatty-acid elongase for long sphingolipid biosynthesis) was downregulated most in Ca:Cg 1:3 biofilms. Recently, Charlet et al. [205] reported Cg cell wall remodeling as a factor during growth in the gut microbiota signifying that this factor of cell wall structure change (such as sphingolipid content) is important for Cg growth and environmental adaptation.

Transport genes were also significantly expressed in Cg during co-culture growth. Transporters included those for various ions (copper: CAGL0D04708g, choline: CAGL0H03399g, iron), DNA, and transmembrane transport (CAGL0K04609g). *C. albicans* has been reported to potentially absorb copper ions through CaAls1 and CaAls3 [224] and copper ion transporter Ca*FET4* mutation was associated with increased biofilm

formation [225] demonstrating a connection between copper ion transport and increased biofilm formation in *Candida* spp. Additionally, 7 of the down-regulated Cg significant genes were involved in nutrient and energy utilization. Several of these significant genes were involved in glycolysis (Cg*LYS12* – most downregulated in Ca:Cg 1:3 biofilms, Cg*LYS21*, Cg*PYC1*) (Figure 21, Figure 23, Figure 24). Additionally, genes involved in DNA/RNA processes, cell division, and cellular response to oxidative stress (CAGL0E04114g, most downregulated in Ca:Cg 1:3) were significantly downregulated in co-culture biofilms (Table 18). Similar to Cg, an oxidative stress response gene Ca*PST1* was also modulated in *C. albicans* biofilms (up-regulated). It was reported by Pemmaraju et al. that *C. albicans* under exogenous oxidative stress increased biofilm matrix production and modulated virulence factors and cell wall mannan content [226]. *C. glabrata* is highly resistant to oxidative stress [227] and more tolerant to oxidative stress as a biofilm over planktonic cells [228].

Table 18. Down-regulated *C. glabrata* genes in co-culture biofilms.

	Systematic name	Standard name	Description
Cell membrane	CAGL0J04378g		Ortholog(s) have role in glycolipid translocation and endoplasmic reticulum membrane localization
	CAGL0K01001g		Ortholog(s) have role in protein localization to plasma membrane, protein targeting to vacuole, receptor-mediated endocytosis, response to pheromone and actin cortical patch, cytosol, endosome, plasma membrane localization
	CAGL0K12848g	SEC53	Putative phosphomannomutase; protein differentially expressed in azole resistant strain [203, 214]
	CAGL0L08184g	FEN1	Predicted fatty acid elongase with role in sphingolipid biosynthetic process; mutants show reduced sensitivity to caspofungin and increased sensitivity to micafungin [212]
	CAGL0M08448g		Ortholog(s) have mannose-ethanolamine phosphotransferase activity and role in ATP transport, GPI anchor biosynthetic process, conidium formation, regulation of growth rate
	CAGL0M13849g	GAS2	Putative glycoside hydrolase of the Gas/Phr family; predicted GPI-anchor [209]
	CAGL0D01034g	VIG9	GDP-mannose pyrophosphorylase involved in the synthesis of GDP-mannose for protein glycosylation [210]
	CAGL0D05742g		Has domain(s) with predicted dolichyl-diphosphooligosaccharide-protein glycotransferase activity, role in protein glycosylation and endoplasmic reticulum, integral component of membrane localization
	CAGL0G04851g	SUR4	Predicted fatty acid elongase involved in production of very long chain fatty acids for sphingolipid biosynthesis; mutants show reduced sensitivity to caspofungin and increased sensitivity to micafungin [212]
	CAGL0I00484g		Ortholog(s) have cell adhesion molecule binding, glucan endo-1,6-beta-glucosidase activity, glucan exo-1,3-beta-glucosidase activity
	CAGL0F07865g	UPC2B	Putative Zn(2)-Cys(6) binuclear cluster transcriptional regulator of ergosterol biosynthesis [213]
	CAGL0F08437g		Ortholog(s) have steryl deacetylase activity, role in response to toxic substance, sterol deacetylation and endoplasmic reticulum lumen, integral component of membrane, lipid droplet localization

Table 18. Continued.

	Systematic name	Standard name	Description
Nutrient and energy utilization	CAGL0I01210g		Ortholog(s) have [cytochrome c]-lysine N-methyltransferase activity, role in peptidyl-lysine methylation and cytosol localization
	CAGL0J06402g		Ortholog(s) have homocitrate synthase activity, role in DNA repair, histone displacement, lysine biosynthetic process via aminoadipic acid and nucleus localization
	CAGL0K12870g		Ortholog(s) have role in mitochondrial respiratory chain complex IV assembly and mitochondrion localization
	CAGL0L11088g		Ortholog(s) have phosphatase activity and role in dephosphorylation
	CAGL0M14025g		Has domain(s) with predicted oxidoreductase activity and role in oxidation-reduction process
	CAGL0F06941g	PYC1	Putative pyruvate carboxylase isoform; gene is upregulated in azole-resistant strain [211]
	CAGL0G02585g	LYS12	Homo-isocitrate dehydrogenase [203]
DNA/RNA	CAGL0I08371g		Ortholog(s) have DNA replication origin binding activity and role in DNA replication initiation, chromatin silencing at silent mating-type cassette, pre-replicative complex assembly involved in nuclear cell cycle DNA replication
	CAGL0K11506g		Ortholog(s) have 5'-3' exodeoxyribonuclease activity involved in UV-damage excision repair, 5'-flap endonuclease activity, double-stranded DNA 5'-3' exodeoxyribonuclease activity, single-stranded DNA 5'-3' exodeoxyribonuclease activity
	CAGL0K00913g		Ortholog(s) have formate-tetrahydrofolate ligase activity, methenyltetrahydrofolate cyclohydrolase activity, methylenetetrahydrofolate dehydrogenase (NADP+) activity, single-stranded DNA binding activity

Table 18. Continued.

	Systematic name	Standard name	Description
DNA/RNA	CAGL0L01397g		Ortholog(s) have DNA replication origin binding, MCM complex binding, chromatin binding, single-stranded DNA-dependent ATP-dependent DNA helicase activity
	CAGL0L09867g		Ortholog(s) have adenylate kinase activity, uridylate kinase activity, role in 'de novo' pyrimidine nucleobase biosynthetic process and mitochondrion, nucleus localization
	CAGL0D01716g		Ortholog(s) have DNA polymerase processivity factor activity
	CAGL0D01012g		Ortholog(s) have RNA polymerase II proximal promoter sequence-specific DNA binding, transcriptional activator activity, RNA polymerase II proximal promoter sequence-specific DNA binding activity
	CAGL0F02431g	ACO2	Ortholog(s) have role in mitochondrial translation and mitochondrion, nucleus localization
	CAGL0H07183g		Ortholog(s) have role in regulation of DNA methylation
Cell division	CAGL0J05676g	INN1	Ortholog(s) have enzyme regulator activity, role in chromosome organization, division septum assembly and HICS complex, cellular bud neck contractile ring localization
	CAGL0A03190g		Ortholog(s) have kinetochore localization
	CAGL0D04444g		Ortholog(s) have role in mitotic sister chromatid cohesion, negative regulation of chromosome condensation, negative regulation of maintenance of mitotic sister chromatid cohesion and nuclear cohesin complex localization
	CAGL0I05764g		Ortholog(s) have repressing transcription factor binding, transcription factor activity, transcription factor binding activity and role in negative regulation of transcription involved in G1/S transition of mitotic cell cycle
unknown	CAGL0C05313g		Protein of unknown function

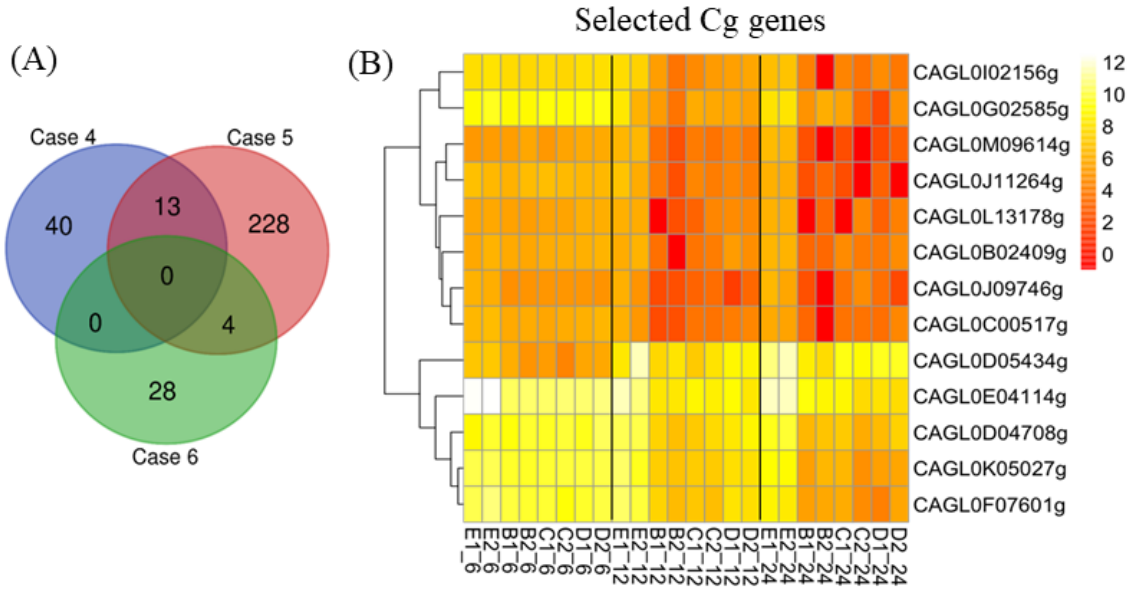

Figure 22. (A): Venn diagram of Cg significant genes in co-culture at 12 and 24 hours. Case 4: 12 hour, Case 5: 24 hour, Case 6: Cg mono-culture.(B): Heat map of Cg significant genes in co-culture at 12 and 24 hours. E: Cg, B: Ca:Cg 3:1, C: Ca:Cg 1:1, D: Ca:Cg 1:3. 2 biological replicates (i.e. E1 and E2). Normalized count data Log_2(counts).

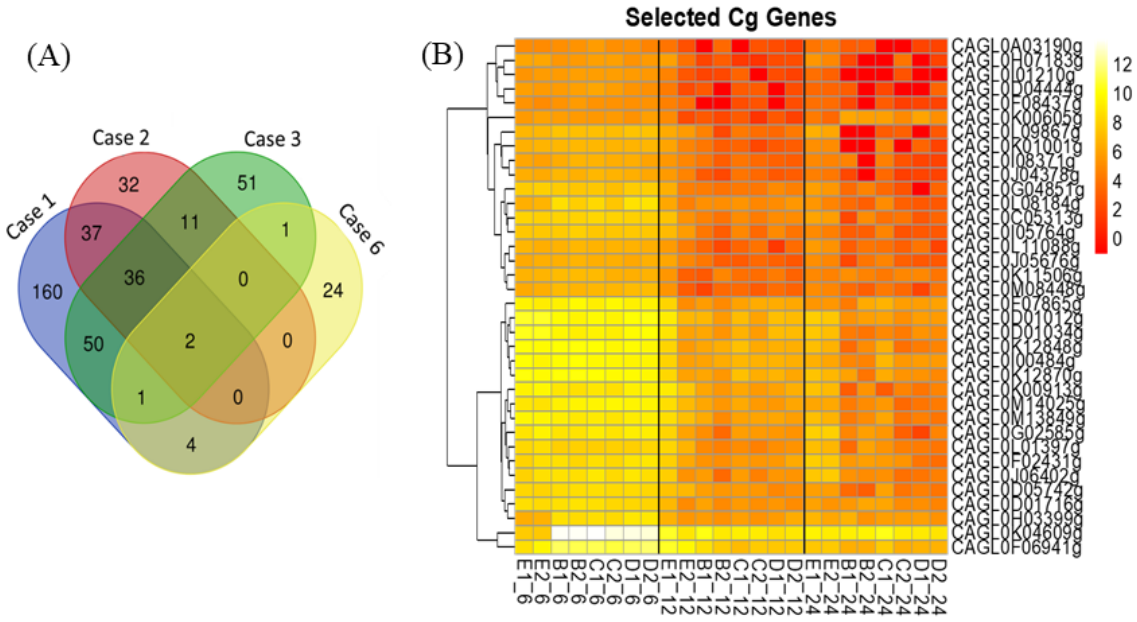

Figure 23. (A): Venn diagram of Cg significant genes in co-culture compared to monoculture. Case 1: Ca:Cg 3:1 biofilm, Case 2: Ca:Cg 1:1 biofilm, Case 3: Ca:Cg 1:3 biofilm, Case 6: Cg mono-culture. (B): Heat map of Cg significant genes in co-culture at 6, 12, and 24 hours. A: Ca, B: Ca:Cg 3:1, C: Ca:Cg 1:1, D: Ca:Cg 1:3. 2 biological replicates (i.e. A1 and A2). Normalized count data Log_2(counts).

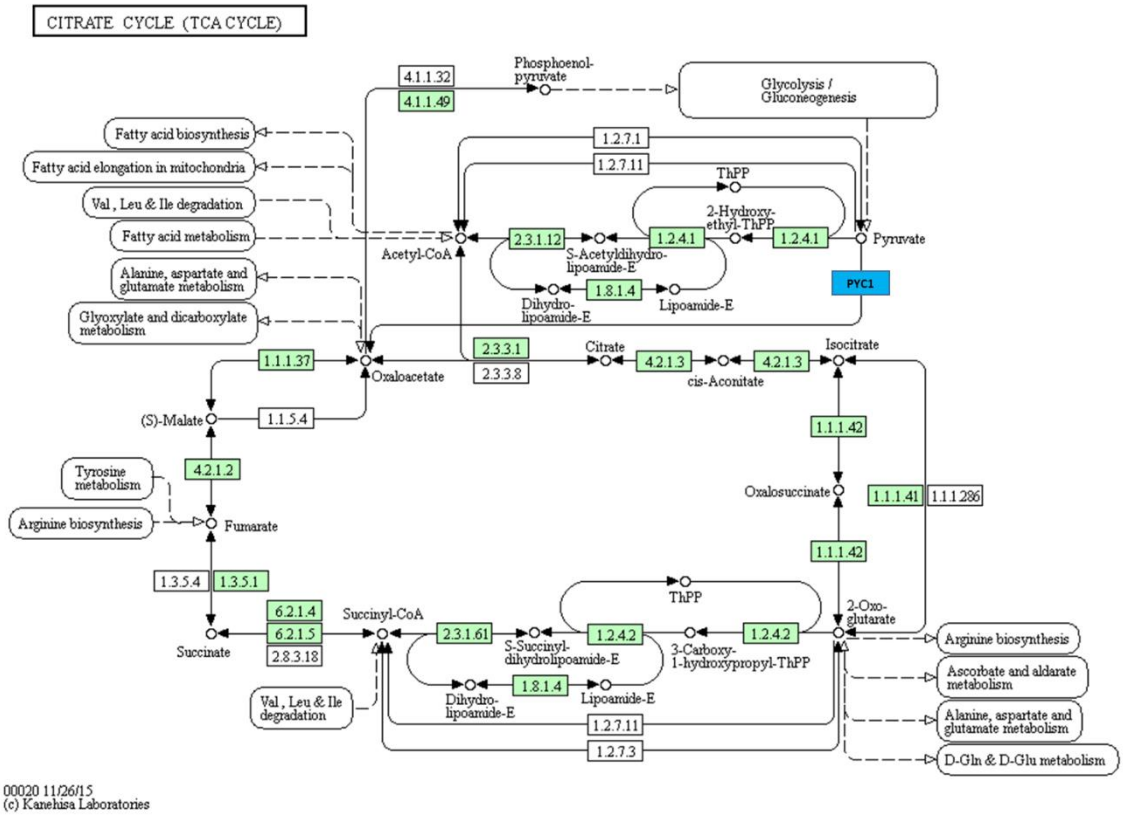

Figure 24. *C. glabrata* KEGG pathway for citrate cycle [218-220].

3.4.4 Increased cell wall lipids in C. albicans in Co-Culture Ca:Cg 1:3 biofilm

It is generally accepted that cell wall proteins and the extracellular matrix contribute to increased biofilm formation and antifungal resistance in *Candida* biofilms [229-233]. Our RNA-seq results indicated that the cell membrane lipids were significantly perturbed in both Ca and Cg in co-culture biofilms. In order to determine and visualize any differences in cell wall lipid composition between mono-culture and co-culture biofilms, filipin dye was used to stain lipids in both Ca and Cg biofilm cells. Filipin is known to interact with the 3-β-hydroxyl group of sterols and preferentially stains

ergosterol in the cell membrane and in lipid rafts. Here, we stained biofilm-derived cells of Ca, Ca:Cg 3:1, and Ca:Cg 1:3 with filipin and then imaged cells with a confocal microscope (see Materials and Methods). Filipin stained lipid rafts were visible in all three conditions, but there was an observed increased abundance of lipid staining on hyphal cell walls in co-culture biofilms Ca:Cg 3:1 and Ca:Cg 1:3 (Figure 25). Comstat2 was used to calculate the occupied surface area of filipin-stained cells. Figure 26 shows the Ca RFP-associated filipin surface area averages from 10 images per replicate. As demonstrated in Figure 26, Ca:Cg 1:3 biofilm had an overall increased lipid content compared to Ca mono-culture and Ca:Cg 3:1 biofilms, although this increase was not statistically significant. In biofilm assays, Ca:Cg 1:3 biofilm was the highest biofilm former and also demonstrated a modulation of lipid biosynthesis gene expression in RNA-seq analysis. For example, Ca*IPT1* was downregulated in co-culture biofilms and was most downregulated in Ca:Cg 1:3. Image analysis results confirm the RNA-seq reported findings, that cell membrane lipids are indeed modulated in *Candida* co-culture biofilms and most significantly in the highest biofilm former Ca:Cg 1:3. Overall, our study suggests modification to the cell wall for lipid biosynthesis and membrane transporters in both *C. albicans* and *C. glabrata* during co-culture biofilm formation. An increase in cell wall lipid content may contribute to increased biofilm formation in *Candida* co-cultures.

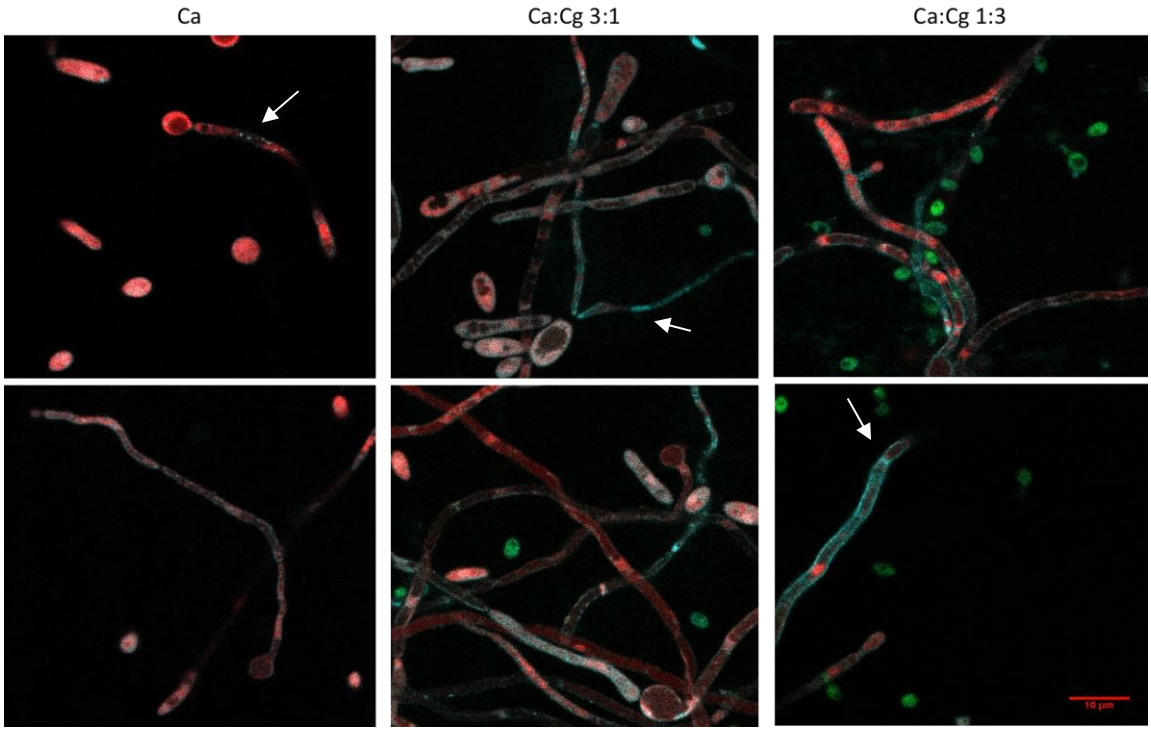

Figure 25. Confocal imaging of filipin-stained biofilm derived cells. Filipin (cyan), RFP (*C. albicans*), GFP (*C. glabrata*). White arrows point to lipid rafts.

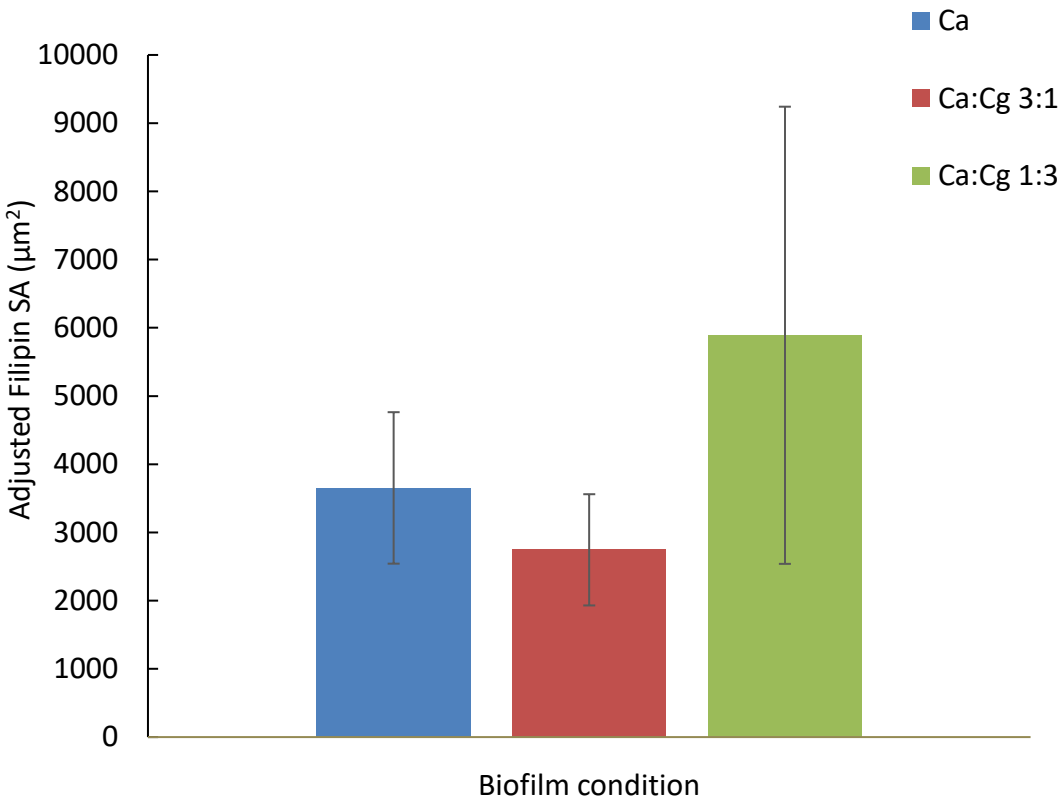

Figure 26. Quantification of surface area of filipin-stained lipids in *C. albicans* cell membrane between biofilm conditions. Error bars are standard error from 3 biological replicates and 10 images per replicate.

4. ELUCIDATING THE MECHANISMS OF FARNESOL, A CANDIDA QUORUM SENSING MOLECULE, ON CANDIDA CO-CULTURE BIOFILM FORMATION

4.1 Summary

Candida spp. are fungal commensal microorganisms that often resides on mucosal surfaces and grow as polymicrobial biofilms. If an individual is immunocompromised, prescribed antibiotics, or experiences inflammation, *Candida* spp. have the potential to become pathogenic and cause infection throughout the body. *Candida* infections are very difficult to treat due to biofilm persistence and inherent resistance to antifungal therapies. The two most common co-isolated *Candida* spp. are *C. albicans* (Ca) and *C. glabrata* (Cg), and co-cultures of these two species have been shown to exhibit increased virulence, biofilm formation, and antifungal drug resistance. A major factor during biofilm formation in *Candida* spp. is the production and response to quorum sensing molecules. One particular molecule, farnesol, is most significantly produced in *C. albicans* and regulates the Ca yeast-to-hyphae transition, decreases Ca hyphae formation, and overall has been shown to decrease biofilm formation. In this work, we aim to elucidate the mechanisms and role of farnesol in Ca:Cg co-culture biofilm formation. By using a *C. albicans* Δ*DPP3* strain (KWN2; *DPP3* is responsible for farnesol biosynthesis from FPP), we saw that biofilm formation increased in mono-culture biofilms but formation was not significantly affected in co-cultures. In KWN2, there was increased hyphae formation compared to wild type Ca and there was a further increase in hyphae in the highest biofilm former of Ca:Cg 1:3. When biofilms were exposed to exogenous farnesol during growth, biofilm formation

decreased in all conditions and the Ca:Cg 1:3 biofilm had less biofilm reduction with addition of 5 μM farnesol (~37% reduction) compared to Ca:Cg 1:1 (~45% reduction) using the wild type Ca strain. To investigate the potential role of Cg in modulating farnesol concentrations in *in vitro* Ca:Cg co-culture biofilms, intracellular farnesol uptake in Cg suspension cultures was measured via GC-MS. Preliminary results show that Cg suspension cultures do indeed sequester and/or possibly consume farnesol from the extracellular medium. Further studies plan to investigate these results, which will include calculating an overall farnesol mass balance in Cg cultures and farnesol downstream metabolite analysis in Cg as a result of possible Cg farnesol catabolism.

4.2 Introduction

The human microbiota is composed of a variety of fungal and bacterial species, many of which reside on mucosal surfaces. *Candida* is a commensal opportunistic pathogen [131] that has recently been described by Auchtung et al. as a transient fungal species [132] with the potential to expand and cause infection (*i.e.* candidiasis) in individuals with weakened immune systems or dysbiosis of the microbiome [6]. Once a *Candida* infection enters the blood stream and becomes systemic, mortality rates may reach as high as 50 percent [8]. *Candida* and other microbes often reside in the human body as biofilms, which is often a polymicrobial cellular structure that acts as a protective niche for microorganisms from external environments and antimicrobial treatments. *Candida* biofilms increases the pathogen's virulence through increased expression of virulence-associated adhesion genes and increased resistance to antifungal drugs [89, 139,

234-238]. Biofilms are commonly associated with mucosal surfaces, and high *Candida* mucosal colonization is linked to an increased risk of candidiasis infection and several gastrointestinal tract diseases such as Crohn's disease and ulcerative colitis [239]. *C. albicans* is the most common *Candida* spp. isolate from patients with candidiasis or candidemia [240-242], followed by *C. glabrata* as a common second most common isolate [7, 241, 243, 244]. *C. albicans* and *C. glabrata* are often co-isolated together during infection [83], which is also perpetuated by the inherent resistance of *C. glabrata* to many antifungal drugs (*e.g.* azole drugs) [245, 246]. Due to the variation in drug response and other factors, there is an emergence of infections from non-*albicans* pathogenic *Candida* spp. such as *C. glabrata* [247]. *C. albicans* and *C. glabrata* co-isolation is also associated with high levels of inflammation [84] and the presence of *C. albicans* with *C. glabrata* increases *C. glabrata* adhesion to *C. albicans* hyphae (an important virulence factor) and increases invasion of *C. glabrata* in vitro [12, 248].

Quorum sensing (QS) is the regulation of gene expression and group behavior in response to changes in cell population density. QS molecules are used by *Candida* spp. to sense cell density and control group behaviors such as virulence and biofilm formation. The two major QS molecules in *C. albicans* and *C. glabrata* are *E,E*-farnesol and tyrosol. Both molecules are produced by each species, where *C. albicans* produces more of each molecule than *C. glabrata*. *C. albicans* has been reported to produce ~ 10 – 60 µM farnesol (depending on the medium), whereas *C. glabrata* only produces on the order of ~ 1 µM farnesol [43]. Ca*DPP3* is considered the main gene responsible for the conversion of farnesyl pyrophosphate to farnesol in *C. albicans*, and a report by Navarathna et al.

demonstrated the reduction of farnesol production in *C. albicans DPP3* knockout strain [52]. The *C. glabrata* gene CAGL0H01177g has orthologs in *S. cerevisiae* (*DPP1*) with a role in farnesol biosynthesis. In *C. albicans*, farnesol is produced at higher cell population densities and promotes the yeast form of cell growth [39]. In *C. glabrata*, treatment with *E*,*E*-farnesol does not affect biofilm formation but slightly decreases the growth rate [43]. *Candida* biofilm formation is affected by farnesol and tyrosol during different stages of development. In the early biofilm growth stages, tyrosol concentration is higher and promotes adhesion and filamentation of *C. albicans*. As the biofilm grows, more farnesol is produced, which has a dominant effect over tyrosol and promotes the growth of more yeast cells that can ultimately lead to the final stage of dispersal of the biofilm [42]. Additionally, farnesol was shown by Ramage et al. to reduce biofilm formation in *C. albicans* and farnesol reduced hyphal growth, which is a major component of biofilm formation in *C. albicans* [41]. Farnesol has also been demonstrated to impact gene expression involved in the hyphal morphogenesis transformation in *C. albicans*. In general, farnesol affected the expression of genes belonging to the following categories: cell cycle, cell wall, stress response, drug resistance, heat shock, amino acid and carbon metabolism, and iron transport [249-253]. Our lab recently published that during *C. albicans – C. glabrata* co-culture biofilm growth there was increased biofilm formation, increased *C. albicans* (Ca) hyphae length as well as increased *C. glabrata* (Cg) attachment to Ca hyphae [139]. What we aim to further understand in this study is the impact of observed Ca-Cg interactions on overall farnesol concentration in biofilm cultures. We are interested in the impact of farnesol on biofilm formation and elucidating potential *C.*

glabrata mechanisms of farnesol mediation in *Candida* cultures such as farnesol sequestration or catabolism.

4.3 Materials and Methods

4.3.1 Microorganisms and growth conditions

C. albicans (SN152 and KWN2 (Δ*DPP3*), K. Nickerson) [52] and *C. glabrata* (ATCC 2001, GFP-labeled) were used in this study. Prior to the experiments, strains were cultured on Yeast Peptone Dextrose (YPD) agar plates for 48 hours at 30°C. For all experiments, single colonies were isolated from YPD agar plates and inoculated into 25 mL YNB medium (50 mM glucose and pH 7, Amresco) supplemented with 40 mg/L of arginine, histidine, and leucine. Cultures were grown overnight at 30°C and 170 rpm for 12 hours prior to experiments.

4.3.2 Construction of RFP-labeled Candida albicans strains

ENO1-RFP::Nat fusion in SN152 and KWN2 strains were constructed using overlap PCR. Primers used for amplification are listed in Table 19. Using *C. albicans* SC5314 ENO1-RFP::Nat gDNA as template, PCR1 (5' upstream, MO_RFPver_F and MO_ENO1US_R) and PCR2 (RFP-Nat and 3' downstream, MO_CaRFPNAT_F and MO_CaRFPamp_R) were amplified using Phusion High-Fidelity DNA Polymerase (Thermo Scientific^{TM}) using 58°C annealing temperature, 2 minute extension time at 72°C, and manufacturer concentration recommendations. PCR1 and PCR2 were gel-purified, and overlap PCR was performed using 50 ng of each template (PCR1 and PCR2), primers MO_RFPver_F and MO_CaRFPamp_R, with 58°C annealing temperature and

2:10 extension time at 72°C. A total of 10, 50 uL PCRs were pooled, cleaned and concentrated, and transformed into SN152 and KWN2 using the Zymo Research Frozen-EZ Yeast Transformation II Kit™. Modifications to the manufacturer protocol included: back-dilute an overnight culture 1:100 in 3 mL YPD and grow cells until OD_{600} of 0.8-1.0, incubate cells in EZ 3 solution for 3 hours, then after 3 hours add 2 mL YPD to cells for an outgrowth phase of 2 hours at 30°C. After the outgrowth phase, cells were centrifuged at 500 x g for 4 minutes, 3 mL of fresh YPD was added to cells and cells were allowed to grow overnight in a test tube at 30°C and 100 rpm. Cells were plated the next day on YPD+200 µg/ml Nourseothricin (Nourseothricin Sulfate, GoldBio), and allowed to grow for 2 days at 30°C. Successful transformants were confirmed via colony PCR and DNA sequencing.

Table 19. Primer list for amplification of *C. albicans* RFP integration cassette.

Name	Direction	Sequence (5' to 3')
MO_RFPver_F	forward	GATTTCCGAATACCCAATTGTT
MO_ENO1US_R	reverse	TAATAACATCTTCAGTGTTATCCATCAATTGAGAAGCCTTTTGGAAAT
MO_CaRFPNAT_F	forward	AGATTTCCAAAAGGCTTCTCAATTGATGGATAACACTGAAGATGTTATTA
MO_CaRFPNAT_R	reverse	TTTTTTTATTTAATCAGAGGCAAACGTAAAACGACGGCCAGTGAA
MO_ENO1DS_F	forward	TCGAATTCACTGGCCGTCGTTTTACGTTTGCCTCTGATTAAATAAAAA
MO_CaRFPamp_R	reverse	CATTATGTTTCAACCGCATTTC

4.3.3 Mycelium growth on agar plates

Candida albicans (SC5314, J. Berman, ENO1-RFP::Nat1) [92] and *Candida glabrata* (ATCC 2001, GFP-labeled) were used for mycelium growth studies. Prior to the experiments, strains were cultured on Yeast Peptone Dextrose (YPD) agar plates for 48 hours at 30°C. Mycelium formation on YPD agar plates was performed in accordance with prior studies [254]. Fresh colonies were lifted from the YPD agar surface and streaked out onto a YPD agar plate using a sterile inoculation loop. Distances between streaks were 5 – 10 mm. Agar plates were placed vertically at 30℃ for 3 days. As seen in Figure 27, growth between streaks is referred to as "inside" and growth not in-between is referred to as "outside". Images were taken with a Canon Powershot G10 on a Zeiss Axio Scope A.1 inverted light microscope using an N-ACHROPLAN 10x/0.25 objective.

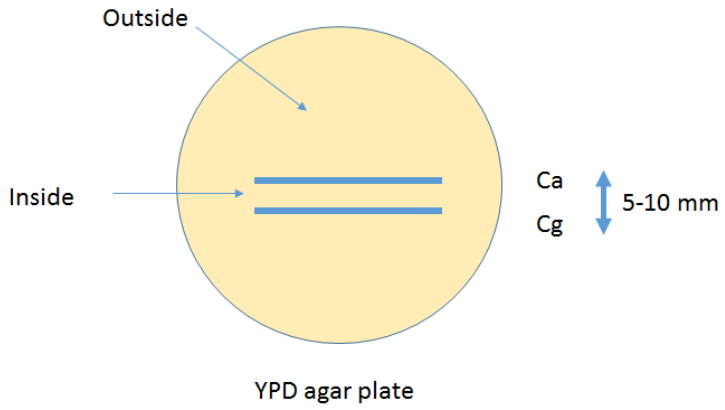

Figure 27. Experimental design for *Candida* mycelium growth. Ca = *C. albicans*, Cg = *C. glabrata*

4.3.4 Biofilm quantification assay

Biofilms were grown in 96-well polystyrene microtiter plates (Corning®). Wells were incubated overnight with heat-inactivated fetal bovine serum (HI FBS) at 37°C. Prior to experiment, wells were washed once in 1X phosphate buffered saline (PBS, pH 7.4). Overnight cultures were washed twice with PBS and resuspended in fresh YNB medium. A hemocytometer was used to calculate cell density and cell cultures were diluted to a final concentration of 10^7 cells/mL. A final volume of 100 µL per well was added to the 96-well plates. For the exogenous farnesol-addition biofilm assay, farnesol dilutions (4M, Sigma-Aldrich) were prepared fresh in ethanol and added to wells at time zero of initial biofilm seeding. Final ethanol concentration in medium was 1% and was kept constant between all farnesol concentrations. Ethanol only addition was used as the control 0 µM farnesol medium. Biofilms were allowed to grow at 37°C for 48 hours without agitation. After 48 hours, wells were washed twice with 200 µL PBS. 200 µL of 99% methanol was added to each biofilm. After 15 minutes, excess methanol was removed from the well and biofilms were allowed to dry completely. Once dry, 200 µL of 0.1% crystal violet was added to each biofilm and incubated at room temperature for 20 minutes [93]. Plates were rinsed gently under DI water to remove excess crystal violet stain from the wells and biofilms. Excess water was removed from the well and 150 µL of 33% acetic acid was added to each biofilm. Acetic acid samples were diluted 10-fold in a clear walled clear bottom 96-well Corning® plate and absorbance was measured at 590 nm in a plate reader (Molecular Devices SpectraMax® 340PC).

4.3.5 Confocal Laser Scanning Microscopy

For CLSM biofilm analysis, biofilms were grown in 2-well chambered coverglass slides (Nunc® Lab-Tek™) that were pre-incubated overnight with HI FBS at 37°C. Cultures of *C. albicans* and *C. glabrata* were grown overnight in YNB medium. Cultures were washed twice in PBS and adjusted to a cell density of 10^7 cells/mL. A final volume of 2 mL per well was used. Biofilms were allowed to grow for 24 hours at 37°C and no agitation. After 24 hours growth, biofilms were washed gently with PBS and fixed with 4% paraformaldehyde (room temperature, dark, 30 min). Images were acquired using Leica Confocal Microscope SP-8 (Leica, USA) using the HC PL APO CS 40x/0.85 dry objective with 488 nm and 561 nm laser lines to image GFP and RFP simultaneously. To analyze the structure of the biofilms, a series of optical sections were taken at 1 μm intervals throughout the depth of the biofilm. 3 biological replicates were imaged and 3 images were taken per biofilm sample and used in both Comstat2 and ImageJ analysis. Image J [94] was used to adjust brightness of images and quantify hyphae length. Comstat2 [95, 96] was used for calculating biofilm thickness.

4.3.6 Farnesol uptake test in C. glabrata suspension cultures

C. glabrata was grown overnight in 5 mL of YNB medium at 250 rpm and 30C. The next day, *C. glabrata* was diluted to an OD600 = 0.5 in fresh YNB medium. 300 μM of farnesol (4M, Sigma-Aldrich; diluted in ethanol) was added to cell culture, using ethanol addition as the control. 2 mL of cell culture was added to screw-cap test tubes and cells were cultured for up to 12 hours at 170 rpm and 30C. At each time point (0, 4, 8, 12 hours), one test tube was sacrificed and 2 mL of cell culture was centrifuged in a cryovial.

Supernatant was removed, and glass beads and 300 µL of hexane was added to each cryovial tube. Cells were disrupted using a Precellys 24 (Bertin Instruments) for 30 seconds at 6000x. Cell suspension was centrifuged at max speed and 200 µL of the hexane layer was collected. Samples were stored in a HPLC vial at -20C prior to GCMS analysis.

4.3.7 GC-MS/MS method for farnesol detection

Gas chromatography mass spectrometry (GC-MS) analyses were carried out with a Thermo Scientific TRACE 1300 GC (Thermo Scientific, Waltham, MA) coupled to a TSQ 8000 Evo operated in Selected Ion Monitoring (SIM) mode. Samples were injected with a TSQ RSH Autosampler (Thermo Scientific) using a 10 µL syringe. Chromatographic separation was achieved on a DB-1MS column (30m x 0.250mm x0.25um) from Agilent Technologies (Santa Clara, CA). The carrier gas was helium at a constant flow rate of 1 mL min^{-1}. The temperatures of MS transfer line and ionization source were set at 250 and 200 °C, respectively. The injection volume was 1 µL for all standards and samples. The inlet temperature was set to 250 °C and all injections were made in split mode at a ratio of 10:1. The 3 step ramp temperature program started at 50 °C, held for 0.5 min; increased until 170 °C at a rate of 40 °C min^{-1}, held for 1 min; increased to 190 °C at a rate of 4 °C min^{-1}, held for 1 min; and finally increased to 300 °C at a rate of 40 °C min^{-1} and held for 2 min. The total run time was 15.5 min. Data processing was performed with Xcalibur and TraceFinder software (Thermo Scientific). The following were the 4 ions for Farnesol at Retention Time 9.11 min within a 2 min scan range: m/z 41.1, 69.1, 81.1 and 93.1.

4.4 Results

4.4.1 Increased mycelium growth between C. albicans and C. glabrata cultures

To look at Ca-Cg interactions, we started by looking at mycelium growth between species on an agar plate. Cg does not produce hyphae, so no mycelium growth was expected from Cg to Ca cells (Figure 28). At 2 days growth on agar plates, no mycelium was seen between Ca-Ca streaks but filamentous clusters between the Ca-Cg streaks start to form (Figure 29). At 3 days growth, the mycelium formed between Ca-Ca are thinner filaments evenly distributed across the inside streaks. For the Ca-Cg plate, Ca still forms mycelium towards Cg but the hyphae are sparser and larger clusters of hyphae with extensive blastospore formation are observed (Figure 30). The observation of larger hyphae clusters between Ca-Cg compared to Ca-Ca may indicate that Cg is secreting a molecule to induce this behavior in Ca. Interestingly, there was no mycelium growth on the outside of the Ca streaks, indicating a concentration dependent response as often seen with quorum sensing or signaling molecules (Figure 28).

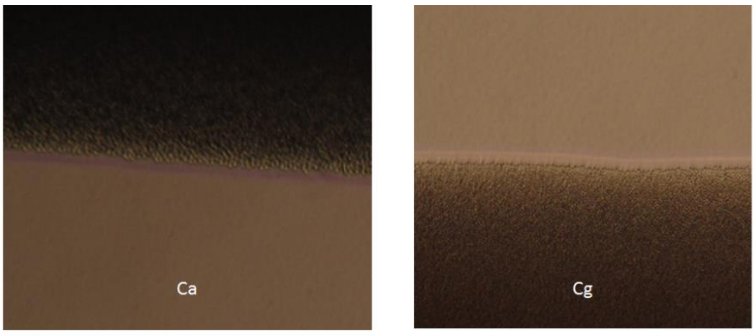

Figure 28. Outside of Ca and Cg agar streaks.

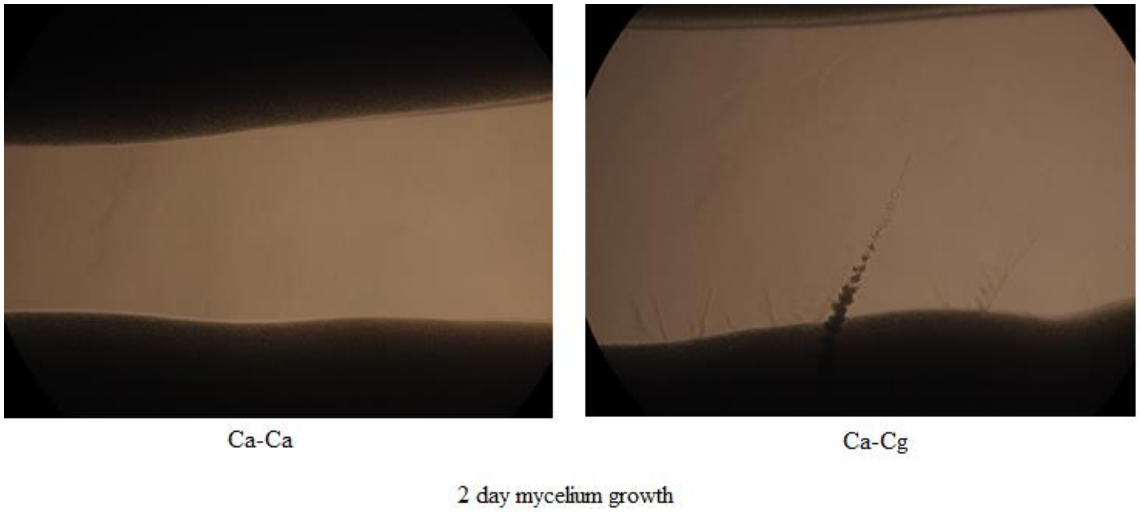

Figure 29. 2 day mycelium growth.

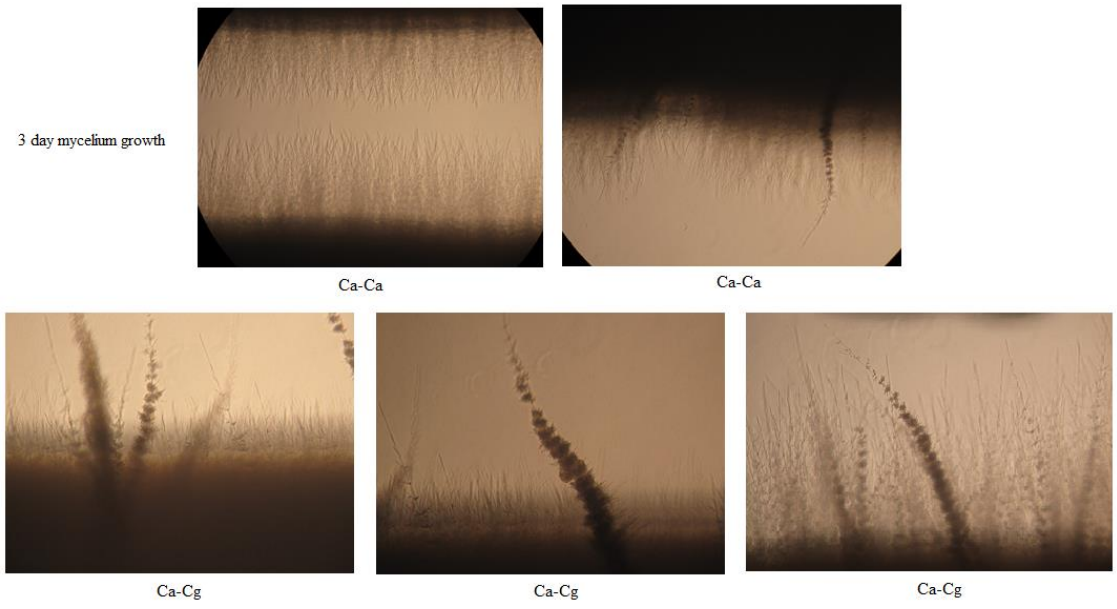

Figure 30. 3 day mycelium growth.

4.4.2 Biofilm formation in DPP3 knockout C. albicans strain KWN2

The *DPP3* gene is involved in the biosynthesis of farnesol in *C. albicans*. SN152, a wild type Ca species, was co-cultured with Cg at varying Ca:Cg ratios (Figure 31, Figure 32). The trend of co-culture biofilm formation was similar to previously published results using a different strain of Ca [139]. The Ca strain KWN2, a double allele *DPP3* knockout strain, was used to investigate the role of endogenous farnesol production on *Candida* mono-culture and co-culture biofilm formation. What was observed was that there was an overall increase in biofilm formation in KWN2 mono-culture and co-culture biofilms compared to the SN152 strain (Figure 31, Figure 32). KWN2 mono-culture biofilm formation was significantly higher than SN152 mono-culture (which has the DPP3 gene for farnesol production) (Figure 31), which demonstrates that endogenous farnesol production by *C. albicans* impacts mono-culture biofilm formation. This also shows that there are other factors involved besides farnesol production in co-culture biofilm growth that results in very high biofilm formation in Ca:Cg 1:1 and Ca:Cg 1:3 (Figure 31, Figure 32).

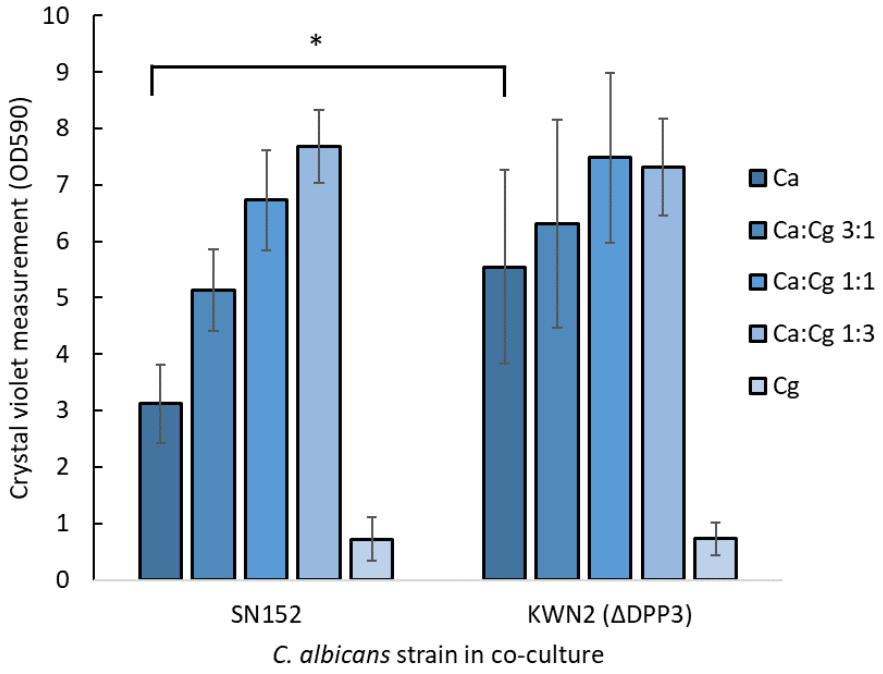

Figure 31. Biofilm formation in 96-well polystyrene plates. 48 hours growth. Data from average of 15 biological replicates per condition. Student's t-test, *:p-value < 0.05 compared with *C. albicans* SN152. Error bars are standard error of samples.

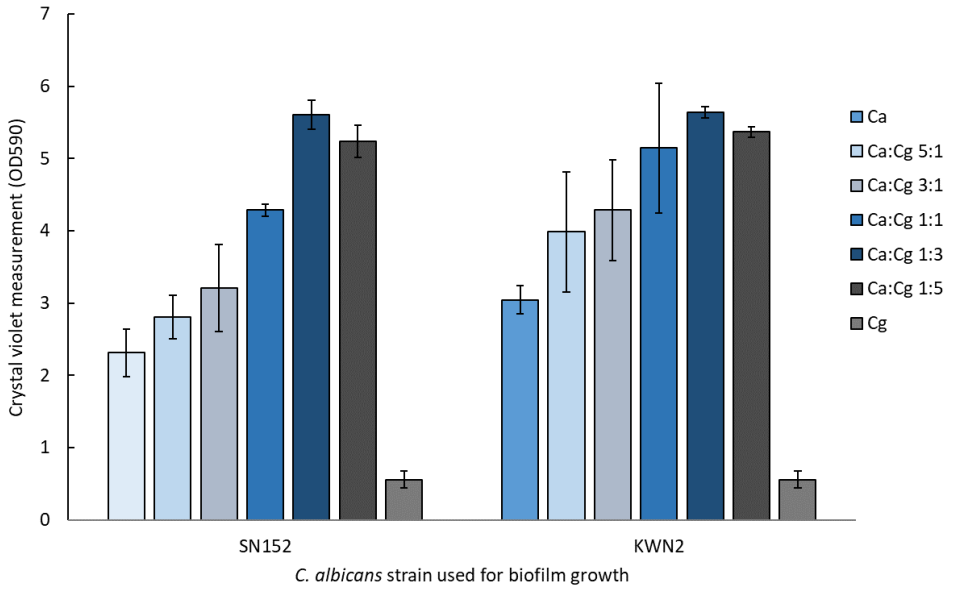

Figure 32. Biofilm formation between *C. albicans* species SN152 and KWN2 in mono-culture and co-culture biofilms, expanded ratios. 3 biological replicates. Error bars are standard error of samples.

4.4.3 Increased hyphae formation in DPP3 knockout C. albicans strain KWN2 biofilm

Confocal microscopy was utilized to further visualize and quantify biofilm formation in KWN2 compared to SN152 in both mono-culture and co-cultures to understand the impact of endogenous farnesol production on Ca morphology and biofilm formation. What was observed was that compared to SN152 cultures (Ca and Ca:Cg 1:3) (Figure 33), in KWN2 there was a significant increase in hyphae formation in both mono-culture and Ca:Cg 1:3 (Figure 34). KWN2 formed very long Ca hyphae throughout the entire biofilm, whereas SN152 formed some long hyphae with clustering in mono-culture but with a noticeable increase in hyphae and clustering in SN152:Cg 1:3 biofilms.

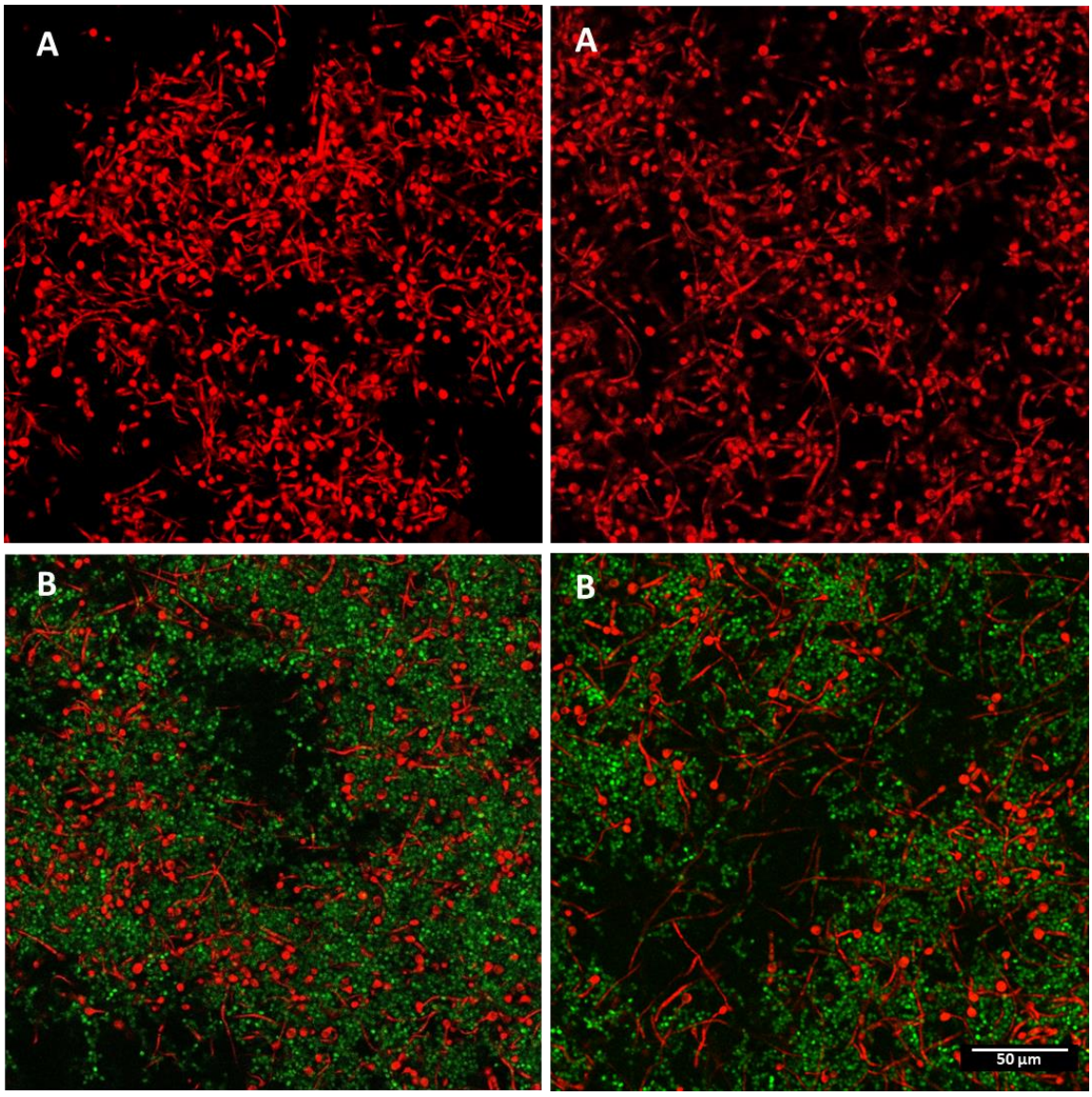

Figure 33. Biofilm structure shown through z-slice of SN152 (A) and SN152:Cg 1:3 (B) after 24 hours growth.

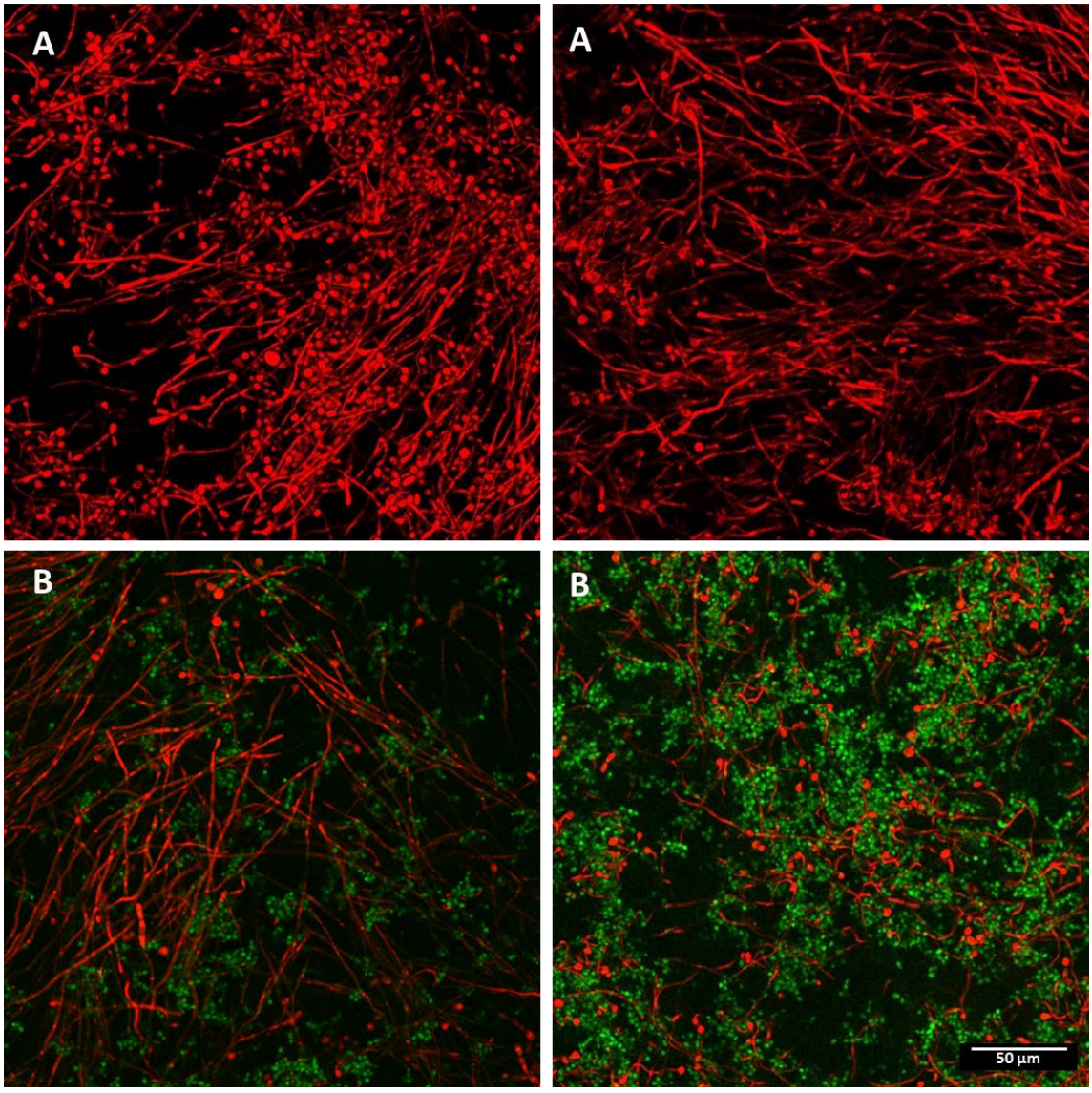

Figure 34. Biofilm structure shown through a representative z-slice of KWN2 (A) and KWN2:Cg 1:3 (B) after 24 hours growth.

Following confocal microscopy visual analysis, image analysis was used to quantify Ca hyphal length and overall biofilm thickness. There was an increase in Ca hyphae length in SN152:Cg 1:3 compared to SN152 mono-culture, and an increase in hyphae length in KWN2:Cg 1:3 compared to KWN2 (Figure 35). KWN2 mono-culture also had increased hyphae compared to mono-culture SN152 biofilms (Figure 35), which is mostly the result of decreased farnesol production which is known to increase hyphae formation in *C. albicans*. Surprisingly, biofilm thickness was only significantly different between KWN2 and KWN2:Cg and was relatively the same overall thickness between SN152, SN152:Cg 1:3, and KWN2 (Figure 36). What should be noted and was previously reported in our lab [139], is that there were still noticeable changes in biofilm topology between mono-culture and co-culture for both SN152 and KWN2 species where Ca:Cg 1:3 co-culture had an increase in varied thickness topology (data not shown). Overall, these results demonstrate the significant impact of farnesol on Ca mono-culture and co-culture biofilm formation and that there are additional factors involved besides farnesol production that results in increased biofilm formation in Ca:Cg 1:3 co-culture conditions.

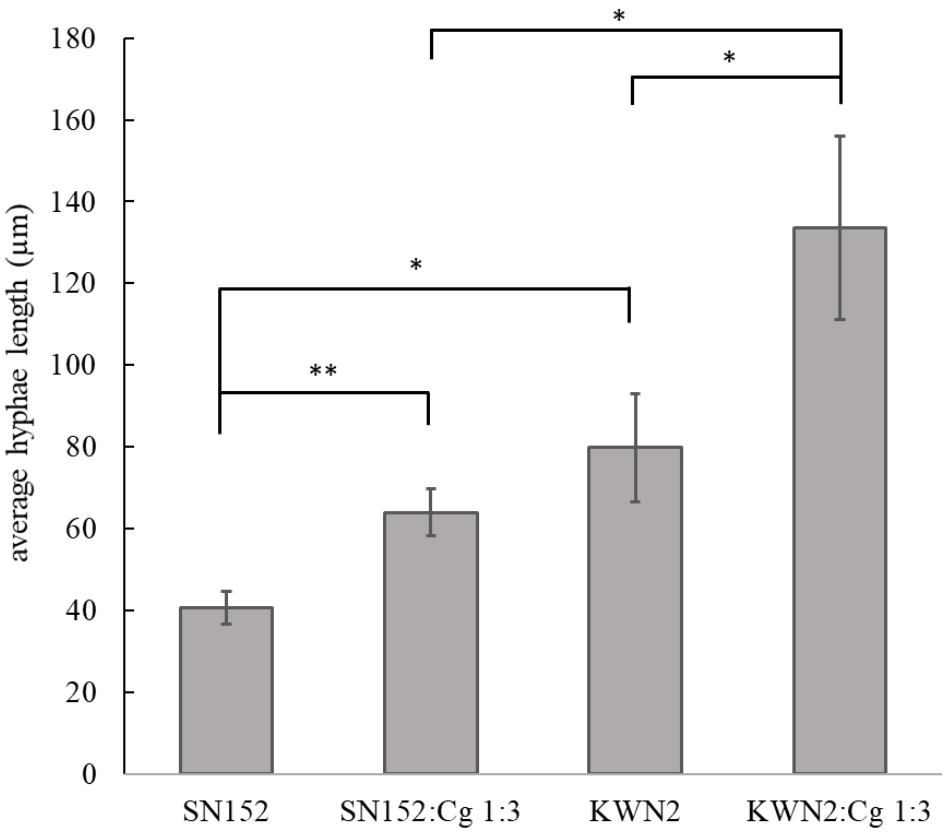

Figure 35. Average *C. albicans* hyphae length in biofilm. 3 biological replicates. Student's t-test, *:p-value < 0.05, **:p-value < 0.01. Error bars are standard error of samples.

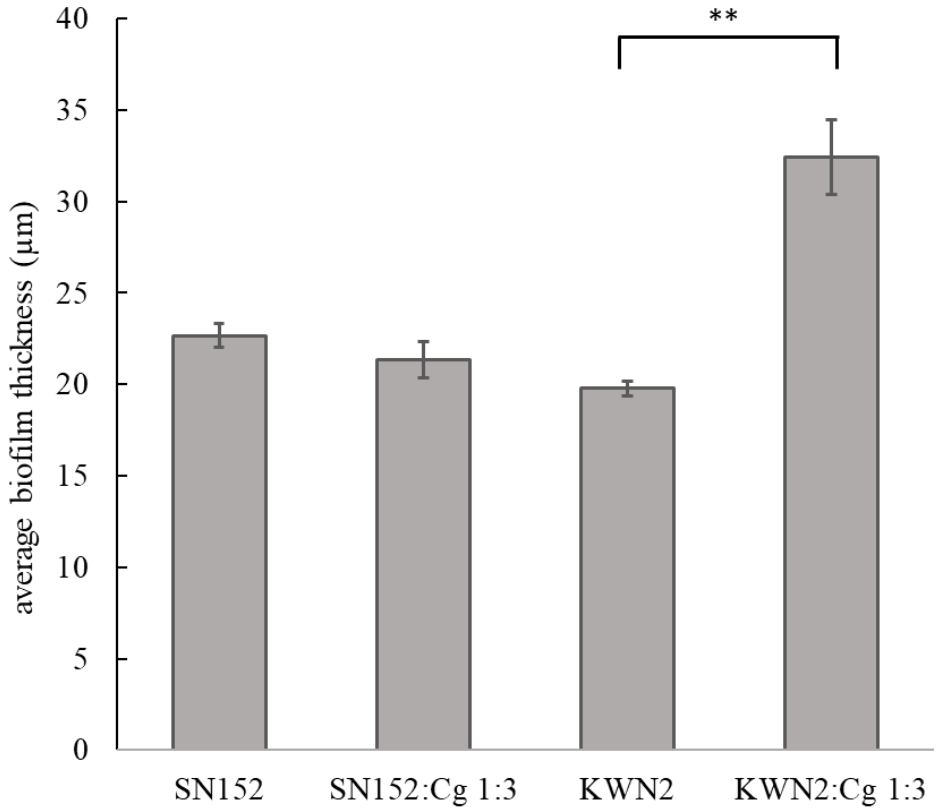

Figure 36. Average biofilm thickness between monoculture and co-culture *Candida* biofilms. 3 biological replicates. Student's t-test, **:p-value < 0.01 compared to monoculture *C. albicans* KWN2. Error bars are standard error of samples.

4.4.4 Biofilm formation with exogenous farnesol addition

To determine the effect of farnesol on biofilm development, exogenous farnesol was added to biofilms at the time of initial seeding into wells. Both strains SN152 and KWN2 were tested and in the 0 µM farnesol biofilm, growth was comparable between the two strains (Figure 37, Figure 38). Biofilm formation proved to be variable in KWN2 (Figure 31), most likely due to the fact that the *DPP3* knockout is not a clean deletion or complete removal of farnesol production in Ca. Biofilm formation in Ca and Ca:Cg 3:1

was not significantly impacted by exogenous farnesol addition, and biofilm formation remained low and close to the same over 0 to 1000 µM farnesol addition (Figure 37, Figure 38). In both SN152:Cg and KWN2:Cg co-culture biofilms, the percentage of biofilm decrease between untreated and farnesol treated biofilms was lower in the Ca:Cg 1:3 biofilm ratio. In SN152:Cg 1:1 there was a decrease of 45% between 0 and 5 µM farnesol, whereas Ca:Cg 1:3 only had a decrease of 37% (Figure 37). In KWN2:Cg 1:1, there was a decrease in biofilm formation of 34% and a decrease of 24% in Ca:Cg 1:3 (Figure 38). This signifies that Ca:Cg 1:3 biofilm formation, the highest biofilm former, is more resilient to exogenous farnesol addition during biofilm growth and development and is able to maintain high biofilm formation in the presence of up to 5 µM farnesol.

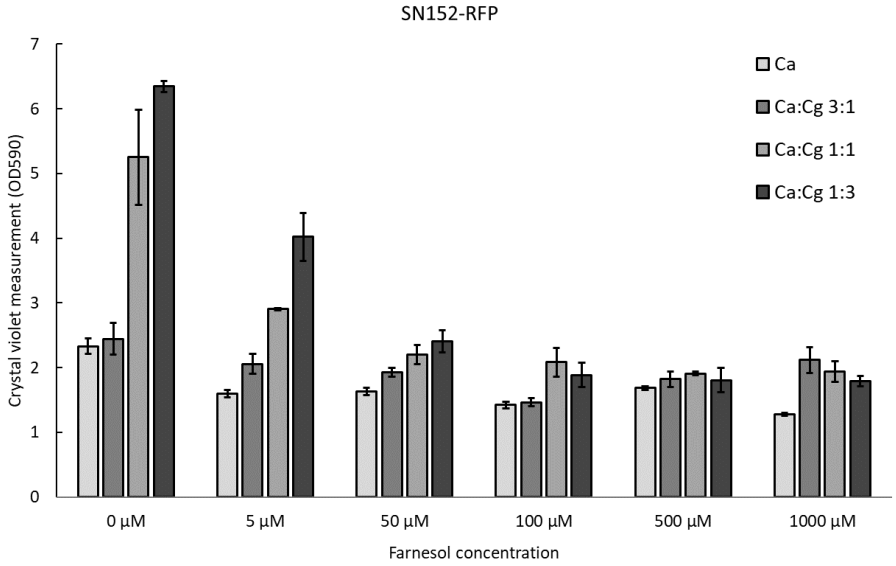

Figure 37. Biofilm formation of SN152 (Ca) and Ca:Cg with the addition of exogenous farnesol. 3 biological replicates. Error bars are standard error of samples.

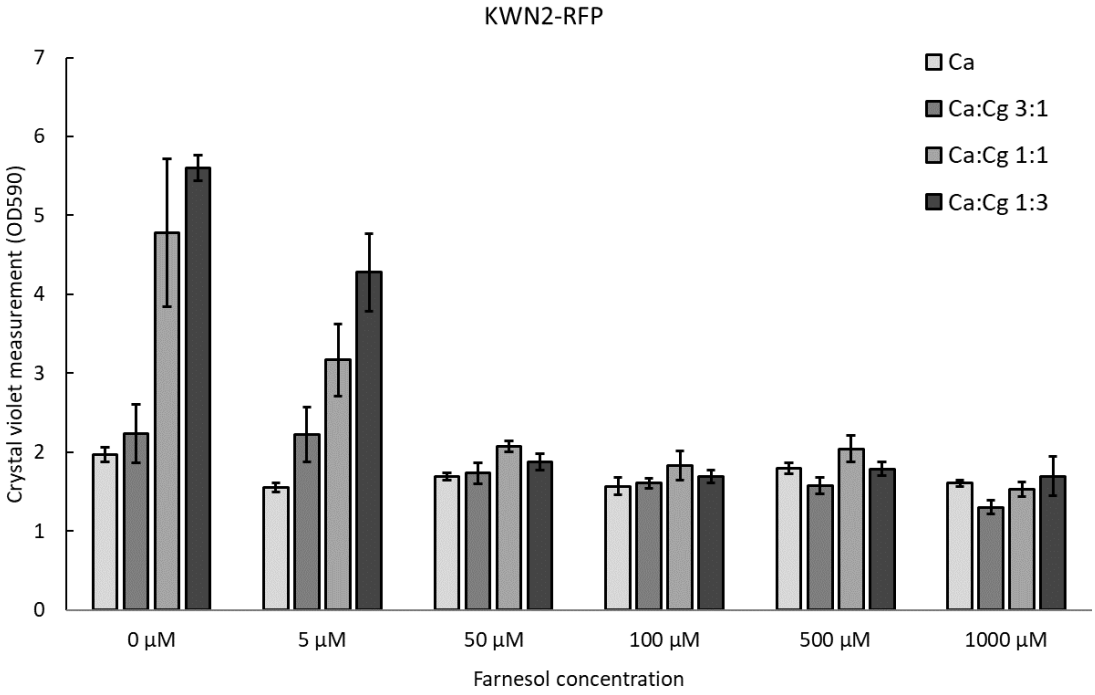

Figure 38. Biofilm formation of KWN2 (Ca) and Ca:Cg with the addition of exogenous farnesol. 3 biological replicates. Error bars are standard error of samples.

4.4.5 C. glabrata farnesol uptake in suspension cultures

In co-culture biofilms, Cg preferentially adhered to Ca hypha. Increased hypha formation was also observed under co-culture conditions. It is hypothesized that Cg may be playing a role in Ca farnesol mediation that would result in increased hypha. To better understand the impact and fate of farnesol in Cg during growth, the cellular uptake of farnesol in Cg suspension cultures was quantified over 12 hours growth using a GCMS (Figure 39, see Materials and Methods). We observed that upon immediate exposure of

Cg cells to farnesol via exogenous farnesol addition to culture medium, farnesol had a high affinity for the Cg cell wall and concentration of farnesol at time = 0h was ~35 µM. After 4 hours of growth, Cg farnesol concentration decreased to ~15 µM and remained at similar levels over 12 hours (Figure 39). Overall, these results support the hypothesis that Ca-Cg interactions involve farnesol mediation by Cg and that Cg is able to acquire and possibly metabolize farnesol. There are ongoing studies to further understand the uptake and possible conversion of farnesol in Cg.

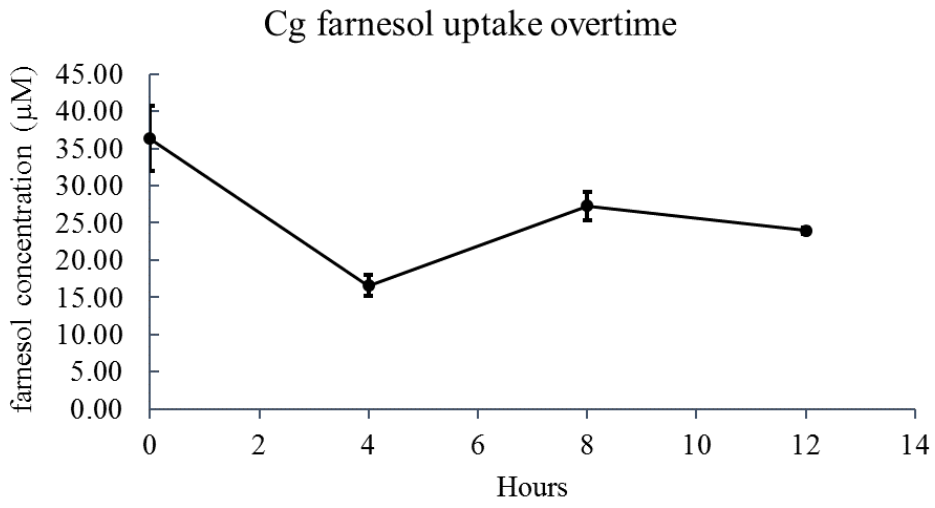

Figure 39. Farnesol concentration in *C. glabrata* suspension-grown cell pellets over time. Data represents two biological replicates and error bars are the standard error of samples.

4.5 Discussion

Candida spp. are commensal yet opportunistic fungal pathogens that are capable of causing superficial and serious life-threatening systemic infections. These infections

most frequently occur in hospital environments, where there is prevalent use of antibiotics and invasive measures (*e.g.* catheters). *Candida* spp. generally grow as biofilms, which are often polymicrobial cellular communities that act as a protective niche for microorganisms from external environments. Due to the protective nature of biofilms, biofilms are inherently difficult to treat with antibiotic therapies and can often perpetuate the cycle of infection by dispersal of biofilm cells to many different areas of the body to continue infection [89, 255-257]. *C. albicans*, the most commonly isolated *Candida* species [7], is capable of forming hyphae which increases biofilm formation. Additionally, *C. glabrata* is often the second most common isolate species from candidiasis [241, 243] and is naturally more resistant to antifungal drugs which makes this species very difficult to treat [246, 258]. *C. albicans* and *C. glabrata* are often co-isolated and when they are isolated together there is a reported increase in inflammation [84]. Previous studies have found that *C. glabrata* actually binds to *C. albicans* hyphae in biofilm formation [12] and that the co-culture of Ca:Cg biofilms yields to increased biofilm formation, virulence gene expression, and antifungal caspofungin drug resistance [23, 139].

Farnesol, a *Candida* spp. quorum sensing molecule, is produced as a part of the sterol biosynthesis pathway [57] and controls the yeast-to-hyphae transition and biofilm formation in *C. albicans* [41]. *C. albicans* is capable of producing up to ~60 uM farnesol in cultures, whereas *C. glabrata* produces very small amounts [43]. Farnesol is also an unstable molecule and most likely undergoes degradation and inactivation by modification of the farnesol molecule [67, 259]. The production and degradation, if any, of farnesol in *C. albicans* is still not well characterized or understood [53, 59]. What was investigated

in this work was the impact of farnesol on *C. albicans* and *C. glabrata* co-culture biofilm formation and also if *C. glabrata* actively sequesters farnesol in suspension cultures. What was observed was that in the *DPP3* knockout *C. albicans* strain KWN2 (*DPP3* converts FPP to farnesol), biofilm formation increased significantly in the mono-culture biofilm but not in Ca:Cg co-cultures. This result was expected because farnesol decreases biofilm formation [41], so by removing a majority of farnesol biosynthesis via *DPP3* deletion [52], biofilm formation is expected to increase. Ca hyphae length also increased in the KWN2 strain biofilms, where KWN2:Cg 1:3 had the longest Ca hyphae in all biofilm conditions. Farnesol reduces hyphae formation in *C. albicans* and the presence of hyphae is often associated with increased pathogenicity [41, 260-262]. When farnesol was exogenously added to the medium, it was observed that the co-culture Ca:Cg 1:1 and 1:3 biofilms were more resistant to biofilm biomass reduction compared to mono-culture biofilms. Ca:Cg 1:3 had the least reduction of biofilm biomass during farnesol exposure compared to the other co-culture conditions. This suggests that Ca:Cg 1:3 is more tolerant to farnesol or is more adept at overcoming the effects of exogenous farnesol, which results in the ability to form robust biofilms. Furthermore, preliminary results demonstrate that Cg sequesters farnesol to some degree in suspension cultures. It was previously reported by our lab that there were increased interactions between Ca and Cg in co-culture biofilms [139], and it is possible that these increased interactions result in Cg modulating the farnesol concentration in *in vitro* biofilms via either sequestration alone or in combination with enhanced farnesol degradation. Further investigation into these mechanisms are needed. Taken together, these results suggest that farnesol production (and possibly

reduction thereof) impacts *Candida* co-culture biofilm formation and that there are other factors besides farnesol that are involved in robust Ca:Cg co-culture biofilm formation.

4.6 Acknowledgements

We would like to thank the Nickerson lab for generously providing the SN152 and KWN2 *C. albicans* strains used in this study.

5. CONCLUSIONS AND RECOMMENDATIONS

5.1 Conclusions

In this work, we investigated the impact of the relative abundances of *C. albicans* and *C. glabrata* on overall biofilm formation and gene expression, and the significance and mechanisms of farnesol on *C. glabrata* and Ca:Cg co-culture biofilm formation. What was observed was that the relative starting ratio of Ca:Cg influences biofilm formation, and the ratio of Ca:Cg 1:3 was the highest biofilm former. With increasing Cg in co-culture Ca:Cg biofilms, there was an increase in biofilm formation, Ca:Cg interactions, Ca hyphal length, Ca virulence gene expression, and overall antifungal (caspofungin) drug resistance. Transcriptomic analysis was performed to better understand gene expression and regulation in *Candida* co-culture biofilms. What was discovered was that genes involved in lipid and cell wall biosynthesis were significantly perturbed in both Ca and Cg in co-culture biofilms, which was confirmed through *in vitro* confocal microscopy analysis. In Cg, transporter genes involved in iron and copper and genes involved in glycolysis and the citrate cycle were all significantly down-regulated which suggests a modulation of cell metabolism during co-culture biofilm formation. From the observation of increased biofilm formation and interactions between Ca and Cg in co-culture biofilms, the role of farnesol was further investigated due to its known impact on *Candida* hyphae and biofilm formation. Farnesol decreased *Candida* biofilm formation and there was increased biofilm formation in the KWN2 (*DPP3*) strain in both mono-culture and co-culture Ca:Cg 1:3 over wild type. To determine if Cg had any role in farnesol sequestration

or mediation of farnesol culture concentrations, Cg farnesol uptake was tested, where it was reported that Cg does indeed sequester exogenous farnesol while in suspension cultures. These results may shed light on the role of Cg in Ca:Cg co-culture biofilms and why with increasing Cg in co-culture, there is increased biofilm formation and virulence.

5.2 Recommendations for Further Research

To follow up RNA-seq results, it would be beneficial to have a more rigorous quantitative assay for lipids between mono-culture and co-culture *Candida* biofilms. RNA-seq results demonstrated that major components of the cell wall were modulated in both Ca and Cg during co-culture growth, so it would be interesting to see if that is able to be measured more robustly. Possible avenues for this type of quantification include electron microscopy for imaging localization of mannoprotein constituents [236], dry weight determination of cell wall components [236], or two-dimensional gel electrophoresis of extracted cell wall proteins [263]. For additional lipid-specific analysis, lipid extraction followed by lipid characterization (thin-layer chromatography and/or electrospray ionization-tandem mass spectrometry) is another option for cell wall lipid quantification [147]. Furthermore, genes involving biosynthesis of other cell wall components such as mannose were shown to be significantly down-regulated in *C. glabrata*. More extensive quantification could be done to determine cell wall component differences between co-culture and mono-culture biofilms.

In order to progress this work, the fate of farnesol needs to be further understood and studied in *Candida albicans* and *Candida glabrata* co-culture biofilms. This would

help elucidate the role and fate of farnesol in *C. glabrata*, and if *C. glabrata* actively sequesters or consumes farnesol in cultures in order to enhance overall biofilm formation of Ca:Cg co-cultures. We are currently investigating the impact of exogenous farnesol in *C. glabrata* suspension cultures to determine if Cg actively acquires farnesol from culture medium. Furthermore, downstream farnesol metabolite analysis of Cg cultures exposed to farnesol would be useful to understand the degradation products, if any, from Cg farnesol catabolism.

Still looking at the effect of farnesol on co-culture *Candida* biofilms, it would be beneficial to quantify the concentration of farnesol produced in *Candida* mono-culture and co-culture biofilms. In addition to farnesol quantification efforts in biofilms, it would also be useful to quantify and image lipid rafts in *Candida* co-culture biofilms of the Δ*DPP3* farnesol pathway knockout to study the impact of endogenous farnesol production on *Candida* cell membrane lipid rafts and cell wall biosynthesis. Furthermore, it would be useful to investigate the impact of farnesol on Cg biofilm and virulence gene expression and to look at the differential gene expression of virulence genes between Cg suspension, Cg mono-culture biofilm, and Cg co-culture biofilm with and without the addition of farnesol. This same gene expression analysis could be applied to Ca virulence gene expression.

REFERENCES

1. Gow, N.A.R., et al., *Candida albicans morphogenesis and host defence: discriminating invasion from colonization.* Nat Rev Micro, 2012. **10**(2): p. 112-122.
2. Kumamoto, C.A. and M.D. Vinces, *Alternative Candida albicans Lifestyles: Growth on Surfaces.* Annu. Rev. Microbiol., 2005. **59**: p. 113-33.
3. Wenzel, R.P. and M.B. Edmond, *The impact of hospital-acquired bloodstream infections.* Emerg Infect Dis, 2001. **7**(2): p. 174-177.
4. Pappas, P.G., F.P. Silveira, and A.S.T.I.D.C.o. Practice, *Candida in solid organ transplant recipients.* Am J Transplant, 2009. **9 Suppl 4**: p. S173-9.
5. Moran, C., et al., *Candida albicans and non-albicans bloodstream infections in adult and pediatric patients: comparison of mortality and costs.* Pediatr Infect Dis J, 2009. **28**(5): p. 433-5.
6. Huffnagle, G.B. and M.C. Noverr, *The emerging world of the fungal microbiome.* Trends Microbiol, 2013. **21**(7): p. 334-41.
7. Wisplinghoff, H., et al., *Nosocomial bloodstream infections due to Candida spp. in the USA: species distribution, clinical features and antifungal susceptibilities.* Int J Antimicrob Agents, 2014. **43**(1): p. 78-81.
8. Kabir, M.A., M.A. Hussain, and Z. Ahmad, *Candida albicans: A Model Organism for Studying Fungal Pathogens.* ISRN Microbiol, 2012. **2012**: p. 538694.

9. Nguyen, M.H., et al., *The Changing Face of Candidemia: Emergence of Non-Candida albicans Species and Antifungal Resistance.* Am J Med, 1996. **100**: p. 617-623.

10. Pfaller, M.A., R.N. Jones, and M. Castanheira, *Regional data analysis of Candida non-albicans strains collected in United States medical sites over a 6-year period, 2006-2011.* Mycoses, 2014. **57**(10): p. 602-11.

11. Azie, N., et al., *The PATH (Prospective Antifungal Therapy) Alliance(R) registry and invasive fungal infections: update 2012.* Diagn Microbiol Infect Dis, 2012. **73**(4): p. 293-300.

12. Tati, S., et al., *Candida glabrata Binding to Candida albicans Hyphae Enables Its Development in Oropharyngeal Candidiasis.* PLoS Pathog, 2016. **12**(3): p. e1005522.

13. Silva, S., et al., *Adherence and biofilm formation of non-Candida albicans Candida species.* Trends Microbiol, 2011. **19**(5): p. 241-7.

14. Hawser, S.P. and L.J. Douglas, *Resistance of Candida albicans biofilms to antifungal agents in vitro.* Antimicrob Agents Chemother, 1995. **39**(9): p. 2128-31.

15. Davies, D., *Understanding biofilm resistance to antibacterial agents.* Nat Rev Drug Discov, 2003. **2**(2): p. 114-22.

16. Chandra, J., et al., *Biofilm Formation by the Fungal Pathogen Candida albicans: Development, Architecture, and Drug Resistance.* J. Bacteriol., 2001. **183**(18): p. 5385-5394.

17. Nobile, C.J. and A.D. Johnson, *Candida albicans Biofilms and Human Disease.* Annu Rev Microbiol, 2015. **69**: p. 71-92.

18. Gulati, M. and C.J. Nobile, *Candida albicans biofilms: development, regulation, and molecular mechanisms.* Microbes Infect, 2016. **18**(5): p. 310-21.

19. Bonhomme, J. and C. d'Enfert, *Candida albicans biofilms: building a heterogeneous, drug-tolerant environment.* Curr Opin Microb, 2013. **16**(4): p. 398-403.

20. Douglas, L.J., *Candida biofilms and their role in infection.* Trends Microb, 2003. **11**(1): p. 30-36.

21. Kumamoto, C.A., *Candida biofilms.* Curr Opin Microb, 2002. **5**(6): p. 608-611.

22. Lopez-Ribot, J.L., *Large-scale biochemical profiling of the Candida albicans biofilm matrix: new compositional, structural, and functional insights.* MBio, 2014. **5**(5): p. e01781-14.

23. Kucharikova, S., et al., *Detailed comparison of Candida albicans and Candida glabrata biofilms under different conditions and their susceptibility to caspofungin and anidulafungin.* J Med Microbiol, 2011. **60**(Pt 9): p. 1261-9.

24. Pathak, A.K., S. Sharma, and P. Shrivastva, *Multi-species biofilm of Candida albicans and non-Candida albicans Candida species on acrylic substrate.* J Appl Oral Sci, 2012. **20**(1): p. 70-5.

25. Iraqui, I., et al., *The Yak1p kinase controls expression of adhesins and biofilm formation in Candida glabrata in a Sir4p-dependent pathway.* Mol Microbiol, 2005. **55**(4): p. 1259-71.

26. Batova, M., et al., *Molecular and phenotypic analysis of mutations causing anionic phospholipid deficiency in closely related yeast species.* Folia Microbiol (Praha), 2009. **54**(1): p. 30-6.

27. Culakova, H., et al., *Mutation of the CgPDR16 gene attenuates azole tolerance and biofilm production in pathogenic Candida glabrata.* Yeast, 2013. **30**(10): p. 403-14.

28. Bastidas, R.J., J. Heitman, and M.E. Cardenas, *The protein kinase Tor1 regulates adhesin gene expression in Candida albicans.* PLoS Pathog, 2009. **5**(2): p. e1000294.

29. Finkel, J.S. and A.P. Mitchell, *Genetic control of Candida albicans biofilm development.* Nat Rev Microbiol, 2011. **9**(2): p. 109-18.

30. Barros, P.P., et al., *Influence of Candida krusei and Candida glabrata on Candida albicans gene expression in in vitro biofilms.* Arch Oral Biol, 2016. **64**: p. 92-101.

31. Silva, S., et al., *The effect of silver nanoparticles and nystatin on mixed biofilms of Candida glabrata and Candida albicans on acrylic.* Med Mycol, 2013. **51**(2): p. 178-84.

32. Pereira-Cenci, T., et al., *The effect of Streptococcus mutans and Candida glabrata on Candida albicans biofilms formed on different surfaces.* Arch Oral Biol, 2008. **53**(8): p. 755-64.

33. Pesee, S., et al., *In vitro activity of Caspofungin combined with Fluconazole on mixed Candida albicans and Candida glabrata biofilm.* Med Mycol, 2016. **54**(4): p. 384-93.

34. Fidel, J., Paul L., J.A. Vazquez, and J.D. Sobel, *Candida glabrata: Review of Epidemiology, Pathogenesis, and Clinical Disease with Comparison to C. albicans.* Clin Microbiol Rev, 1999. **12**(1): p. 80-96.

35. Ng, T.S., et al., *Growth, biofilm formation, antifungal susceptibility and oxidative stress resistance of Candida glabrata are affected by different glucose concentrations.* Infect Genet Evol, 2016. **40**: p. 331-8.

36. Vavala, E., et al., *Characterization of biofilms in drug-sensitive and drug-resistant strains of Candida albicans.* J Chemother, 2013. **25**(2): p. 87-95.

37. Cataldi, V., et al., *Candida species isolated from different body sites and their antifungal susceptibility pattern: Cross-analysis of Candida albicans and Candida glabrata biofilms.* Med Mycol, 2016.

38. Chen, H., et al., *Tyrosol is a quorum-sensing molecule in Candida albicans.* Proc Natl Acad Sci, 2004. **101**(14): p. 5048-5052.

39. Hornby, J.M., et al., *Quorum sensing in the dimorphic fungus Candida albicans is mediated by farnesol.* Appl Environ Microbiol, 2001. **67**(7): p. 2982-2992.

40. Oh, K.B., et al., *Purification and characterization of an autoregulatory substance capable of regulating the morphological transition in Candida albicans.* Proc Natl Acad Sci, 2001. **98**(8): p. 4664-4668.

41. Ramage, G., et al., *Inhibition of Candida albicans Biofilm Formation by Farnesol, a Quorum-Sensing Molecule.* Appl Environ Microbiol, 2002. **68**(11): p. 5459-5463.

42. Alem, M.A., et al., *Production of tyrosol by Candida albicans biofilms and its role in quorum sensing and biofilm development.* Eukaryot Cell, 2006. **5**(10): p. 1770-9.

43. Weber, K., B. Schulz, and M. Ruhnke, *The quorum-sensing molecule E,E-farnesol--its variable secretion and its impact on the growth and metabolism of Candida species.* Yeast, 2010. **27**(9): p. 727-39.

44. Cremer, J., V. Vatou, and I. Braveny, *2,4-(hydroxyphenyl)-ethanol, an antioxidative agent produced by Candida spp., impairs neutrophilic yeast killing in vitro.* FEMS Microbiol Lett, 1999. **170**(2): p. 319-325.

45. Monteiro, D.R., et al., *Effect of tyrosol on adhesion of Candida albicans and Candida glabrata to acrylic surfaces.* Med Mycol, 2015. **53**(7): p. 656-65.

46. Ghosh, S., et al., *Regulation of aromatic alcohol production in Candida albicans.* Appl Environ Microbiol, 2008. **74**(23): p. 7211-8.

47. Kradolfer, P., P. Niederberger, and R. Hutter, *Tryptophan degradation in Saccharomyces cerevisiae: characterization of two aromatic aminotransferases.* Arch Microbiol, 1982. **133**(3): p. 242-8.

48. Sentheshanmuganathan, S. and S.R. Elsden, *The mechanism of the formation of tyrosol by Saccharomyces cerevisiae.* Biochem J, 1958. **69**(2): p. 210-8.

49. Nakayama, H., et al., *Depletion of the squalene synthase (ERG9) gene does not impair growth of Candida glabrata in mice.* Antimicrob Agents Chemother, 2000. **44**(9): p. 2411-8.

50. Song, J.L., et al., *Antifungal activity of fluconazole in combination with lovastatin and their effects on gene expression in the ergosterol and prenylation pathways in Candida albicans.* Med Mycol, 2003. **41**(5): p. 417-25.

51. Davis, D.A., et al., *Candida albicans Mds3p, a conserved regulator of pH responses and virulence identified through insertional mutagenesis.* Genetics, 2002. **162**(4): p. 1573-81.

52. Navarathna, D.H., et al., *Effect of farnesol on a mouse model of systemic candidiasis, determined by use of a DPP3 knockout mutant of Candida albicans.* Infect Immun, 2007. **75**(4): p. 1609-18.

53. Polke, M., et al., *Farnesol signalling in Candida albicans - more than just communication.* Crit Rev Microbiol, 2018. **44**(2): p. 230-243.

54. Zhang, L., et al., *Bisbibenzyls, a new type of antifungal agent, inhibit morphogenesis switch and biofilm formation through upregulation of DPP3 in Candida albicans.* PLoS One, 2011. **6**(12): p. e28953.

55. Chang, W., et al., *Retigeric acid B attenuates the virulence of Candida albicans via inhibiting adenylyl cyclase activity targeted by enhanced farnesol production.* PLoS One, 2012. **7**(7): p. e41624.

56. Nickerson, K.W., A.L. Atkin, and J.M. Hornby, *Quorum sensing in dimorphic fungi: farnesol and beyond.* Appl Environ Microbiol, 2006. **72**(6): p. 3805-13.

57. Hornby, J.M., B.W. Kebaara, and K.W. Nickerson, *Farnesol biosynthesis in Candida albicans: cellular response to sterol inhibition by zaragozic acid B.* Antimicrob Agents Chemother, 2003. **47**(7): p. 2366-9.

58. Han, T.L., R.D. Cannon, and S.G. Villas-Boas, *The metabolic response of Candida albicans to farnesol under hyphae-inducing conditions.* FEMS Yeast Res, 2012. **12**(8): p. 879-89.

59. Nickerson, K.W. and A.L. Atkin, *Deciphering fungal dimorphism: Farnesol's unanswered questions.* Mol Microbiol, 2017. **103**(4): p. 567-575.

60. Dumitru, R., et al., *In vivo and in vitro anaerobic mating in Candida albicans.* Eukaryot Cell, 2007. **6**(3): p. 465-72.

61. Hargarten, J.C., et al., *Candida albicans Quorum Sensing Molecules Stimulate Mouse Macrophage Migration.* Infect Immun, 2015. **83**(10): p. 3857-64.

62. Dumitru, R., J.M. Hornby, and K.W. Nickerson, *Defined anaerobic growth medium for studying Candida albicans basic biology and resistance to eight antifungal drugs.* Antimicrob Agents Chemother, 2004. **48**(7): p. 2350-4.

63. Langford, M.L., et al., *Activity and toxicity of farnesol towards Candida albicans are dependent on growth conditions.* Antimicrob Agents Chemother, 2010. **54**(2): p. 940-2.

64. Kebaara, B.W., et al., *Candida albicans Tup1 is involved in farnesol-mediated inhibition of filamentous-growth induction.* Eukaryot Cell, 2008. **7**(6): p. 980-7.

65. Kadosh, D. and A.D. Johnson, *Induction of the Candida albicans filamentous growth program by relief of transcriptional repression: a genome-wide analysis.* Mol Biol Cell, 2005. **16**(6): p. 2903-12.

66. Polke, M., et al., *A functional link between hyphal maintenance and quorum sensing in Candida albicans.* Mol Microbiol, 2017. **103**(4): p. 595-617.

67. Shchepin, R., et al., *Quorum sensing in Candida albicans: probing farnesol's mode of action with 40 natural and synthetic farnesol analogs.* Chem Biol, 2003. **10**(8): p. 743-50.

68. Forman, B.M., et al., *Identification of a nuclear receptor that is activated by farnesol metabolites.* Cell, 1995. **81**(5): p. 687-93.

69. Crick, D.C., D.A. Andres, and C.J. Waechter, *Farnesol is utilized for protein isoprenylation and the biosynthesis of cholesterol in mammalian cells.* Biochem Biophys Res Commun, 1995. **211**(2): p. 590-9.

70. Edwards, P.A. and J. Ericsson, *Sterols and isoprenoids: signaling molecules derived from the cholesterol biosynthetic pathway.* Annu Rev Biochem, 1999. **68**: p. 157-85.

71. Thai, L., et al., *Farnesol is utilized for isoprenoid biosynthesis in plant cells via farnesyl pyrophosphate formed by successive monophosphorylation reactions.* Proc Natl Acad Sci U S A, 1999. **96**(23): p. 13080-5.

72. Mateos, R., L. Goya, and L. Bravo, *Metabolism of the olive oil phenols hydroxytyrosol, tyrosol, and hydroxytyrosyl acetate by human hepatoma HepG2 cells.* J Agric Food Chem, 2005. **53**(26): p. 9897-905.

73. Corona, G., et al., *The fate of olive oil polyphenols in the gastrointestinal tract: implications of gastric and colonic microflora-dependent biotransformation.* Free Radic Res, 2006. **40**(6): p. 647-58.

74. Underhill, D.M. and I.D. Iliev, *The mycobiota: interactions between commensal fungi and the host immune system.* Nat Rev Immunol, 2014. **14**(6): p. 405-16.

75. Cho, I. and M.J. Blaser, *The human microbiome: at the interface of health and disease.* Nat Rev Genet, 2012. **13**(4): p. 260-70.

76. Bansal, T., et al., *The bacterial signal indole increases epithelial-cell tight-junction resistance and attenuates indicators of inflammation.* Proc Natl Acad Sci U S A, 2010. **107**(1): p. 228-33.

77. Berg, R.D., *The indigenous gastrointestinal microflora.* Trends Microbiol, 1996. **4**(11): p. 430-5.

78. Claesson, M.J., et al., *Gut microbiota composition correlates with diet and health in the elderly.* Nature, 2012. **488**(7410): p. 178-84.

79. Garrett, W.S., J.I. Gordon, and L.H. Glimcher, *Homeostasis and inflammation in the intestine.* Cell, 2010. **140**(6): p. 859-70.

80. Costello, E.K., et al., *Bacterial community variation in human body habitats across space and time.* Science, 2009. **326**(5960): p. 1694-7.

81. Qin, J., et al., *A human gut microbial gene catalogue established by metagenomic sequencing.* Nature, 2010. **464**(7285): p. 59-65.

82. Arumugam, M., et al., *Enterotypes of the human gut microbiome.* Nature, 2011. **473**(7346): p. 174-180.

83. Okada, K., et al., *A Clinical Study of Candida albicans and Candida glabrata Co-infection of Oral Candidiasis.* Ronen Shika Igaku, 2016. **31**(3): p. 346-353.

84. Coco, B.J., et al., *Mixed Candida albicans and Candida glabrata populations associated with the pathogenesis of denture stomatitis.* Oral Microbiol Immunol, 2008. **23**(5): p. 377-83.

85. Pfaller, M.A., et al., *In vitro activities of ravuconazole and voriconazole compared with those of four approved systemic antifungal agents against 6,970 clinical isolates of Candida spp.* Antimicrob Agents Chemother, 2002. **46**(6): p. 1723-7.

86. Pfaller, M.A., et al., *Evaluation of the etest method using Mueller-Hinton agar with glucose and methylene blue for determining amphotericin B MICs for 4,936 clinical isolates of Candida species.* J Clin Microbiol, 2004. **42**(11): p. 4977-9.

87. Davies, A., et al., *Oral yeast carriage in patients with advanced cancer.* Oral Microbiol Immunol, 2002. **17**: p. 79-84.

88. Kuhn, D.M., et al., *Antifungal Susceptibility of Candida Biofilms: Unique Efficacy of Amphotericin B Lipid Formulations and Echinocandins.* Antimicrob Agents Chemother, 2002. **46**(6): p. 1773-1780.

89. Uppuluri, P., et al., *Dispersion as an important step in the Candida albicans biofilm developmental cycle.* PLoS Pathog, 2010. **6**(3): p. e1000828.

90. Harriott, M.M. and M.C. Noverr, *Candida albicans and Staphylococcus aureus form polymicrobial biofilms: effects on antimicrobial resistance.* Antimicrob Agents Chemother, 2009. **53**(9): p. 3914-22.

91. Heisel, T., et al., *High-Fat Diet Changes Fungal Microbiomes and Interkingdom Relationships in the Murine Gut.* mSphere, 2017. **2**(5).

92. Huang, M., et al., *Evolutionary Dynamics of Candida albicans during In Vitro Evolution.* Eukaryot Cell, 2011. **10**(11): p. 1413-1421.

93. Peeters, E., H.J. Nelis, and T. Coenye, *Comparison of multiple methods for quantification of microbial biofilms grown in microtiter plates.* J Microbiol Methods, 2008. **72**(2): p. 157-65.

94. Schneider, C.A., W.S. Rasband, and K.W. Eliceiri, *NIH Image to ImageJ: 25 years of image analysis.* Nat Methods, 2012. **9**(7): p. 671-5.

95. Heydorn, A., et al., *Quantification of biofilm structures by the novel computer program COMSTAT.* Microbiology, 2000. **146 (Pt 10)**: p. 2395-407.

96. Vorregaard, M., *Comstat2 - a modern 3D image analysis environment for biofilms.* Informatics and Mathematical Modelling, 2008: p. 85.

97. CLSI, *Reference Method for Broth Dilution Antifungal Susceptibility Testing of Yeasts; Approved Standard, Second Edition. M27-A2.* Clinical and Laboratory Standards Institute, 2002. **22**.

98. Pierce, C.G., et al., *A simple and reproducible 96-well plate-based method for the formation of fungal biofilms and its application to antifungal susceptibility testing.* Nat Protoc, 2008. **3**(9): p. 1494-500.

99. Chandra, J., P.K. Mukherjee, and M.A. Ghannoum, *In vitro growth and analysis of Candida biofilms.* Nat Protoc, 2008. **3**(12): p. 1909-24.

100. Calderone, R.A. and W.A. Fonzi, *Virulence factors of Candida albicans.* Trends Microbiol, 2001. **9**(7): p. 327-35.

101. Sudbery, P.E., *Growth of Candida albicans hyphae.* Nat Rev Microbiol, 2011. **9**(10): p. 737-48.

102. Iraqui, I., et al., *The Yak1p kinase controls expression of adhesins and biofilm formation in Candida glabrata in a Sir4p-dependent pathway.* Mol. Microbiol., 2005. **55**(4): p. 1259-1271.

103. Nobile, C.J., et al., *Function of Candida albicans adhesin Hwp1 in biofilm formation.* Eukaryot Cell, 2006. **5**(10): p. 1604-10.

104. Joo, M.Y., et al., *Expression of SAP5 and SAP9 in Candida albicans biofilms: comparison of bloodstream isolates with isolates from other sources.* Med Mycol, 2013. **51**(8): p. 892-896.

105. Naglik, J.R., et al., *Quantitative expression of the Candida albicans secreted aspartyl proteinase gene family in human oral and vaginal candidiasis.* Microbiology, 2008. **154**(Pt 11): p. 3266-80.

106. Vale-Silva, L.A., et al., *Upregulation of the Adhesin Gene EPA1 Mediated by PDR1 in Candida glabrata Leads to Enhanced Host Colonization.* mSphere, 2016. **1**(2).

107. Lamfon, H., et al., *Susceptibility of Candida albicans biofilms grown in a constant depth film fermentor to chlorhexidine, fluconazole and miconazole: a longitudinal study.* J Antimicrob Chemother, 2004. **53**(2): p. 383-385.

108. Mukherjee, P.K., et al., *Oral Mycobiome Analysis of HIV-Infected Patients: Identification of Pichia as an Antagonist of Opportunistic Fungi.* PLoS Pathog, 2014. **10**(3).

109. Kim, D., et al., *Candida albicans stimulates Streptococcus mutans microcolony development via cross-kingdom biofilm-derived metabolites.* Sci Rep, 2017. **7**: p. 41332.

110. van Leeuwen, P.T., et al., *Interspecies Interactions between Clostridium difficile and Candida albicans.* mSphere, 2016. **1**(6).

111. Redding, S.W., et al., *Candida glabrata is an emerging cause of oropharyngeal candidiasis in patients receiving radiation for head and neck cancer.* Oral Surg Oral Med Oral Pathol Oral Radiol and Endod, 2004. **97**(1): p. 47-52.

112. Rocco, T.R., S.E. Reinert, and H.H. Simms, *Effects of fluconazole administration in critically ill patients - Analysis of bacterial and fungal resistance.* Arch Surg, 2000. **135**(2): p. 160-165.

113. Lortholary, O., et al., *Recent Exposure to Caspofungin or Fluconazole Influences the Epidemiology of Candidemia: a Prospective Multicenter Study Involving 2,441 Patients.* Antimicrob Agents Chemother, 2011. **55**(2): p. 532-538.

114. Guleri, A., et al., *Treatment of Candida Glabrata With Micafungin: A Case Report and Brief Review of the Literature*. 2013. Vol. 4. 2013: Journal of Medical Cases.

115. Chong, P.P., et al., *Genetic relatedness of Candida strains isolated from women with vaginal candidiasis in Malaysia.* J Med Microbiol, 2003. **52**(8): p. 657-666.

116. Rajendran, R., et al., *Biofilm formation is a risk factor for mortality in patients with Candida albicans bloodstream infection-Scotland, 2012-2013.* Clin Microbiol Infect, 2016. **22**(1): p. 87-93.

117. Vazquez, J.A., *Options for the management of mucosal candidiasis in patients with AIDS and HIV infection.* Pharmacotherapy, 1999. **19**(1): p. 76-87.

118. Redding, S.W., et al., *The epidemiology of non-albicans Candida in oropharyngeal candidiasis in HIV patients.* Spec Care Dentist, 2000. **20**(5): p. 178-81.

119. Monteiro, D.R., et al., *Antifungal activity of silver nanoparticles in combination with nystatin and chlorhexidine digluconate against Candida albicans and Candida glabrata biofilms.* Mycoses, 2013. **56**(6): p. 672-80.

120. Hawser, S.P. and L.J. Douglas, *Biofilm formation by Candida species on the surface of catheter materials in vitro.* Infect Immun, 1994. **62**(3): p. 915-921.

121. Pierce, C.G., et al., *The Candida albicans Biofilm Matrix: Composition, Structure and Function.* J Fungi (Basel), 2017. **3**(1).

122. Alonso, M.F., et al., *Macrophage Migration Is Impaired within Candida albicans Biofilms.* J Fungi, 2017. **3**(3): p. 31.

123. Sudbery, P.E., *Growth of Candida albicans hyphae.* Nat Rev Micro, 2011. **9**(10): p. 737-748.

124. Kuhn, D.M., *Comparison of Biofilms Formed by Candida albicans and Candida parapsilosis on Bioprosthetic Surfaces.* Infect Immun, 2002. **70**(2): p. 878-888.

125. Almeida, R.S., et al., *The Hyphal-Associated Adhesin and Invasin Als3 of Candida albicans Mediates Iron Acquisition from Host Ferritin.* PLoS Pathog, 2008. **4**(11): p. e1000217.

126. Sharkey, L.L., et al., *Flanking direct repeats of hisG alter URA3 marker expression at the HWP1 locus of Candida albicans.* Microbiology, 2005. **151**(4): p. 1061-1071.

127. Nailis, H., et al., *Monitoring ALS1 and ALS3 Gene Expression During In Vitro Candida albicans Biofilm Formation Under Continuous Flow Conditions.* Mycopathologia, 2008. **167**(1): p. 9.

128. Halliwell, S.C., et al., *Heterogeneous Expression of the Virulence-Related Adhesin Epa1 between Individual Cells and Strains of the Pathogen Candida glabrata.* Eukaryot Cell, 2012. **11**(2): p. 141-150.

129. Mundy, R.D. and B. Cormack, *Expression of Candida glabrata adhesins following exposure to chemical preservatives.* J Infect Dis, 2009. **199**(12): p. 1891-1898.

130. Domergue, R., et al., *Nicotinic Acid Limitation Regulates Silencing of Candida Adhesins During UTI.* Science, 2005. **308**(5723): p. 866.

131. Gow, N.A. and B. Hube, *Importance of the Candida albicans cell wall during commensalism and infection.* Curr Opin Microbiol, 2012. **15**(4): p. 406-12.

132. Auchtung, T.A., et al., *Investigating Colonization of the Healthy Adult Gastrointestinal Tract by Fungi.* mSphere, 2018. **3**(2).

133. Sender, R., S. Fuchs, and R. Milo, *Revised Estimates for the Number of Human and Bacteria Cells in the Body.* PLoS Biol, 2016. **14**(8): p. e1002533.

134. Iliev, I.D. and I. Leonardi, *Fungal dysbiosis: immunity and interactions at mucosal barriers.* Nat Rev Immunol, 2017. **17**(10): p. 635-646.

135. Mukherjee, P.K., et al., *Oral mycobiome analysis of HIV-infected patients: identification of Pichia as an antagonist of opportunistic fungi.* PLoS Pathog, 2014. **10**(3): p. e1003996.

136. Matsubara, V.H., et al., *Probiotic lactobacilli inhibit early stages of Candida albicans biofilm development by reducing their growth, cell adhesion, and filamentation.* Appl Microbiol Biotechnol, 2016. **100**(14): p. 6415-26.

137. Bendel, C.M., *Colonization and epithelial adhesion in the pathogenesis of neonatal candidiasis.* Semin Perinatol, 2003. **27**(5): p. 357-64.

138. Heisel, T., et al., *High-Fat Diet Changes Fungal Microbiomes and Interkingdom Relationships in the Murine Gut.* mSphere, 2017. **2**(5).

139. Olson, M.L., A. Jayaraman, and K.C. Kao, *Relative Abundances of Candida albicans and Candida glabrata in In Vitro Coculture Biofilms Impact Biofilm Structure and Formation.* Appl Environ Microbiol, 2018. **84**(8).

140. Bruno, V.M., et al., *Comprehensive annotation of the transcriptome of the human fungal pathogen Candida albicans using RNA-seq.* Genome Res, 2010. **20**(10): p. 1451-8.

141. Linde, J., et al., *Defining the transcriptomic landscape of Candida glabrata by RNA-Seq.* Nucleic Acids Res, 2015. **43**(3): p. 1392-406.

142. Biswas, S., P. Van Dijck, and A. Datta, *Environmental sensing and signal transduction pathways regulating morphopathogenic determinants of Candida albicans.* Microbiol Mol Biol Rev, 2007. **71**(2): p. 348-76.

143. Lorenz, M.C. and G.R. Fink, *The glyoxylate cycle is required for fungal virulence.* Nature, 2001. **412**(6842): p. 83-86.

144. Bensen, E.S., et al., *Transcriptional profiling in Candida albicans reveals new adaptive responses to extracellular pH and functions for Rim101p.* Mol Microbiol, 2004. **54**(5): p. 1335-51.

145. Enjalbert, B., et al., *Role of the Hog1 stress-activated protein kinase in the global transcriptional response to stress in the fungal pathogen Candida albicans.* Mol Biol Cell, 2006. **17**(2): p. 1018-32.

146. Rajendran, R., et al., *Integrating Candida albicans metabolism with biofilm heterogeneity by transcriptome mapping.* Sci Rep, 2016. **6**: p. 35436.

147. Lattif, A.A., et al., *Lipidomics of Candida albicans biofilms reveals phase-dependent production of phospholipid molecular classes and role for lipid rafts in biofilm formation.* Microbiology, 2011. **157**(Pt 11): p. 3232-42.

148. Whaley, S.G., et al., *Azole Antifungal Resistance in Candida albicans and Emerging Non-albicans Candida Species.* Front Microbiol, 2016. **7**: p. 2173.

149. Rodrigues, C.F. and M. Henriques, *Portrait of Matrix Gene Expression in Candida glabrata Biofilms with Stress Induced by Different Drugs.* Genes (Basel), 2018. **9**(4).

150. Afgan, E., et al., *The Galaxy platform for accessible, reproducible and collaborative biomedical analyses: 2016 update.* Nucleic Acids Res, 2016. **44**(W1): p. W3-W10.

151. Trapnell, C., L. Pachter, and S.L. Salzberg, *TopHat: discovering splice junctions with RNA-Seq.* Bioinformatics, 2009. **25**(9): p. 1105-11.

152. Bolger, A.M., M. Lohse, and B. Usadel, *Trimmomatic: a flexible trimmer for Illumina sequence data.* Bioinformatics, 2014. **30**(15): p. 2114-20.

153. Anders, S., P.T. Pyl, and W. Huber, *HTSeq--a Python framework to work with high-throughput sequencing data.* Bioinformatics, 2015. **31**(2): p. 166-9.

154. Love, M.I., W. Huber, and S. Anders, *Moderated estimation of fold change and dispersion for RNA-seq data with DESeq2.* Genome Biol, 2014. **15**(12): p. 550.

155. Skrzypek, M.S., et al., *The Candida Genome Database (CGD): incorporation of Assembly 22, systematic identifiers and visualization of high throughput sequencing data.* Nucleic Acids Res, 2017. **45**(D1): p. D592-D596.

156. Nobile, C.J., et al., *A recently evolved transcriptional network controls biofilm development in Candida albicans.* Cell, 2012. **148**(1-2): p. 126-38.

157. Bonhomme, J., et al., *Contribution of the glycolytic flux and hypoxia adaptation to efficient biofilm formation by Candida albicans.* Mol Microbiol, 2011. **80**(4): p. 995-1013.

158. Nett, J.E., et al., *Time course global gene expression analysis of an in vivo Candida biofilm.* J Infect Dis, 2009. **200**(2): p. 307-13.

159. Kamthan, M., et al., *Quantitative proteomics and metabolomics approaches to demonstrate N-acetyl-D-glucosamine inducible amino acid deprivation response as morphological switch in Candida albicans.* Fungal Genet Biol, 2012. **49**(5): p. 369-78.

160. Elson, S.L., et al., *An RNA transport system in Candida albicans regulates hyphal morphology and invasive growth.* PLoS Genet, 2009. **5**(9): p. e1000664.

161. Singh, R.P., et al., *Cap2-HAP complex is a critical transcriptional regulator that has dual but contrasting roles in regulation of iron homeostasis in Candida albicans.* J Biol Chem, 2011. **286**(28): p. 25154-70.

162. Tsong, A.E., et al., *Evolution of a combinatorial transcriptional circuit: a case study in yeasts.* Cell, 2003. **115**(4): p. 389-99.

163. Palige, K., et al., *Global transcriptome sequencing identifies chlamydospore specific markers in Candida albicans and Candida dubliniensis.* PLoS One, 2013. **8**(4): p. e61940.

164. Garcia-Sanchez, S., et al., *Global roles of Ssn6 in Tup1- and Nrg1-dependent gene regulation in the fungal pathogen, Candida albicans.* Mol Biol Cell, 2005. **16**(6): p. 2913-25.

165. Bennett, R.J. and A.D. Johnson, *The role of nutrient regulation and the Gpa2 protein in the mating pheromone response of C. albicans.* Mol Microbiol, 2006. **62**(1): p. 100-19.

166. Srikantha, T., et al., *Identification of genes upregulated by the transcription factor Bcr1 that are involved in impermeability, impenetrability, and drug*

resistance of Candida albicans a/alpha biofilms. Eukaryot Cell, 2013. **12**(6): p. 875-88.

167. Kunze, D., et al., *Functional analysis of the phospholipase C gene CaPLC1 and two unusual phospholipase C genes, CaPLC2 and CaPLC3, of Candida albicans.* Microbiology, 2005. **151**(Pt 10): p. 3381-94.

168. Sellam, A., et al., *Experimental annotation of the human pathogen Candida albicans coding and noncoding transcribed regions using high-resolution tiling arrays.* Genome Biol, 2010. **11**(7): p. R71.

169. Ramsdale, M., et al., *MNL1 regulates weak acid-induced stress responses of the fungal pathogen Candida albicans.* Mol Biol Cell, 2008. **19**(10): p. 4393-403.

170. Copping, V.M., et al., *Exposure of Candida albicans to antifungal agents affects expression of SAP2 and SAP9 secreted proteinase genes.* J Antimicrob Chemother, 2005. **55**(5): p. 645-54.

171. Bishop, A.C., et al., *Robust utilization of phospholipase-generated metabolites, glycerophosphodiesters, by Candida albicans: role of the CaGit1 permease.* Eukaryot Cell, 2011. **10**(12): p. 1618-27.

172. Ramirez, M.A. and M.C. Lorenz, *The transcription factor homolog CTF1 regulates {beta}-oxidation in Candida albicans.* Eukaryot Cell, 2009. **8**(10): p. 1604-14.

173. Li, L., et al., *Flavodoxin-Like Proteins Protect Candida albicans from Oxidative Stress and Promote Virulence.* PLoS Pathog, 2015. **11**(9): p. e1005147.

174. Gonzalez-Hernandez, R.J., et al., *Phosphomannosylation and the Functional Analysis of the Extended Candida albicans MNN4-Like Gene Family.* Front Microbiol, 2017. **8**: p. 2156.

175. Yeh, Y.C., H.Y. Wang, and C.Y. Lan, *Candida albicans Aro1 affects cell wall integrity, biofilm formation and virulence.* J Microbiol Immunol Infect, 2018.

176. Ahn, C.H., et al., *A farnesoic acid-responsive transcription factor, Hot1, regulates yeast-hypha morphogenesis in Candida albicans.* FEBS Lett, 2017. **591**(9): p. 1225-1235.

177. Heymann, P., et al., *The siderophore iron transporter of Candida albicans (Sit1p/Arn1p) mediates uptake of ferrichrome-type siderophores and is required for epithelial invasion.* Infect Immun, 2002. **70**(9): p. 5246-55.

178. Lee, S.A., et al., *Overexpression of a dominant-negative allele of YPT1 inhibits growth and aspartyl protease secretion in Candida albicans.* Microbiology, 2001. **147**(Pt 7): p. 1961-70.

179. Lee, S.A., et al., *Intracellular trafficking of fluorescently tagged proteins associated with pathogenesis in Candida albicans.* Med Mycol, 2005. **43**(5): p. 423-30.

180. Hynes, M.J., et al., *Regulatory genes controlling fatty acid catabolism and peroxisomal functions in the filamentous fungus Aspergillus nidulans.* Eukaryot Cell, 2006. **5**(5): p. 794-805.

181. Liu, T.T., et al., *Genome-wide expression profiling of the response to azole, polyene, echinocandin, and pyrimidine antifungal agents in Candida albicans.* Antimicrob Agents Chemother, 2005. **49**(6): p. 2226-36.

182. Wiltshire, C., S. Black, and A.J. Brown, *Over-expression of Candida albicans mitochondrial ribosomal protein S9 (MrpS9p) disturbs mitochondrial function in Saccharomyces cerevisiae.* Yeast, 1999. **15**(2): p. 139-43.

183. Newport, G., et al., *Inactivation of Kex2p diminishes the virulence of Candida albicans.* J Biol Chem, 2003. **278**(3): p. 1713-20.

184. Fanning, S., et al., *Divergent targets of Candida albicans biofilm regulator Bcr1 in vitro and in vivo.* Eukaryot Cell, 2012. **11**(7): p. 896-904.

185. Sanyal, K. and J. Carbon, *The CENP-A homolog CaCse4p in the pathogenic yeast Candida albicans is a centromere protein essential for chromosome transmission.* Proc Natl Acad Sci U S A, 2002. **99**(20): p. 12969-74.

186. Sanyal, K., M. Baum, and J. Carbon, *Centromeric DNA sequences in the pathogenic yeast Candida albicans are all different and unique.* Proc Natl Acad Sci U S A, 2004. **101**(31): p. 11374-9.

187. Baum, M., et al., *Formation of functional centromeric chromatin is specified epigenetically in Candida albicans.* Proc Natl Acad Sci U S A, 2006. **103**(40): p. 14877-82.

188. Joglekar, A.P., et al., *Molecular architecture of the kinetochore-microtubule attachment site is conserved between point and regional centromeres.* J Cell Biol, 2008. **181**(4): p. 587-94.

189. Shivaraju, M., et al., *Cell-cycle-coupled structural oscillation of centromeric nucleosomes in yeast.* Cell, 2012. **150**(2): p. 304-16.

190. Harcus, D., et al., *Transcription profiling of cyclic AMP signaling in Candida albicans.* Mol Biol Cell, 2004. **15**(10): p. 4490-9.

191. Seneviratne, C.J., et al., *Candida albicans biofilm formation is associated with increased anti-oxidative capacities.* Proteomics, 2008. **8**(14): p. 2936-47.

192. Prasad, T., et al., *Functional analysis of CaIPT1, a sphingolipid biosynthetic gene involved in multidrug resistance and morphogenesis of Candida albicans.* Antimicrob Agents Chemother, 2005. **49**(8): p. 3442-52.

193. Pasrija, R., T. Prasad, and R. Prasad, *Membrane raft lipid constituents affect drug susceptibilities of Candida albicans.* Biochem Soc Trans, 2005. **33**(Pt 5): p. 1219-23.

194. Stehr, F., et al., *Expression analysis of the Candida albicans lipase gene family during experimental infections and in patient samples.* FEMS Yeast Res, 2004. **4**(4-5): p. 401-8.

195. Fernández-Arenas, E., et al., *Integrated Proteomics and Genomics Strategies Bring New Insight into Candida albicans Response upon Macrophage Interaction.* Molecular & Cellular Proteomics, 2007. **6**(3): p. 460-478.

196. Lan, C.Y., et al., *Regulatory networks affected by iron availability in Candida albicans.* Mol Microbiol, 2004. **53**(5): p. 1451-69.

197. Tournu, H., et al., *Global role of the protein kinase Gcn2 in the human pathogen Candida albicans.* Eukaryot Cell, 2005. **4**(10): p. 1687-96.

198. Karababa, M., et al., *Comparison of gene expression profiles of Candida albicans azole-resistant clinical isolates and laboratory strains exposed to drugs inducing multidrug transporters.* Antimicrob Agents Chemother, 2004. **48**(8): p. 3064-79.

199. Hube, B., et al., *Secreted lipases of Candida albicans: cloning, characterisation and expression analysis of a new gene family with at least ten members.* Arch Microbiol, 2000. **174**(5): p. 362-74.

200. Garcera, A., et al., *Anchorage of Candida albicans Ssr1 to the cell wall, and transcript profiling of the null mutant.* Res Microbiol, 2005. **156**(9): p. 911-20.

201. MacCallum, D.M., et al., *Property Differences among the Four Major Candida albicans Strain Clades.* Eukaryot Cell, 2009. **8**(3): p. 373-387.

202. Kamran, M., et al., *Inactivation of transcription factor gene ACE2 in the fungal pathogen Candida glabrata results in hypervirulence.* Eukaryot Cell, 2004. **3**(2): p. 546-52.

203. Stead, D., et al., *Proteomic changes associated with inactivation of the Candida glabrata ACE2 virulence-moderating gene.* Proteomics, 2005. **5**(7): p. 1838-48.

204. de Groot, P.W., et al., *The cell wall of the human pathogen Candida glabrata: differential incorporation of novel adhesin-like wall proteins.* Eukaryot Cell, 2008. **7**(11): p. 1951-64.

205. Charlet, R., et al., *Remodeling of the Candida glabrata cell wall in the gastrointestinal tract affects the gut microbiota and the immune response.* Sci Rep, 2018. **8**(1): p. 3316.

206. Denisse Ramírez-Quijas, M., et al., *Effect of oxidative stress on cell wall morphology in four pathogenic Candida species*. Vol. Mycol Progress. 2015.

207. Srikantha, T., et al., *Phenotypic switching in Candida glabrata accompanied by changes in expression of genes with deduced functions in copper detoxification and stress.* Eukaryot Cell, 2005. **4**(8): p. 1434-45.

208. Gomez-Molero, E., et al., *Proteomic analysis of hyperadhesive Candida glabrata clinical isolates reveals a core wall proteome and differential incorporation of adhesins.* FEMS Yeast Res, 2015. **15**(8).

209. Weig, M., et al., *Systematic identification in silico of covalently bound cell wall proteins and analysis of protein-polysaccharide linkages of the human pathogen Candida glabrata.* Microbiology, 2004. **150**(Pt 10): p. 3129-44.

210. Ohta, A., et al., *The VIG9 gene products from the human pathogenic fungi Candida albicans and Candida glabrata encode GDP-mannose pyrophosphorylase.* Biochim Biophys Acta, 2000. **1475**(3): p. 265-72.

211. Vermitsky, J.P., et al., *Pdr1 regulates multidrug resistance in Candida glabrata: gene disruption and genome-wide expression studies.* Mol Microbiol, 2006. **61**(3): p. 704-22.

212. Healey, K.R., et al., *CRS-MIS in Candida glabrata: sphingolipids modulate echinocandin-Fks interaction.* Mol Microbiol, 2012. **86**(2): p. 303-13.

213. Nagi, M., et al., *Transcription factors CgUPC2A and CgUPC2B regulate ergosterol biosynthetic genes in Candida glabrata.* Genes Cells, 2011. **16**(1): p. 80-9.

214. Rogers, P.D., et al., *Proteomic analysis of experimentally induced azole resistance in Candida glabrata.* J Antimicrob Chemother, 2006. **58**(2): p. 434-8.

215. Ohta, A., et al., *The VIG9 gene products from the human pathogenic fungi Candida albicans and Candida glabrata encode GDP-mannose pyrophosphorylase.* Biochimica et Biophysica Acta (BBA) - General Subjects, 2000. **1475**(3): p. 265-272.

216. Alfatah, M., et al., *Critical role for CaFEN1 and CaFEN12 of Candida albicans in cell wall integrity and biofilm formation.* Sci Rep, 2017. **7**: p. 40281.

217. Iyer, V.R., et al., *Genomic binding sites of the yeast cell-cycle transcription factors SBF and MBF.* Nature, 2001. **409**(6819): p. 533-8.

218. Kanehisa, M., et al., *KEGG: new perspectives on genomes, pathways, diseases and drugs.* Nucleic Acids Res, 2017. **45**(D1): p. D353-D361.

219. Kanehisa, M., et al., *KEGG as a reference resource for gene and protein annotation.* Nucleic Acids Res, 2016. **44**(D1): p. D457-D462.

220. Kanehisa, M. and S. Goto, *KEGG: Kyoto Encyclopedia of Genes and Genomes.* Nucleic Acids Res, 2000. **28**(1): p. 27-30.

221. Gupta, P., R.C. Meena, and N. Kumar, *Functional analysis of selected deletion mutants in Candida glabrata under hypoxia.* 3 Biotech, 2017. **7**(3): p. 193.

222. Yan, D., et al., *Crz1p regulates pH homeostasis in Candida glabrata by altering membrane lipid composition.* Appl Environ Microbiol, 2016.

223. Heidler, S.A. and J.A. Radding, *Inositol phosphoryl transferases from human pathogenic fungi.* Biochim Biophys Acta, 2000. **1500**(1): p. 147-52.

224. Zheng, S., et al., *Als1 and Als3 regulate the intracellular uptake of copper ions when Candida albicans biofilms are exposed to metallic copper surfaces.* FEMS Yeast Res, 2016. **16**(3).

225. d'Enfert, C. and G. Janbon, *Biofilm formation in Candida glabrata: What have we learnt from functional genomics approaches?* FEMS Yeast Res, 2016. **16**(1): p. fov111.

226. Pemmaraju, S.C., et al., *Impact of oxidative and osmotic stresses on Candida albicans biofilm formation.* Biofouling, 2016. **32**(8): p. 897-909.

227. Cuellar-Cruz, M., et al., *High resistance to oxidative stress in the fungal pathogen Candida glabrata is mediated by a single catalase, Cta1p, and is controlled by the transcription factors Yap1p, Skn7p, Msn2p, and Msn4p.* Eukaryot Cell, 2008. **7**(5): p. 814-825.

228. Seneviratne, C.J., et al., *Proteomics of drug resistance in Candida glabrata biofilms.* Proteomics, 2010. **10**(7): p. 1444-54.

229. Mitchell, K.F., R. Zarnowski, and D.R. Andes, *Fungal Super Glue: The Biofilm Matrix and Its Composition, Assembly, and Functions.* PLoS Pathog, 2016. **12**(9): p. e1005828.

230. Mitchell, K.F., et al., *Role of matrix beta-1,3 glucan in antifungal resistance of non-albicans Candida biofilms.* Antimicrob Agents Chemother, 2013. **57**(4): p. 1918-20.

231. Vediyappan, G., T. Rossignol, and C. d'Enfert, *Interaction of Candida albicans biofilms with antifungals: transcriptional response and binding of antifungals to beta-glucans.* Antimicrob Agents Chemother, 2010. **54**(5): p. 2096-111.

232. Nett, J.E., et al., *Genetic basis of Candida biofilm resistance due to drug-sequestering matrix glucan.* J Infect Dis, 2010. **202**(1): p. 171-5.

233. Takahashi, S., et al., *Significant differences in the cell-wall mannans from three Candida glabrata strains correlate with antifungal drug sensitivity.* FEBS J, 2012. **279**(10): p. 1844-56.

234. Chandra, J., et al., *Biofilm Formation by the Fungal Pathogen Candida albicans: Development, Architecture, and Drug Resistance.* J Bacteriol, 2001. **183**(18): p. 5385-5394.

235. Samaranayake, Y.H., et al., *Human serum promotes Candida albicans biofilm growth and virulence gene expression on silicone biomaterial.* PLoS One, 2013. **8**(5): p. e62902.

236. Angiolella, L., et al., *Increase of virulence and its phenotypic traits in drug-resistant strains of Candida albicans.* Antimicrob Agents Chemother, 2008. **52**(3): p. 927-36.

237. Kucharikova, S., et al., *In vivo Candida glabrata biofilm development on foreign bodies in a rat subcutaneous model.* J Antimicrob Chemother, 2015. **70**(3): p. 846-56.

238. Pfaller, M.A., *Antifungal drug resistance: mechanisms, epidemiology, and consequences for treatment.* Am J Med, 2012. **125**(1 Suppl): p. S3-13.

239. Kumamoto, C.A., *Inflammation and gastrointestinal Candida colonization.* Curr Opin Microbiol, 2011. **14**(4): p. 386-91.

240. de Sousa, L., et al., *Isolation and identification of Candida species in patients with orogastric cancer: susceptibility to antifungal drugs, attributes of virulence in vitro and immune response phenotype.* BMC Infect Dis, 2016. **16**: p. 86.

241. Kim, G.Y., J.S. Jeon, and J.K. Kim, *Isolation Frequency Characteristics of Candida Species from Clinical Specimens.* Mycobiology, 2016. **44**(2): p. 99-104.

242. Yapar, N., et al., *Evaluation of species distribution and risk factors of candidemia: a multicenter case-control study.* Med Mycol, 2011. **49**(1): p. 26-31.

243. Horn, D.L., et al., *Epidemiology and outcomes of candidemia in 2019 patients: data from the prospective antifungal therapy alliance registry.* Clin Infect Dis, 2009. **48**(12): p. 1695-703.

244. Pfaller, M.A., et al., *International surveillance of bloodstream infections due to Candida species: frequency of occurrence and in vitro susceptibilities to fluconazole, ravuconazole, and voriconazole of isolates collected from 1997 through 1999 in the SENTRY antimicrobial surveillance program.* J Clin Microbiol, 2001. **39**(9): p. 3254-9.

245. Barchiesi, F., et al., *Electrophoretic karyotyping and triazole susceptibility of Candida glabrata clinical isolates.* Eur J Clin Microbiol Infect Dis, 1999. **18**(3): p. 184-7.

246. Vermitsky, J.P. and T.D. Edlind, *Azole resistance in Candida glabrata: coordinate upregulation of multidrug transporters and evidence for a Pdr1-like transcription factor.* Antimicrob Agents Chemother, 2004. **48**(10): p. 3773-81.

247. Papon, N., et al., *Emerging and emerged pathogenic Candida species: beyond the Candida albicans paradigm.* PLoS Pathog, 2013. **9**(9): p. e1003550.

248. Silva, S., et al., *Candida glabrata and Candida albicans co-infection of an in vitro oral epithelium.* J Oral Pathol Med, 2011. **40**(5): p. 421-7.

249. Shareck, J. and P. Belhumeur, *Modulation of morphogenesis in Candida albicans by various small molecules.* Eukaryot Cell, 2011. **10**(8): p. 1004-12.

250. Cao, Y.Y., et al., *cDNA microarray analysis of differential gene expression in Candida albicans biofilm exposed to farnesol.* Antimicrob Agents Chemother, 2005. **49**(2): p. 584-9.

251. Cho, T., et al., *Transcriptional changes in Candida albicans Genes by both farnesol and high cell density at an early stage of morphogenesis in N-acetyl-D-glucosamine medium.* Nihon Ishinkin Gakkai Zasshi, 2007. **48**(4): p. 159-67.

252. Enjalbert, B. and M. Whiteway, *Release from quorum-sensing molecules triggers hyphal formation during Candida albicans resumption of growth.* Eukaryot Cell, 2005. **4**(7): p. 1203-10.

253. Sato, T., et al., *Farnesol, a morphogenetic autoregulatory substance in the dimorphic fungus Candida albicans, inhibits hyphae growth through suppression of a mitogen-activated protein kinase cascade.* Biol Pharm Bull, 2004. **27**(5): p. 751-2.

254. Fleischmann, J., C.D. Broeckling, and S. Lyons, *Candida krusei form mycelia along agar surfaces towards each other and other Candida species.* BMC Microbiol, 2017. **17**(1): p. 60.

255. Costerton, J.W., et al., *Microbial biofilms.* Annu Rev Microbiol, 1995. **49**: p. 711-45.

256. O'Toole, G., H.B. Kaplan, and R. Kolter, *Biofilm formation as microbial development.* Annu Rev Microbiol, 2000. **54**: p. 49-79.

257. Mah, T.F. and G.A. O'Toole, *Mechanisms of biofilm resistance to antimicrobial agents.* Trends Microbiol, 2001. **9**(1): p. 34-9.

258. Ostrosky-Zeichner, L., et al., *Antifungal susceptibility survey of 2,000 bloodstream Candida isolates in the United States.* Antimicrob Agents Chemother, 2003. **47**(10): p. 3149-54.

259. Crick, D.C., D.A. Andres, and C.J. Waechter, *Novel salvage pathway utilizing farnesol and geranylgeraniol for protein isoprenylation.* Biochem Biophys Res Commun, 1997. **237**(3): p. 483-7.

260. Mosel, D.D., et al., *Farnesol concentrations required to block germ tube formation in Candida albicans in the presence and absence of serum.* Appl Environ Microbiol, 2005. **71**(8): p. 4938-40.

261. Pukkila-Worley, R., et al., *Candida albicans hyphal formation and virulence assessed using a Caenorhabditis elegans infection model.* Eukaryot Cell, 2009. **8**(11): p. 1750-8.

262. Jacobsen, I.D., et al., *Candida albicans dimorphism as a therapeutic target.* Expert Rev Anti Infect Ther, 2012. **10**(1): p. 85-93.

263. Vitali, A., et al., *Cell wall composition and biofilm formation of azoles-susceptible and -resistant Candida glabrata strains.* J Chemother, 2017. **29**(3): p. 164-172.